5-2005

Climatic and Lithogenic Controls on Soil Organic Matter-Mineral Associations

Rota Wagai

CLIMATIC AND LITHOGENIC CONTROLS ON SOIL ORGANIC MATTER-MINERAL ASSOCIATIONS

By

Rota Wagai

B.S. University of Wisconsin-Madison, 1996

M.S. Oregon State University, 1999

A THESIS

Submitted in Partial Fulfillment of the

Requirements for the Degree of

Doctor of Philosophy

(in Ecology and Environmental Sciences)

The Graduate School

The University of Maine

May, 2005

Advisory Committee:

Lawrence M. Mayer, Professor of Marine Biogeochemistry, Advisor

Christopher S. Cronan, Professor of Ecosystems and Biogeochemistry

Ivan, J. Fernandez, Professor of Forest Soils and Element Cycling

Gary M. King, Professor of Microbial Ecology and Biogeochemistry

Tsutomu Ohno, Professor of Soil Chemistry

CLIMATIC AND LITHOGENIC CONTROLS ON SOIL ORGANIC MATTER-MINERAL ASSOCIATIONS

By Rota Wagai

Thesis Advisor: Dr. Lawrence M. Mayer

An Abstract of the Thesis Presented
in Partial Fulfillment of the Requirements for the
Degree of Doctor of Philosophy
(in Ecology and Environmental Sciences)
May, 2005

Interactions of organic matter (OM) with soil mineral phases strongly affect the storage and dynamics of soil OM as well as other ecosystem processes. This study examined aspects of organo-mineral associations in soils at different scales. First, I assessed the potential controls of climate and parent rock type on organo-mineral associations using two sets of undisturbed tropical forest soils developed on two contrasting rocks along an altitudinal gradient in Borneo, Southeast Asia. Density fractionations showed that OM stored in surface mineral soils partitioned towards plant detritus fraction under cooler climates on both rock types. Thus climate exerted stronger control on soil OM storage and partitioning patterns than parent rock in the study area. The plant detritus associated with soil mineral grains also increased its standing stock under cooler climates, suggesting that abundance of mineral-free detritus and its comminution had stronger control than soil mineralogical factors.

Second, gas sorption approaches were applied to the same sets of soils to assess OM associations with soil mineral surfaces. Surface characterization before and after OM removal revealed that, with increasing altitude and OM loading, OM appear to

accumulate in globular forms that incidentally encapsulate fine mineral grains, rather than accumulating via sorption onto all mineral surfaces. Similar control of soil OM loading on the organo-mineral arrangements was found in soils of different geographic areas and soil types (n = 33), suggesting much wider generality of this relationship.

Third, I examined the importance of hydrous iron oxides (FeOx), a common soil mineral phase known to have strong sorptive capacity, for soil OM storage using a wider range of mineral soils spanning eight soil orders. With a modified selective FeOx dissolution method, I achieved the first quantification of the organic carbon (OC) that can be released from FeOx phases. Iron-bound OC accounted for only minor fractions of total soil OC (mean: 11%, range: 0-37%), indicating limited capacity of FeOx to sorptively store bulk of soil OM. The mass ratios of OC to iron (OC:Fe) of the extracts in some low pH, organic samples (e.g., spodic horizons) implied the presence of organo-iron complexes rather than adsorbed forms.

DEDICATION

In memory of my grandfather, Michio Wagai, and
my best friend, Takashi Ishii.

You are always my inspiration.

ACKNOWLEDGMENTS

My last five years in Maine have been the most challenging and enriching experience. I could not have accomplished my thesis work without support from many people for various aspects of my academic and personal life.

First of all, I'd like to thank my advisor and mentor, Larry Mayer, for guiding me with patience, providing this exciting challenge, teaching me the depth and freedom of science, and sharing his passion and humor with me. He cultivated my curiosity, sharpened my thinking, and inspired me to be a scientist and a teacher. I feel very fortunate to have discovered him here in the Maine woods. Linda Schick was a tremendous resource for all practical aspects of my research projects. Her wisdom of how to conduct science from overall management to detail analyses was critical for the success of my projects and is something I can only hope to achive myself someday.

Gratitude is also extended to my committee members: Chris Cronan for critical advice from the start to the end of my projects, Gary King for the use of his lab and discussions, and Tsutomu Ohno for his encouragements and helpful comments on my project. Ivan Fernandez has been a great contributor and mentor towards my Ph.D. program including use of his lab facility and scientific advice.

I am greatly appreciative of Professor Kanehiro Kitayama at Kyoto University, Japan, for substantial field support as well as for his patient encouragement and advice throughout my program. Crucial field support from Sabah Park Service, particularly from EcoKinabalu team, is kindly acknowledged.

I'd also like to thank my fellow graduate students and other scientists in Mayer's lab: Ivan Voparil, Anders Giessing, Dave Shull, and Kathy Hardy, for many valuable

discussions and advice. Many others at the Darling Marine Center have been supportive during my last four years. I'd like to especially thank Shawn Shellito, Carolyn Skinder, Heather Uhden, Lesley Harris, Eric Weissberger, Kelly Dorgan, Anne Simpson, Pete Jumars, Karen Templeton, Katherine Sackmann, Lisa Auriemma, Linda Healy, Tim Miller, and the two wonderful shuttle drivers, Lynne Sparrow and Steve Cust.

Steve Norton greatly helped my understanding of geology of my study area.I'd like to thank Laurie Osher for inviting me to The University of Maine. Discussions with her, Yuriko Yano, and Karin Merritt significantly advanced my understanding of soil organic matter in the early stages of my Ph.D. program. Phil Sollins offered invaluable feedback on my research (as long as I could catch him!). I've also benefited from stimulating discussions with Klaus Kaiser, Karin Eusterhues, and Udo Schwertmann on organo-mineral interactions, and practical advice from Chris Swanston and Jen Parker on soil density separation. Better insight into the organic composition of my soils was made possible by generous analytical support from Heike Knicker.

I was very fortunate to have various supports from excellent labs in Orono campus. Soil Analytical Lab, particularly Bruce Hoskins, provided vital advice on analytical issues as well as high-quality chemical analyses. Cheryl Spencer at Forest Soils Lab, Tiffany Wilson and Therese Anderson at George J. Mitchell Center for Environmental and Watershed Research, and Wayne Honeycutt and Tim Griffin at New England Plant Soil and Water Lab, are also greatly thanked for methodological advice and use of their equipments and facilities.

NASA's Earth System Science Fellowship provided me latitude to conduct a cross-disciplinary and rather ambitious project. Their support of my Ph.D. program shows that they truly value international collaboration in science.

Special thanks to Anne Pfeiffer and Beth Whitman for, among other things, their excellent help on my English writing at many odd hours! Carol Zahner has been a great neighbor and companion for cooking and laughter. In addition to the ones mentioned earlier, I am also extremely thankful to Will Holme, Holly Baldwin, Jennifer Dorsen, Malissa, David, & Rosalee Landry, Yu-Yun Chen, Sarah Granville, Sheree Fickling, Mindy Crandal, Zoe Armstrong, Erika Clesceri, Chris & Eva Flannagan, Kai Snyder & Sandra Coveny, Shizuo Suzuki, Kenji Nanba, Tetsuya Kiyosawa, Shinichi Saoshiro, Takehito Iimura, my Sundai-Kofu brothers, and late Pat McGurty. Their friendship (and the Clarks Cove Road Chai and Yoga Institute!) gave me focus and daily stability for my thesis work. My last year in Maine was particularly enriched by Cristina Lopez-Gallego, John Titus the Congo teacher, Marcela Morane, Nohora Estes, Angela, Kenneth & Conrad Kortemeier, and Jessie Mae MacDougall.

Finally, I would like to thank my partner, Naoko Izumi, and my parents, Michiumi and Fusayo Wagai, for understanding me so well and encouraging me to pursue my path.

TABLE OF CONTENTS

LIST OF TABLES

LIST OF FIGURES

Chapter 1 – General Introduction

Accumulation and loss of soil organic carbon (OC) greatly influences the global carbon cycle. Soil contains 1500 Pg C, which is roughly three times the terrestrial plant carbon pool and twice the atmospheric CO_2 pool (Schlesinger, 1991). The majority of soil carbon is in an organic form, associated with minerals in the upper portion of the lithosphere to form soil organic matter (SOM). Amount and composition of SOM significantly affect ecosystem processes and functions through the storage of carbon and nutrients, development of soil structure, and alteration of nutrient cycling.

Our predictive capability of the long-term responses of SOM to climatic and anthropogenic perturbations, however, remains poor. This difficulty is largely due to the complexity in (a) soil-climate-rock-biota interactions and feedback processes among them at larger spatio-temporal scales, and (b) interactions between OM of different decay stages with a suite of soil minerals at shorter and finer scales (e.g., Baldock and Skjemstad, 2000).

The larger-scale complexity may be overcome by field SOM studies with careful control of state factors (e.g., climo-, chrono-, and hillslope sequence, Sollins et al., 1996). The finer-scale complexity may be resolved by aggregate/molecular level examinations of OM-mineral associations in model and field conditions. In addition, the gap between the two scales needs to be filled. For instance, climate effects on submicrometer-scale interactions between OM and minerals should be taken into account to predict long-term responses of SOM pools to climate and land-use changes.

Over the last three decades, multiple biologically and physically distinctive SOM pools have been recognized and successfully separated. One of these separation methods

is based on the variations in the density and strengths of organo-mineral associations among soil constituents (Christensen, 1992; Golchin et al., 1994): light-density materials (e.g., plant detritus) relatively free of soil mineral grains are more labile and accessible for microbes than microbially-processed, heavy-density fractions containing organic materials strongly associated with soil minerals. Recent studies using ^{13}C-NMR spectroscopy and ^{14}C tracer provided a basis for mechanistic conceptual models linking plant detritus with SOM dynamics (Golchin et al., 1997; Braisden et al., 2002). Yet, the factors controlling the nature and fate of mineral-associated OM pools are still too uncertain to build simulation models based on the density fractions.

Mineral controls on SOM stabilization have been deduced from three lines of studies in literature: (1) Field soil analyses showed a co-variation between clay abundance and soil OC content among a wide variety of soils (e.g., Jenny, 1941; Post et al., 1982; Buol et al., 1990; Feller and Beare, 1997) and between mineralogical factors and OC turnover rates (Torn et al., 1997; Masiello et al., in press). (2) Laboratory analyses revealed a high biodegradability of OC once exposed from organo-mineral aggregates by physical disruption for soils (Gregorich et al., 1989; Hassink 1996) or by chemical extraction for sediments (Keil et al., 1994). (3) Experimental mixing of labile OC with a variety of soil clays or model minerals provided some direct evidence that certain minerals (e.g., clays, iron and aluminum oxides, and allophanes) stabilize OC and/or retard OC degradation (Martin *et al.*, 1966; Boudot et al., 1989; Saggar et al., 1996; Jones and Edwards, 1998). Yet, mechanistic understanding of mineral controls on soil OC dynamics remains limited (Sollins et al., 1996; Baldock and Skjemstad, 2000).

Increasing research efforts have been made to examine temperature and climatic controls on SOM after the atmospheric greenhouse effect was recognized. Conclusive evidence exists on the temperature sensitivity of soil OC among controlled incubation studies (e.g., Katterer et al., 1998; Kirschbaum, 2000). Yet the response of in-situ SOM to temperature is under debate (e.g., Liski et al., 1999; Epstein et al., 2002) partly because the sensitivity of mineral soils, consisting largely of organo-mineral associations, is unclear (e.g., Giardina and Ryan, 2000; Davidson et al., 2000).

Simulation models are an increasingly important tool to better understand and manage SOM dynamics. Current SOM simulation models, however, have some serious limitations for realistic predictions. For example, soil texture (abundance of clay-size minerals) is the only modifier of OC turnover time in a commonly-used CENTURY model (Parton et al., 1987). Recent studies suggest that mineralogy (Torn et al., 1997; Masiello et al., in press) and fine pores that exclude microbes and/or their enzymes (Adu and Oades, 1978; Mayer et al., 2004) may have more direct controls over SOM stabilization than texture, implying the need for more mechanism-based model development for long-term SOM predictions. Most current simulation models account for multiple biophysically-distinct OM pools present in actual soils by designing model structures with multiple "conceptual" pools of different turnover times. Virtually all of these models, however, assume that all of the "conceptual" pools respond to temperature similarly, which contradicts current theories and field data of SOM turnover (Burke et al., 2003). Current simulation as well as conceptual models of SOM dynamics therefore seem to be impeded by the limited understanding of (and lack of field data on) the temperature and mineral controls on the SOM pools including mineral-associated OM pool.

Here, I studied a series of undisturbed forest soils developed on two contrasting parent material types along an altitudinal gradient in Borneo, Southeast Asia, to better understand the climatic and lithogenic controls on SOM storage, its partitioning into biophysically-meaningful fractions, and organo-mineral association modes. In Chapter 1, I demonstrate that the SOM pools that responded most strongly to the climate gradient were light-density fractions, including the mineral-covered plant detritus fraction, and that microbially-processed, organo-mineral materials remained relatively constant.

Despite strong partitioning of SOM storage towards the light fractions under cooler climates, 50-86% of OC and nitrogen was strongly associated with minerals among the studied soils. This type of OM presumably represents the SOM pool of slow turnover and thus long-term OC sink (Braisden et al., 2002). While sorption is often considered as an important mechanism contributing to the long-term SOM storage (e.g., Oades, 1988; Baldock and Skjemstad, 2000), little is known about the extent of OM coverage of mineral surfaces or the factors controlling it. Thus in Chapter 2, I examine the potential climatic and lithogenic controls on OM-mineral surface relationship using the same set of study sites.

In the course of these studies, I found significant contribution of hydrous iron oxides (FeOx) to soil surface area, and potentially to SOM accumulation, under certain parent rock and climate regimes (e.g., weathered tropical soils on FeOx-rich rocks and cool temperate soils on glaciated materials). FeOx is ubiquitous in soils and often accounts for large fractions of soil mineral surface area (Borggaard, 1982), and its importance to dissolved OM sorption (Tipping, 1981; Kaiser et al., 1997) and SOM storage in podzolic soils (Buol et al., 1989) is well-known. More recently, its importance

in a wider range of soils has been suggested (Masiello et al., in press). Yet no information is available on the amounts of OC sorptively stabilized by FeOx in field soils. Thus, in Chapter 3, I examine the significance of FeOx on SOM storage using a range of mineral soils spanning eight soil orders. I modified a selective iron dissolution technique to quantify the OC that can be released from soil FeOx phases. The results indicate that direct adsorption of OC by FeOx accounts for only minor fractions of SOM, and implies more complex mechanisms of organo-iron interactions such as OM-FeOx-clay ternary association and organo-metal complexation.

Chapter 2 - Climate and parent material influences on soil organic matter storage and partitioning into physical fractions in tropical forest ecosystems

2.1. Abstract

Long-term responses of soil organic matter (SOM) pools to environmental perturbations are uncertain due to our limited understanding of SOM-climate-parent rock-biota interactions. Temperature sensitivity of SOM turnover remains unresolved partly because soil contains multiple SOM pools of different biochemistry and degrees of mineral association. We hypothesized that the amount of OM associated with soil minerals (heavy density fraction, HF) changes little while that in light-density plant detritus (f-LF) and mineral-associated detritus (m-LF) increases along a warm to cool climate gradient. This trend is expected because OM in HF is likely buffered against microbial processing and presumably against temperature change, and the formation of m-LF is likely controlled by the abundance of f-LF which has been shown to be a temperature-sensitive pool. We tested this hypothesis for the top 10 cm in two sets of undisturbed tropical forest soils, one developed from sedimentary rock and the other from ultrabasic igneous rock, along an altitudinal gradient (700-2700 m) in Borneo.

HF and m-LF accounted for 50-85% and 2-37% of total organic carbon (OC) while f-LF was always <8%, indicating the quantitative importance of m-LF especially under cooler climates. The OC stored in the 0-10cm as LFs, particularly as m-LF, increased (from 0.3-0.7 to 1.4-3 kg m^{-2}) while that as HF remained relatively constant (ca. 3 kg m^{-2}). The amounts of OC stored in O-horizons and as in the 0-10cm A-horizon as >4-mm plant detritus also increased with altitude and were similar to the OC storage

in m-LF. Large O-horizon accumulation at the mid-altitude sedimentary site corresponded to low abundance of soil macrofauna. Formation of m-LF appeared to be controlled by the abundance and fragmentation of mineral-free plant detritus. C:N ratios (and ^{13}C-NMR spectroscopy for the sedimentary series) indicate more humified nature of HF compared to f-LF at all sites. Climate or parent rock appeared not to affect the OM composition in f-LF and HF. In contrast, m-LF showed significantly higher C:N and aliphaticity at mid-altitude compared to low and high altitudes on both rock types, consistent with abundant, resinous plant detritus found at this altitude. Assessment of the variations in chemical composition and size (surface area-to-volume ratio) of plant detritus deserves further study to establish a better understanding of the nature of m-LF and the partitiong of plant detritus between f-LF and m-LF.

Our results indicate that climate exerted a stronger control on the SOM storage and partitioning than parent rock in the studied forest ecosystems, and showed that responses of the density fractions to the temperature gradient significantly differed between the light and heavy fractions.

2.2. Introduction

Soil organic matter (SOM) plays a critical role in ecosystem functioning through the storage of carbon and nutrients, improvement of aeration and water-holding capacity, and thus affects primary production and biogeochemical cycling. Long-term responses of SOM, a significant carbon reservoir on the earth's surface, to environmental perturbations remain uncertain largely due to complex feedback processes among soil, climate, parent rock, and biota.

Temperature sensitivity of soil organic carbon (OC) processing is well-established from controlled incubation studies (Katterer et al., 1998). Yet the response of SOM in the field to temperature is under debate (e.g., Liski et al., 1999; Epstein et al., 2002). Significant temperature control on the in-situ decomposition of labile soil OC (e.g., plant detritus) has been demonstrated using bomb ^{14}C tracer (Bird et al., 1996; Trumbore et al., 1996). Yet, recalcitrant or whole soil OC dynamics have appeared insensitive to temperature (Paul et al., 1997; Giardina and Ryan, 2000). Thus predictive capability of current SOM simulation models, that apply the same temperature sensitivity to all of their "conceptual" OC pools of different biophysical properties and/or turnover times, is questionable (Burke et al., 2003). In addition, lack of physically-definable pools corresponding to the "conceptual" pools limits further development of these models (Christensen, 1996). Identification of biologically-relevant, physical pools and examination of the factors controlling these pools are among the first steps to better understand climate controls on SOM dynamics.

The density fractionation approach allows a separation of heterogeneous SOM into biophysically-distinctive pools (Christensen, 1992): light-density plant detritus relatively free of soil mineral grains (free light fraction, f-LF) and amorphous, microbially-processed organic materials strongly associated with soil minerals (heavy fraction, HF). Large seasonal changes in the amounts of f-LF in mineral soils imply that f-LF is a significant reservoir of labile carbon and nutrients in forest ecosystems (Spycher et al.,1983).

More recently, Golchin et al. (1994) distinguished the plant detritus associated with soil minerals (m-LF) from HF using ultrasound treatment of soil in heavy liquid (ca.

1.6 g cm^{-3}), and showed that m-LF contained 9-18 % and 6-14% of total soil OC and nitrogen (N), respectively, among five native forest and grassland soils. Lower carbohydrate contents of m-LF than f-LF were taken as evidence for a more advanced decomposition state of m-LF, which led to the conceptual model linking plant detritus with SOM dynamics – plant detritus enters soil as f-LF which decays to m-LF as microbial growth and slime production on litter surfaces attract mineral grains, and OC in the m-LF eventually transforms to HF (Golchin et al., 1997). Using ^{14}C tracer, Braisden et al. (2002) has shown that the turnover time of f-LF was <10 years and that of most m-LF materials was 20-40 years among grassland soils of different ages, implying that m-LF represents a distinctive, mineral-protected, plant detritus pool. Despite clear morphological and compositional difference, OC turnover times between m-LF and HF were relatively similar (Braisden et al., 2002). Thus the nature and fate of m-LF seem uncertain in current conceptual SOM models based on density separations (Golchin et al., 1997; Braisden et al., 2002).

The role of plant detritus in soil may become greater during global climate change. Atmospheric CO_2 enrichment will likely increase the input of plant detritus to soil due to enhanced plant productivity (Haile-Mariam et al., 2000; Schlesinger and Lichter, 2001). Then the extent of plant detritus association with soil minerals will be an important factor affecting the decomposition rate and thus the temporality of extra carbon sinks. Clay mineralogy directly affects the degradability of plant detritus (e.g., Saggar et al., 1996) and clay abundance appears to enhance the OC accumulation in m-LF (Kölbl and Kögel-Knabner, 2004). Yet climate controls on the plant detritus partitioning to f-LF vs. m-LF, or the formation of the m-LF are virtually unstudied.

To what extent does climate control the accumulation and partitioning of SOM into these physical pools? Christensen (1992) pointed out the general trend of soil OC partitioning towards f-LF from low to high latitudes among 13 forest soils from the literature, though state factors were not likely controlled and the m-LF was not quantified in these studies. Temperature sensitivity of microbial OC decomposition is likely the highest in f-LF among the density fractions because of high substrate quality and accessibility (lack of mineral armoring) as witnessed in lab incubation of plant residues (e.g., Katterer et al., 1998), and less in HF because soil mineral matrix likely acts as a buffer. The temperature sensitivity of m-LF is less clear. We hypothesized that the amount of OM in HF changes little while that in f-LF and m-LF increases along a warm to cool climate gradient because the formation of m-LF is likely controlled by the abundance of f-LF which is temperature sensitive (Bird et al., 1996; Trumbore et al., 1996). Alternatively, similar residence times of the m-LF and HF (Braisden et al., 2002) may suggest high stability of m-LF, in which case m-LF may be less sensitive to temperature, responding to the climate gradient more similarly to HF.

We tested these hypotheses using two sets of undisturbed tropical forest soils, one developed from acidic sedimentary rock and the other from ultrabasic igneous rock, on a mountain slope in Borneo, Southeast Asia. An altitudinal gradient of 700-2700 m above sea level provides a climate gradient. We focused on the standard depth of 0-10cm, where SOM is most concentrated and climate exerts stronger control than at depth, to assess the climate influence on surface soil OM storage and partitioning. We also examined OC composition and stoichiometry of the density fractions to gain insight on the decomposition process and to elucidate potential effects of climate and parent material on

the quality of organic matter. A companion study (Wagai et al. in prep) assessed the climate control on organic covering of soil mineral surfaces using the same set of soils.

2.3. Materials & Methods

2.3.1. Study are

We studied soils on the eastern and southern slopes of Mt. Kinabalu (4095 m, 6°05'N, 160°33' E), developed on both acidic sedimentary and ultrabasic igneous parent materials, under the primary rain forests protected as the Kinabalu Park. The six selected sites (at ca. 700, 1700, and 2700 m above sea level on the two rock types) are part of a long-term ecological study and more detailed site characteristics have been reported elsewhere (Aiba and Kitayama, 1999; Kitayama and Aiba, 2002). Briefly, the climate is humid tropical with weak influences of the Asiatic monsoon. A strong temperature gradient is present along the slope (Table 2.1): mean annual air temperature (MAT) decreases with altitude at a mean lapse rate of 0.0055 $^{\circ}C\ m^{-1}$, with <2 °C intra-annual variations (Kitayama, 1992). Mean annual rainfall is relatively constant (2300-2400 mm yr^{-1}) with altitude, although inter-annual variation can be large (e.g., 1800-3300 mm yr^{-1} during 1996-1999, Kitayama and Aiba, 2002). Air and soil moisture generally increase with altitude (Table 2.2) due to cooling and more frequent cloud cover at upper altitudes.

The sedimentary rocks found in the study area (Trusmadi formation) include Eocene argillite, slates, siltstones, and sandstones (Jacobson, 1970). The ultrabasic igneous rocks consist mostly of peridotite, with various degrees of serpentinization, characterized by high concentrations of MgO, FeO, and heavy metals (Jacobson, 1970). Soil pH of surface mineral horizons was roughly one pH unit higher on the untrabasic

rock than on sedimentary rock at each altitude, reflecting the contrasting chemistry of the two parent materials (Table 2.2). Parent rock above 3000 m is largely granitic massif. All soils were sampled on gentle slope positions (<27°) under closed canopy.

Forests on both sedimentary and ultrabasic sites showed a similar rate of decrease in aboveground net primary productivity (ANPP) with increasing altitude (Table 2.1), suggesting a strong temperature control on forest productivity. The decrease in ANPP with altitude could be explained solely through reduced leaf area (per unit area) with altitude on sedimentary parent materials, while both leaf area and phosphorus deficiency appeared to control the ANPP decrease on ultrabasic parent materials (Kitayama and Aiba, 2002). Soil fauna composition appeared to show a zonation along the altitudinal gradient: termites dominate at the 700-m sites, geophagic earthworms at the 2700-m sites, and the lower presence of both of these faunal groups at the 1700-m sites (M. Ito, personal comm.).

Table 2.1: Climate and ecosystem characteristics of Mt. Kinabalu study sites. Data from Kitayama and Aiba (2002).

	Sedimentary rock series			Ultrabasic rock series		
	Altitude (m)					
	700	1700	2700	700	1700	2700
Actual elevation of each site (m)	650	1560	2590	700	1860	2700
Mean annual air temperature (°C)#	23.8	18.8	13.1	23.3	16.9	12.3
Mean annural rainfall (mm)*	2392	2380	2256	2392	2380	2256
Aboveground biomass (kg m^{-2})	48.1	28	29.5	54.2	21.3	10.8
Aboveground NPP (kg m^{-2} yr^{-1})	1.91	1.22	0.78	1.72	0.81	0.73
Litterfall mass (kg m^{-2} yr^{-1})	1.11	0.80	0.53	1.11	0.63	0.59

based on the weather station at 2700m and the lapse rate of 0.0055 °C per meter.
* from the weather station at each altitude.

Table 2.2: Soil characteristics (0-10 cm A-horizon) of the study sites. S.E. is standard error (n = 5)

		Sedimentary rock series			Ultrabasic rock series		
		Altitude (m)					
		700	1700	2700	700	1700	2700
pH in deionized water	MEAN	3.88	4.13	3.86	4.83	5.45	4.87
	S.E.	0.10	0.11	0.13	0.11	0.10	0.15
pH in $CaCl_2$	MEAN	3.48	3.36	3.09	4.01	4.59	4.19
	S.E.	0.03	0.06	0.05	0.09	0.25	0.20
Total soil OC (%)	MEAN	2.98	4.91	14.22	3.03	6.21	8.30
	S.E.	0.43	0.70	1.83	0.28	0.81	0.77
Total soil N (%)	MEAN	0.25	0.28	0.70	0.21	0.31	0.49
	S.E.	0.03	0.05	0.09	0.02	0.04	0.05
Total soil C:N	MEAN	11.7	18.1	20.3	14.8	20.0	16.9
	S.E.	0.4	0.7	0.7	0.8	0.7	0.2
Soil suborder *		humic	tropical	tropical	peric	tropical	tropical
Soil order *		Ultisol	Alfisol (Incept/Spod)	Inceptisol	Oxisol	Alfisol	Inceptisol

* tentative classification of soils at each site according to U.S. soil taxonomy.

2.3.2. Soil sampling and handling

After the initial soil survey, five soil samples were collected from 2-20 meters apart, to account for heterogeneity, adjacent to the permanent vegetation plots at each site. The 0-10-cm of the A-horizons were sampled by a core and sieved through a 4-mm sieve to reduce soil structural distruction for incubation study (not reported here). Coarser plant detritus and gravels (>4 mm) were dried at 75 and 105 °C, respectively, and weighed for standing stock calculation. Subsets of <4-mm soils were analyzed for soil pH in deionized water and 0.01N calcium chloride at a soil:solution ratio of 1:5 (g:mL) after 0.5-1.0 hour equilibration. Soil water content of the sieved soils was determined by weight loss after 48 hours at 105 °C. The remainder of sieved soils were freeze-dried and kept frozen until the following analyses.

Another set of field soils (n = 4-6 except for the 700-m ultrabasic site, n = 2) was collected at each site for bulk density estimates. At randomly-chosen locations in each site, O-horizon materials from a specific ground area (100-225 cm^2) were carefully sampled using square frames and the average depth of O-horizon was estimated from the depth measurement at four corners. After O-horizon removal, the top 10-cm mineral soil was taken by a metal core (diameter = 4 cm). O-horizon and mineral soil samples were dried at 75 °C and 105 °C for 48 hours, respectively, and weighed for bulk density calculation. The O-horizon materials were ground for further analysis.

2.3.3. Density separation

To quantify OC associated with soil minerals, particulate organic materials were removed from soils by a density separation technique, modified from Golchin et al.

(1994). Samples were gently turned over 20 times by hand with 1.6 g cm^{-3} sodium polytungstate solution. The free light-density fraction (f-LF) was floated and transferred into a Buchner funnel with a glass-fiber filter (Whatman GF/C) and rinsed with deionized water until the electrical conductivity of the rinse water reached < 50 μS, and then oven-dried at 60 °C. The remaining soil slurry was treated with ultrasound (656 J mL^{-1}) using a Fisher-Artek-Dynatech Model 300 sonicator with a 19-mm diameter tip in an ice bath. The sonicator was calorimetrically calibrated (North, 1976). The material floated after the sonication (mineral-associated light fraction, or m-LF) was recovered using the same procedure as the f-LF recovery. Settled materials in the heavy liquid after the sonication (heavy density fraction – HF) were rinsed as above, and then freeze-dried.

2.3.4. Mass and organic matter recovery

Total OC and N in dried bulk samples, density separates, and O-horizon materials were analyzed using a Perkin-Elmer 2400 CHN analyzer (Perkin-Elmer, Norwalk, CT, USA). A pilot test showed the absence of carbonate in the studied soils.

Soil materials were almost fully recovered after the density separation (Fig. 2.1a). Both OC and N are slightly lost during the separation/recovery process, possibly due to dissolution, fine colloids and/or OM stuck on the glass fiber filter during m-LF rinse step (Fig. 2.1b,c). Greater loss of N might result from the loss of low C:N, humified material or inorganic N. High mass recovery refutes the former possibility. Loss of inorganic N into the polytungstate solution or during oven-drying of LFs is a possibility. Analytical or sub-sampling error is also a possibility.

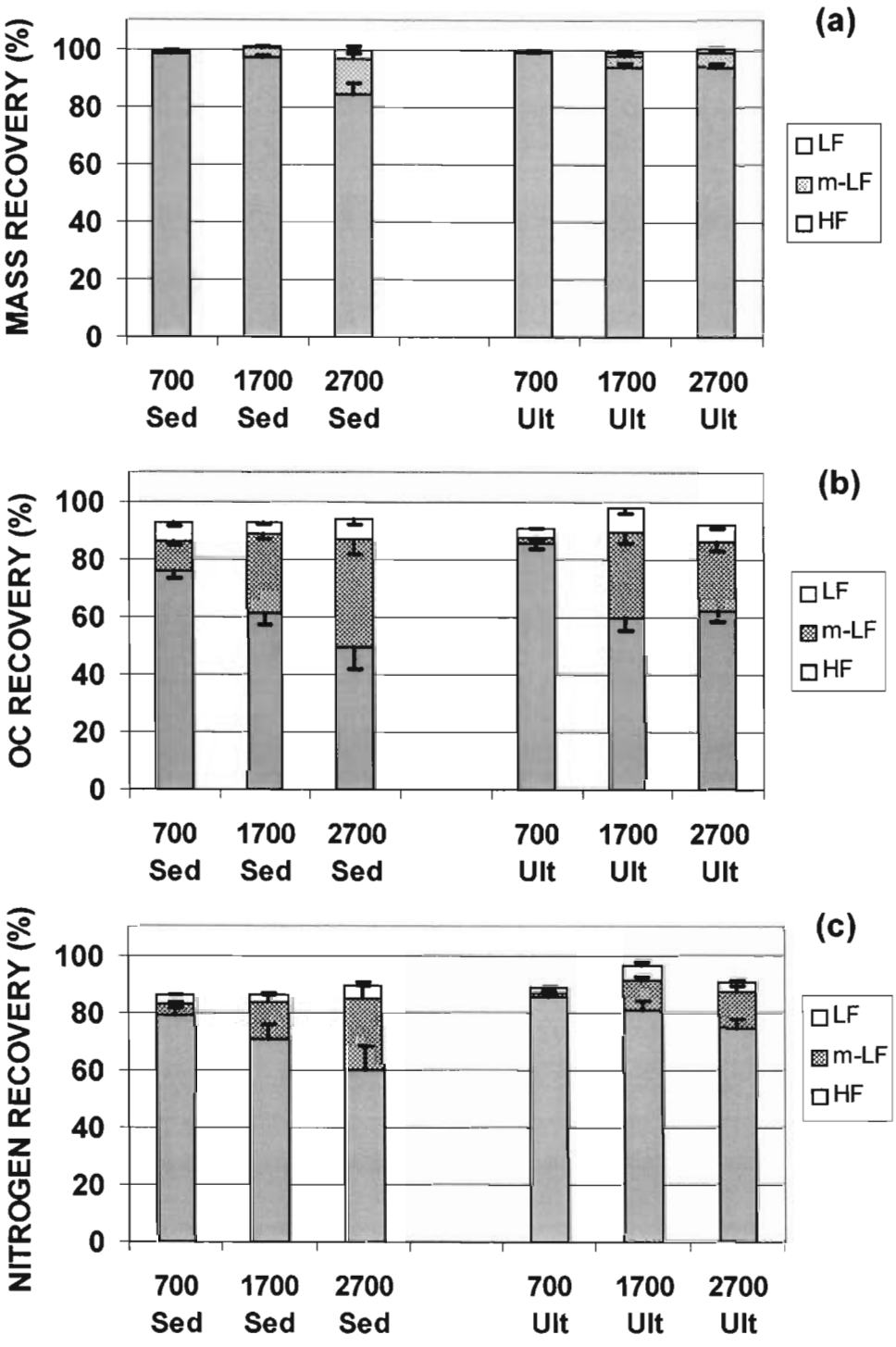

Figure 2.1: Recovery of mass (a), organic carbon (b), and nitrogen (c) among the three density fractions. Error bar = standard error (n = 5)

2.3.5. Solid-state ^{13}C-NMR spectroscopy

For solid-state CPMAS ^{13}C NMR spectroscopy, equal mass of five replicates was combined for each density fraction at each site. For the sedimentary soils, one O-horizon sample was prepared in the same way for each site. For the ultrabasic soils, HF was not analyzed due to the high concentration of iron oxides. The solid-state ^{13}C NMR spectra were obtained on a Bruker DSX 200 spectrometer at a ^{13}C resonance frequency of 50.3 MHz and using a commercial Bruker double-bearing probe with phase-stabilized zirconium dioxide rotors of 7-mm outer diameter. The contact time was 1 ms. Depending on the sensitivity of the samples, between 9700 and 373,000 scans were accumulated using a pulse delay of 100–400 ms. Line broadenings between 50 and 150 Hz were applied prior to Fourier transformation. The 13C chemical shift scale is referenced to tetramethylsilane (= 0 ppm). The NMR spectra were divided into four major chemical shift regions: alkyl C (-10 to 45 ppm), O/N-alkyl C (45 to 110 ppm), aromatic C (110 to 160 ppm), carbonyl C (160 to 220 ppm) (Knicker and Lu¨demann, 1995). The relative carbon distribution was determined by integration of the signal intensity in the different chemical shift regions using an adapted integration routine supplied with the instrument software.

2.3.6. Standing stock calculation

For all five samples from each site, the total OC concentrations in 0-10 cm A-horizons were calculated by summing the OC quantity of the three density fractions in the isolated <4-mm mass and that of >4-mm plant detritus (POM) in the isolated >4-mm mass. Graveles isolated in the >4-mm fraction were assumed to contain no OC. The OC concentrations of the >4-mm POM fractions were not measured but assumed to be the

same as that of f-LF because of their morphological similarity. Analysis of a limited number of the POM samples justified this assumption. The averaged total A-horizon OC concentration (n = 5) at each site was multiplied by the averaged bulk density (n = 2-6) to estimate OC standing stock in the 0-10 cm A-horizon. Error propagation was calculated from the relative standard deviation (RSD) for each value as follow:

$$RSD_{\text{A-horizon OC stock}} = \text{square root of } [(RSD_{\text{OC concentration}})^2 + (RSD_{\text{bulk density}})^2] .$$

Standing stocks of O-horizons were estimated in the same way. The OC standing stocks in the 0-10 cm A-horizons were partitioned into the density fractions by applying the OC mass partitioning ratios among the four fractions.

2.4. Results and Discussion

2.4.1. Microscopic observation

We first examined the morphology of the density fractions using a dissecting microscope to qualitatively determine material origins and the degree of alteration of isolated materials. Materials recovered as f-LF were largely coarse plant detritus (>100 μm) with relatively intact morphology (Fig. 2.2 a-d). Much of the plant detritus, particularly root fragments, was covered with fine mineral crystals or microaggregates (<10-20 μm). In contrast, m-LF was dominated by more fragmented plant detritus (<100 μm) that had little recognizable morphology except for some pollen, spore-like materials (Fig. 2.2 e-h). Plant fragments in this fraction appeared less covered with fine minerals (e.g., Fig. 2.2 e,f,h). Pollen and spores were much less common in f-LF in accord with Baisden et al. (2002), and accounted for no more than one quarter of m-LF materials

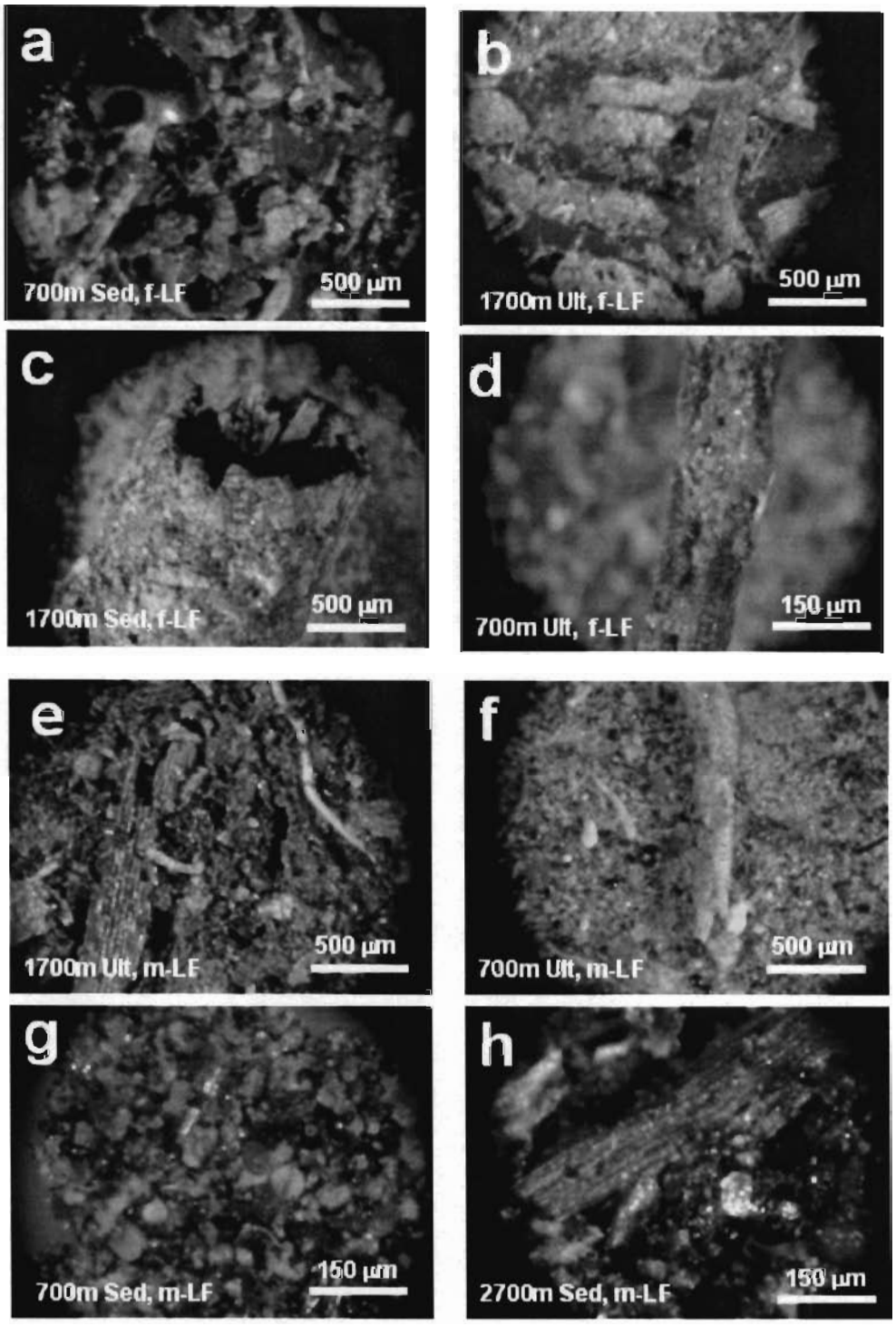

Figure 2.2: Examples of f-LF (a-d) and m-LF materials (e-h) observed by a dissecting light microscope. Black corners are outside of microscope's field of view.

(visual observation) across all sites. Pollen and spores therefore appeared to accumulate preferentially in the m-LF, which may be attributed to their recalcitrance and thus long residence time, allowing their association with mineral grains. No charred materials were recognized in f-LF or m-LF. Heavy density fractions contained no recognizable plant detritus and consisted of mineral grains (presumably microaggregates) with amorphous organic matter (OM). The observed morphological differences among the density fractions are consistent among all six sites, and are in accord with previous studies (Golchin et al., 1994; Baisden et al., 2002).

The f-LF materials appeared to be more covered with mineral grains than m-LF materials, presumably due to the detachment of mineral grains from plant detritus by the ultrasound treatment of the m-LF. The observed greater mineral-covering of f-LF was confirmed by the lower OM concentration (thus higher mineral concentration) of f-LF than m-LF at all six sites (Table 2.3). A similar pattern in the OC concentration between f-LF and m-LF has been reported for other forest and agricultural soils (Parker et al., 2001; Kölbl and Kögel-Knabner, 2004). Note that the original m-LF materials (in field condition) had to be associated with minerals at greater extent than f-LF materials to have the net density >1.6 g cm^{-3} in the initial density separation step.

The size of the plant detritus may have a significant control over the f-LF vs. m-LF partitioning. Materials recovered as m-LF were clearly more fragmented and had higher surface area-to-volume ratios than f-LF materials. Assuming equal likelihood of mineral attachment onto all surfaces of plant detritus, similar amounts of mineral covering per unit surface area of plant detritus will lead to the net density >1.6 g cm^{-3} for smaller materials. If this assumption is true, then smaller or easily-fragmented detritus

enters m-LF faster than coarser detritus regardless of degradation stage. The observed preferential accumulation of pollen in m-LF may therefore be attributable to its small size as well as chemical recalcitrance. The relative importance of size vs. degradation degree of plant detritus is an important issue to study to establish a better understanding of the f-LF vs. m-LF partitioning process.

The OC concentrations of f-LF slightly decreased with increasing altitude on both rock series (Table 2.3). When both rock types were combined, this altitudinal trend was marginally significant ($p = 0.06$), suggesting that f-LF at higher altitude might hold more mineral grains per mass. The higher mineral content of upper altitude f-LF materials may result from longer residence time (slower decay) of plant detritus under cooler climates allowing greater association with mineral grains.

Table 2.3: Concentration of OC in the isolated density fractions. Standard error ($n = 5$) in prentices.

site	f-LF OC (%)	m-LF OC (%)	HF OC (%)
700 Sed	36.39 (0.87)	47.99 (1.24)	2.23 (0.22)
1700 Sed	35.44 (0.87)	50.74 (1.26)	3.06 (0.48)
2700 Sed	34.26 (0.74)	47.18 (0.70)	8.01 (0.97)
700 Ult	35.73 (1.98)	48.06 (1.99)	2.59 (0.20)
1700 Ult	35.50 (1.56)	49.43 (1.23)	3.62 (0.28)
2700 Ult	32.50 (1.28)	43.92 (1.18)	5.36 (0.41)

2.4.2. SOM concentrations

Total soil OC and N concentrations progressively increased by 3-5 fold and 2-3 fold, respectively, with increasing altitude on both rock types (Table 2.2). Despite little difference in annual precipitation along the altitudinal gradient, soil moisture content also increased due to lower evapotranspiration under cooler climate and more frequent cloud formation at 2700 m sites (Kitayama et al., 1998; Hall et al., 2004). In humid tropical forests, however, soil moisture is not likely to limit decomposition rate. The progressive SOM accumulation with altitude, despite a two-fold drop in the OM input rate (Table 2.1), is therefore more attributable to temperature change, reflecting the higher temperature sensitivity of decomposition than OM production (Kirschbaum, 2000).

Heavy fractions accounted for 50-85% of total soil OC and 60-85% of total N in the surface mineral horizon across the study sites (Fig. 2.3). Most of the remaining SOM was accounted for by m-LF (2-37% of total OC and 1-25% of total N). The partitioning of total OC and N shifted mainly from HF to m-LF with increasing altitude on sedimentary rock and, to a lesser extent, on ultrabasic rock. The increase in SOM concentration with altitude was almost entirely achieved by the organic matter increases in m-LF and HF on both rock series (Fig. 2.3). Yet the relative increase in OM concentration from the 700 to 2700 m was the most significant in f-LF. The progressive increase in the OM concentration in HF with altitude was accompanied by organic covering of mineral surfaces (Chapter 3).

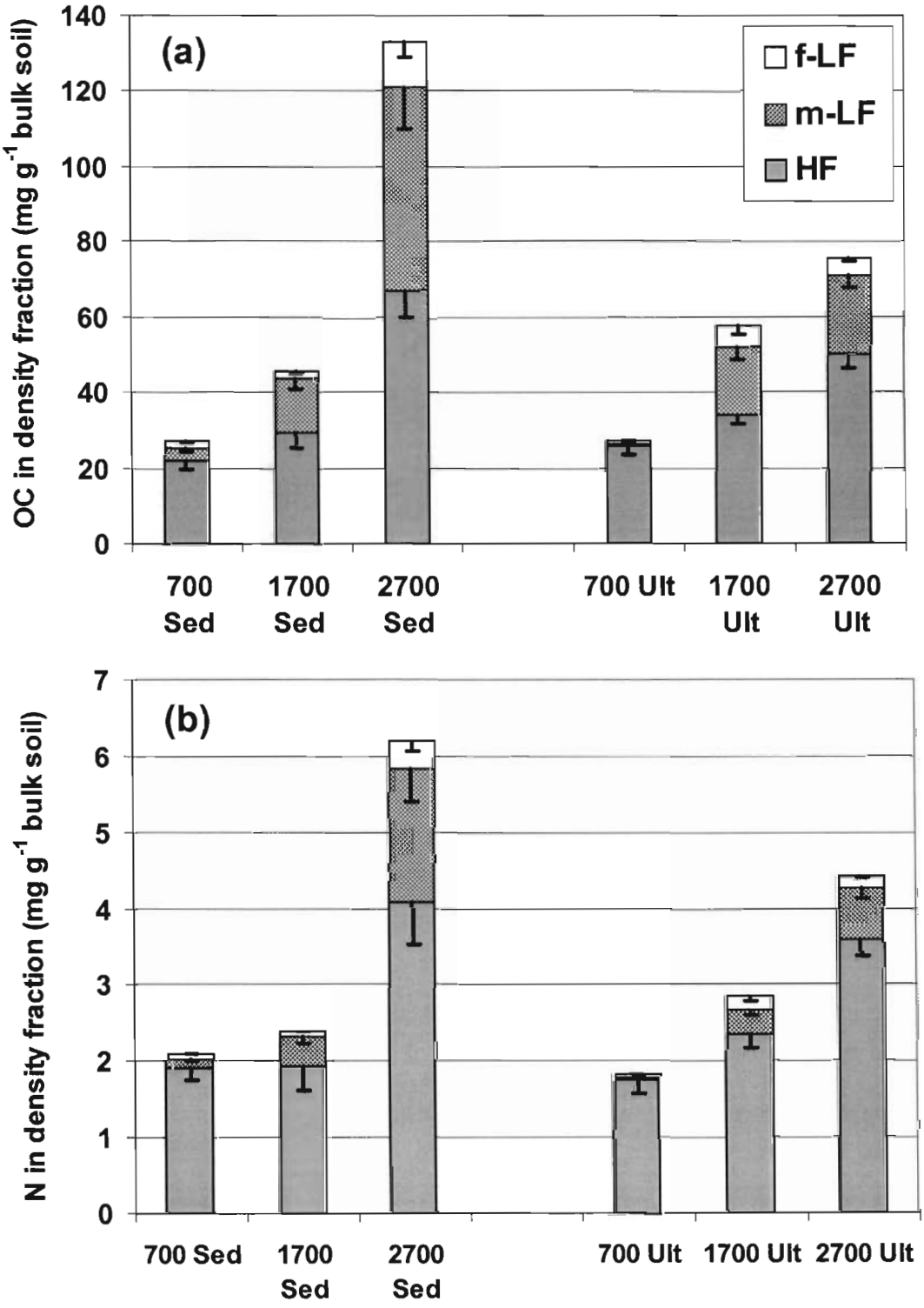

Figure 2.3: Concentration of organic carbon (a) and nitrogen (b) in the density fractions per mass of <4-mm soil. Error bar = standard error (n = 5)

2.4.3. Stoichiometry of SOM fractions

We used the C:N ratio to assess the qualitative aspects of OM in the density fractions to gain insight on the decomposition process. Total soil C:N ratios increased more significantly and consistently in the sedimentary series than the ultrabasic series (Table 2.2). The temperature response of the sedimentary soil C:N ratios was comparable to the averaged one unit of C:N ratio increase per ^{o}C MAT drop found in a review of published data (Jenny, 1980).

Among the detritus pools, the highest C:N ratios were found in freshly fallen litter, the lowest ratios in HF, and intermediate ratios in the O-horizon and LFs at all six sites (Fig. 2.4), in agreement with the general concept of decomposition from high C:N plant litter to low C:N, microbially-processed humic materials with strong association with the soil mineral grains. The general increase in the C:N ratios of litterfall materials with increasing altitude is attributable to the forest's adaptation to cooler climate regimes – trees appeared to increase foliar N concentration to maintain the photosynthetic performance per unit leaf area in higher altitudes, which is partly achieved by higher N resorption efficiency of tree leaves before senescence, resulting in N-depleted litter (Kitayama and Aiba, 2002).

The C:N ratio was consistently higher at the 2700 m than 700 m sites in all of the studied OM fractions on borth parent materials except for HF (Fig. 2.4). However, the C:N ratios of the detritus pools at the mid-altitudinal sites followed the altitudinal trend only in f-LF on the sedimentary series and in litterfall and O-horizon materials on the ultrabasic series. The departre from the altitudinal trend was most clear in m-LF on both

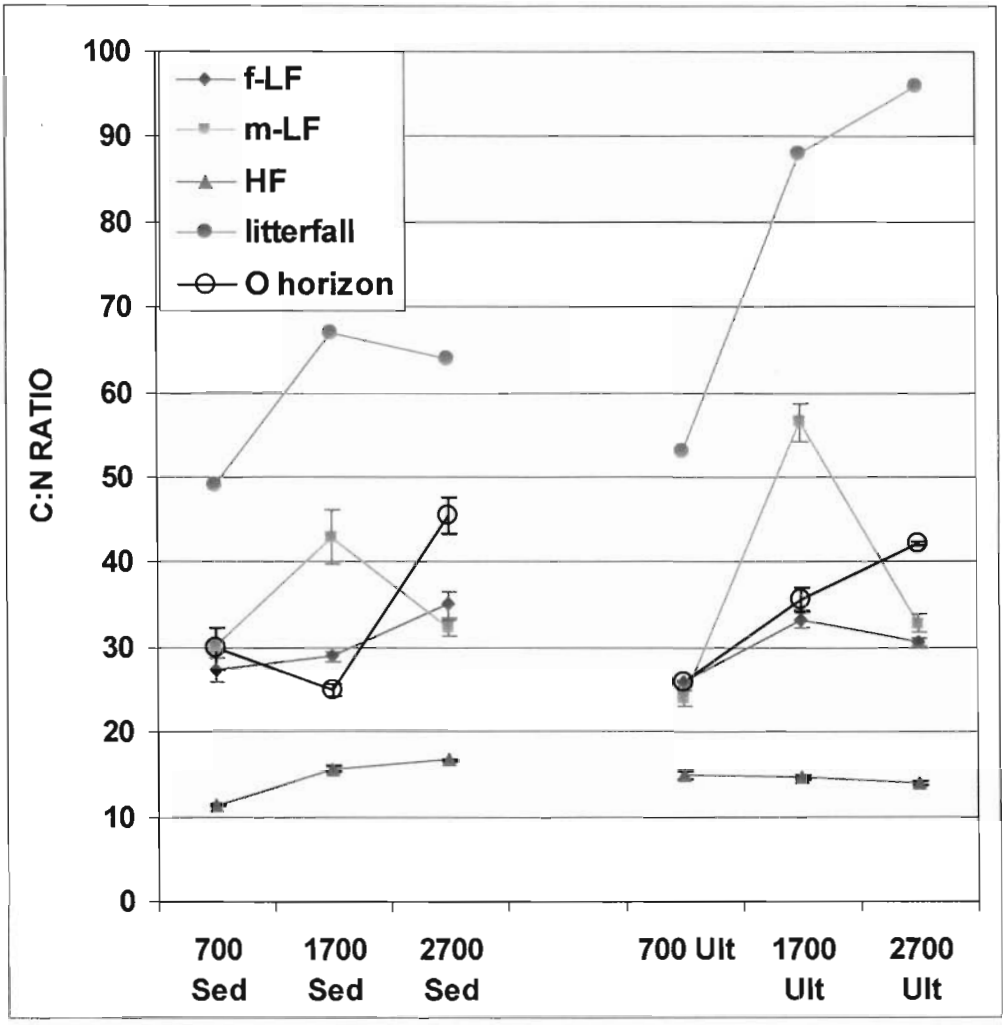

Figure 2.4: Ratio of organic carbon to nitrogen in the density fractions, O-horizon, and litterfall materials across the sites. Error bars = standard error (n = 5 for density fractions, 5 for the O-horizons at 1700-m sites, and 2 for the O-horizons at the other sites). Litterfall data is from Kitayama and Aiba (2002).

parent materials, and the OC-enrichment of m-LF on the sedimentary rock corresponded to that of litterfall material (Fig. 2.4).

The C:N ratios of m-LF are often slightly higher than those of f-LF, and ranged between 10-23 for warmer and cultivated soils (Golchin et al., 1994; Baisden et al., 2002; Kölbl and Kögel-Knabner, 2004) and 21-57 for cool temperate forest soils (Parker et al., 2002). Characteristically high C:N ratios of the m-LF at the 1700-m sites (range: 29-76), close to those of litterfall materials, suggest the possibility that some of the fresh plant detritus at these sites quickly associate with mineral grains (see discussion below).

Despite the OM enrichment in HF with increasing altitude (Fig. 2.3), it's C:N ratios remained low (Fig. 2.4). Lower C:N ratios in the HF than in the LFs support the concept that HF holds amorphous, humified OM resulting from intensive microbial transformation (Golchin et al., 1997; Braisden et al., 2002), and is consistent with microscopic observations. These low ratios of the HFs indicate that microbial processing of plant detritus led to the formation of amorphous OM that sticks to mineral grains strongly enough to survive the ultrasound treatment.

The gap in C:N ratios between initial (litter) and end materials (HF) widened with altitude on both rock series. The high altitude soils appear to require as much N to preserve one unit of OC in the HF as lower altitude soils. In addition to N limitation in the autotrophic processes (Kitayama and Aiba, 2002), in-situ soil net mineralization decreased to near-zero with increasing altitude in the same set of sites (Kitayama et al., 1998; Hall et al., 2004). These results are consistent with the idea that N limits the microbial transformation of LF materials to HF at the higher altitude soils. This idea is in accord with experimental evidence that a ten-year N fertilization increased the OC

storage in the HF of alpine soils (Neff et al., 2002). Nitrogen limitation on soil heterotrophic activity under cooler climate regimes is becoming increasingly recognized (e.g., Schimel and Bennett, 2004).

2.4.4. OC composition revealed by ^{13}C-NMR

Composition of OC in the density fractions was examined using ^{13}C-NMR to further elucidate the degree of decomposition and possible origins of organic materials. The HF of ultrabasic soils were not analyzed for ^{13}C-NMR spectra due to the inteference by high content of paramagnetic iron. For sedimentary soils, O-horizons were included to compare the OC composition between a starting material and with more decomposed materials in the density fractions. Carbohydrate (O-alkyl group) abundance decreased in the order: O-horizon > f-LF > m-LF in all sedimentary sites and f-LF > m-LF in all ultrabasic sites (Fig. 2.5). The decrease in carbohydrate relative to aliphatic-C group from f-LF to m-LF presumably indicates preferential degradation of carbohydrates (Golchin et al., 1994; Golchin et al., 1997). The increase in carbohydrate from m-LF to HF in the sedimentary soils and the low C:N of the HF are supposed to represent microbially-derived carbohydrates in the HF (Golchin et al., 1997).

The OC composition of f-LF (and O-horizon for the sedimentary series) was quite similar along the altitudinal gradient (Fig. 2.5). In contrast, high inter-altitude variation in the OC composition was found in m-LF although there was no consistent change with altitude. Significantly higher carbohydrate and a concurrent increase in C:N ratio in the HF at the 2700-m sedimentary site suggest greater incorporation of plant-derived carbohydrate with increasing altitude.

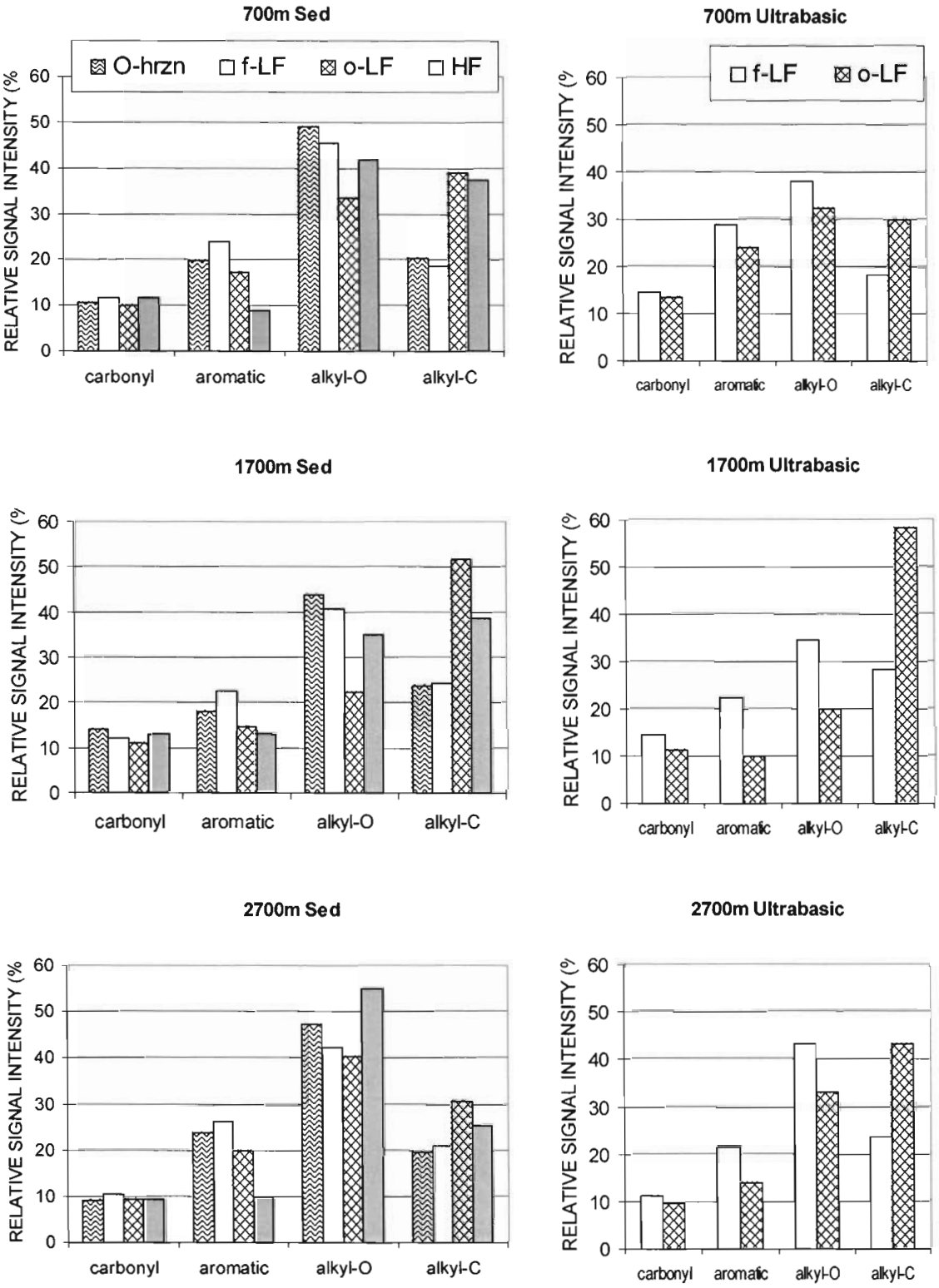

Figure 2.5: Percent of total ^{13}C-NMR spectra assigned to each carbon group for the density fractions and O-horizon for the sedimentary sites.

A unique composition of OM in the m-LF at the 1700-m sites is suspected from the significantly higher C:N ratios (Fig. 2.4) and aliphatic-C (Fig. 2.5) compared to other altitudes or density fractions. High aliphaticity of these m-LFs can result from either preferential degradation of O-alkyl by microbes or selective preservation of aliphatic plant detritus. High C:N ratios of the m-LFs (40-60) argue against the former possibility. Concentration of ethanol-benzene extractable lipid, a highly aliphatic compound, in the litterfall materials was highest at the 1700 m on both rock series (18-24% of litter mass, Kitayama et al., 2004). Plant lipids include waxes and resins that are found in various parts of plants (e.g., leaf and pollen surface coatings, tree bark) and these lipid-rich plant detritus presumably decay slowly, possibly giving longer residence time for OM-mineral association. Aliphaticity at the 1700-m samples was much more pronounced in the m-LF than in the f-LF (and in the O-horizon in the sedimentary series, Fig. 2.6), suggesting the possibility that the highly aliphatic plant detritus (possibly pollen and spores) entered the m-LF rapidly with short residence time in O-horizon or f-LF. We were unable to compare the abundance of pollen in m-LF across sites from the microscopic observation. Lower earthworm and termite abundance at the 1700-m sites (M. Ito, personal comm.) might also contribute to the formation and unique composition of the m-LFs.

While further investigation is clearly needed to substantiate the nature and fate of m-LF, significantly different composition of the m-LF at the 1700-m sites and preferential accumulation of pollen-like materials in the m-LFs at all sites implies that the current concept of decomposition sequence (litter → f-LF → m-LF → HF, Golchin et al., 1997; Braisden et al., 2002) may be improved by accounting for the variations in the chemistry, size, and residence time of plant detritus. It seems possible for some plant

detritus such as fine roots and pollen to rapidly pass though f-LF and accumulate in m-LF.

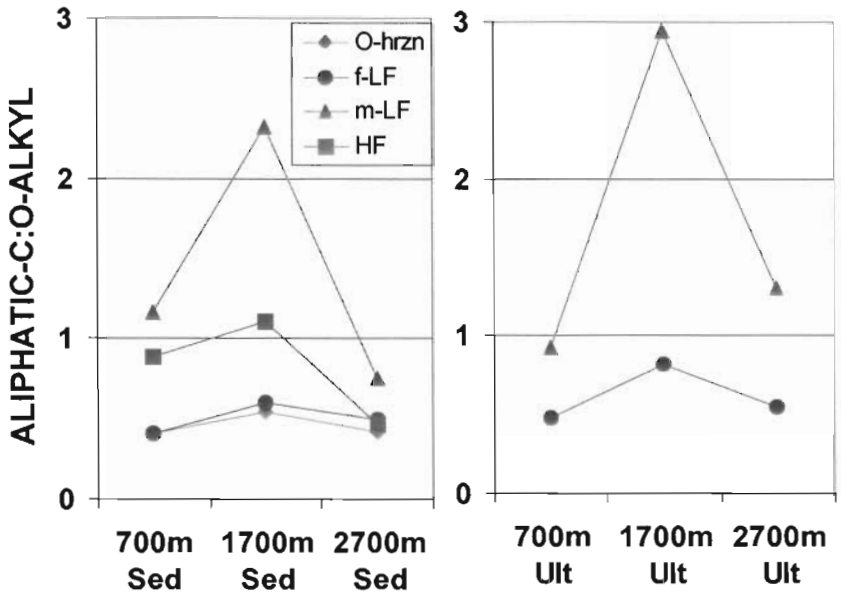

Figure 2.6: Aliphaticity (the ratio of aliphatic carbon to carbohydrate) in the density fractions and O-horizon for the sedimentary sites.

2.4.5. SOM standing stock

The sanding stock of OC in the top 10-cm soil was calculated including O-horizon material and the >4-mm POM fraction in the 0-10 cm of the A-horizon. The 0-10 cm A-horizon stock generally increased with altitude on both rock series (Fig. 2.7). Light-density fractions, particularly m-LF, responded to the climate gradient while HF remained relatively constant, supporting our hypothesis that the amount of OM in LFs increases than that in HF along a warm to cool climate graidnet. These results imply that temperature sensitivity of microbial OM decay was higher in LFs than in HF.

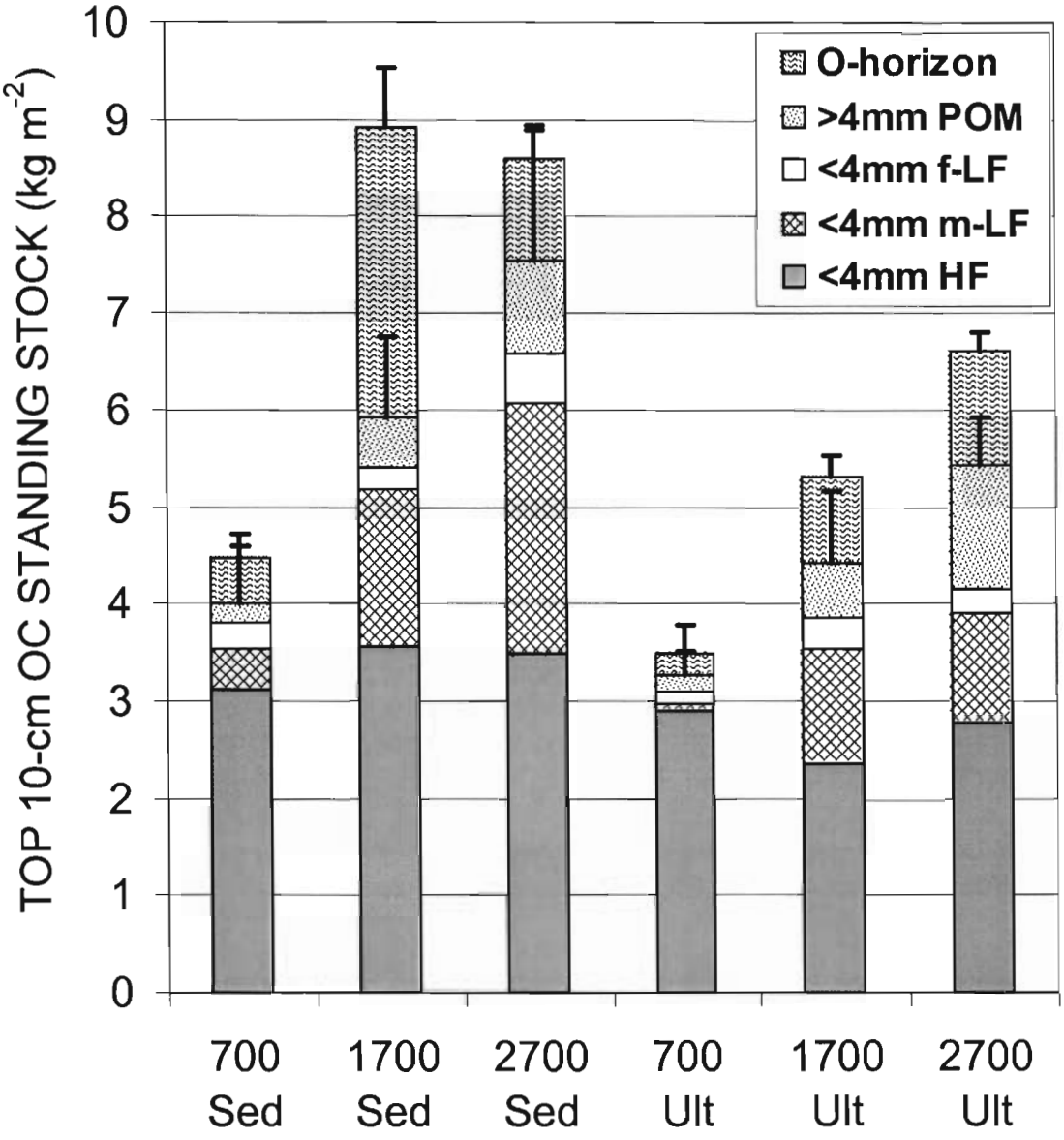

Figure 2.7: Standing stock of OC in 0-10cm A-horizon physical fractions and O-horizon. Upper error bars (standard error, n = 5) are for O-horizon and lower ones are for top 10-cm A-horizon consisting of the three density fractions and >4-mm plant detritus (POM).

While the m-LF had more consistent change in OC stock than f-LF along the climate gradient, the >4-mm POM fraction showed an even stronger response. This latter fraction was morphologically similar to the f-LF but was coarser in size. We assumed that the OC contents of the >4-mm POM fractions equal those of f-LF at each site. The altitudinal trend in the >4-mm POM fractions was largely dictated by their masses – a 13-fold increase from the 700 to 2700 m on both rock series. Due to the huge increase in their masses with altitude, the assumption of their OC contents likely had little impact on our data trends. Both m-LF and less mineral-associated plant detritus in the A-horizon (f-LF + the >4-mm POM fraction) showed similar responses to the climate gradient. These patterns suggest that the m-LF formation in our study sites was strongly influenced by the amount of plant detritus.

The OC stocks in the m-LF at the mid-altitude sites were generally in line with the altitudinal trends despite the fact that these samples were significantly more enriched with aliphatic C relative to N than the m-LF in the 700-m and 2700-m sites (Fig. 2.4 and Fig. 2.5). Thus, the abundance of plant detritus (O-horizon, >4-mm POM, and f-LF) and its fragmentation (high surface area-to-volume ratio) appear to be more important factors accounting for the greater OC stock in the m-LF under cooler climates in our study area. Longer residence time of plant detritus due to slower decay under cooler climates likely gives more opportunity to form m-LF.

These results imply that the operational cutoff size for soil (4-mm in this study, but more commonly 2-mm) could significantly change this partitioning. It is clearly important to account for all SOM fractions when assessing the changes in SOM stock in different forms (e.g., Fernandez et al., 1993).

The constant OC stock in the HF despite a 2-2.5 fold increase in its OC concentration (per mass of bulk soil, Fig. 2.3) resulted from lower bulk densities of soils at higher altitudes. Roughly a 2-fold decline in the bulk density with altitude had less impact on the OC stocks in LFs due to the much greater increase in their OC concentrations with altitude compared to HF. High OM concentration and earthworm activity (see Methods) likely contributed to the low bulk density of upper altitude soils. Thus, the relatively constant OC stock does not indicate that OC storage in HF was independent of climatic control. Instead, the HF under cooler climates held a higher concentration of OM (on mass basis, Table 2.3) within more porous soil structure compared to the HF under the warmer climates.

While the climate showed primary control on the OC stored in the top 10-cm A-horizons on both rock types, the sedimentary soils apparently stored greater OC than the ultrabasic soils at any given altitude. Aboveground net primary productivity (ANPP), estimated as the sum of woody increment and litterfall, was comparable between soil types at 700 m and 2700 m (Table 2.1), but the sedimentary ecosystem had higher ANPP, particularly wood production, at 1700 m (Kitayama and Aiba, 2002). Thus the greater SOM storage in the sedimentary site at the 1700 m, particularly in the O-horizon, might result from the higher input. This site also showed the least abundance of earthworms and termites of all six sites (M. Ito, personal comm.). Significantly higher OC stock in the O-horizon at this site, departing from the altitudinal patterns of other plant detritus fractions (Fig. 6), is consistent with the idea that ecosystem engineers (earthworm and termite) promote the fragmentation and decomposition of plant detritus (e.g., Gonzalez and Seastedt, 2001). At the 700-m altitude, greater fractions of the ANPP were invested in

wood production in the sedimentary forest ecosystem (Kitayama and Aiba, 2002). To the extent that woody materials decompose more slowly than leaf litter, greater woody input may account for the greater OC stocks of plant detritus in the sedimentary soils.

The sedimentary soils also appeared to store more OC in the m-LF than ultrabasic soils at the 700 and 2700-m sites, and possibly at the 1700-m site (Fig. 2.7). Soil mineralogical difference between the two rock types might account for the different OC stocks in the m-LF. Phyllosilicate minerals (kaolinite and illite) dominated the <2 μm fraction in the sedimentary soils while iron oxides and some phyllosilicates were found in the ultrabasic soils (Wagai et al., in prep). Phyllosilicates are platy, have high surface area-to-volume ratios, and thus might be more effective at physically protecting plant detritus than the iron oxides that are generally smaller and rounder. We did not find studies on the mineralogy control on the m-LF formation, but the abundance of clay-size minerals appeared to increase the OC concentration in m-LF per total soil mass (Kölbl and Kögel-Knabner, 2004).

Do other factors account for the greater OC stocks in the m-LF at the sedimentary soils? OM input as litterfall (Table 2.1) as well as the OM composition (Fig. 2.4-2.6) were similar between the two rock types at the 700 and 2700-m sites. Therefore, the amount of initial materials (plant detritus) and their bulk composition are not likely to explain the higher OC stock in m-LF at the sedimentary sites. While the differences in soil fauna/microflora communities between the two rock types may also affect the m-LF formation, the mineralogical difference appeared to be a plausible explanation for the observed difference in the OC stock in m-LF between the rock types. The same

mineralogical factor might also affect the higher OC stocks in HF at the 1700 and 2700-m sedimentary sites.

2.5. Concluding remarks

Strong influences of both climatic and mineralogical factors on SOM storage and dynamics are well known, but to their interactive effect is not well understood. At the regional scale, soil OC stock was not related to MAT but texture across forest soils in the Pacific Northwest U.S. (Homann et al., 1995). In the Great Plains grasslands, on the other hand, soil OC stock increased with precipitation and texture and decreased with MAT (Jenny, 1941). Among cooler end-members of these soils, however, soil OC concentration was not correlated with texture but only with precipitation (Sims and Nielsen, 1986). In our study sites, field observation and soil mineral surface analysis (Chapter 3) suggest that textures in the sedimentary soils are not finer than that in the ultrabasic soils at each altitude despite the higher standing stock of the former soils especially at higher altitudes. Therefore, commonly-found textural controls on SOM storage may not be applicable to the soils formed under cooler climates because the shift in the partitioning of SOM towards LFs would result in high accumulation of OM having little association with mineral grains.

In our study sites, we conclude that climate exerted a stronger control on the SOM storage at the top 10-cm soil and its partitioning pattern into density fractions than parent rock. The difference in the OC storage, composition, and turnover times among the density fractions found in current and previous studies (Golchin et al., 1997; Braisden et al., 2002) indicates the potential applicability of the density fractions to develop a more

mechanistic simulation model (e.g., Christensen, 1996). Our results imply that the responses of the density fractions to temperature are significantly different, particularly between LFs and HF. Therefore, the assumption that all SOM pools similarly respond to temperature used in current simulation models requires modification (Burke et al., 2003) if the density fractions are to be matched with "conceptual" pools in the current models.

Our results indicate the quantitative importance of m-LF for soil OC and N storage under cooler climates and that of HF under warmer climates. Yet the nature and fate of m-LF materials remains unclear. Further investigation on the factors controlling the f-LF vs. m-LF partitioning will be useful to improve new mechanism-based, conceptual models of SOM dynamics (Golchin et al., 1997; Braisden et al., 2002).

Our conclusion may not be applicable to other soils. The studied area had little seasonality. SOM storage under a tropical temperature regime may be significantly different from that under a non-tropical regime even when MAT is similar (e.g., Buol et al., 1990). Soils under different vegetation and human influence (e.g., grassland and tilled soils) may also have different responses to climatic and lithological factors.

Chapter 3 - Climate and parent material controls on soil surface-organic matter relationship in undisturbed forest soils

3.1. Abstract

The interactions of organic matter (OM) with minerals appear to control soil OM preservation. Sorption studies have shown that OM sorbed on limited sections of mineral surfaces such as edges of clays and very small pores. Little is known, however, on how OM associates with minerals at the OM loading greater than the level attributable to sorptive preservation. We hypothesized that, with increasing OM loading, OM accumulates as particles that incidentally encapsulate fine mineral grains (encapsulation mode), rather than accumulating via sorption onto all mineral surfaces (paint mode). These possible modes of organo-mineral arrangements were distinguished by the combination of two previously developed surface-derived variables: (1) fractional organic coverage of untreated soil surfaces ($\%ORG_{untreated}$) and (2) fractional organic occlusion of mineral surfaces ($\%SFA_{occluded}$). Materials with high $\%ORG_{untreated}$ with low $\%SFA_{occluded}$ imply paint mode, while low $\%ORG_{untreated}$ with high $\%SFA_{occluded}$ imply a partial encapsulation mode where some mineral particles are organically occluded but other grains are naked. We tested this approach using a series of tropical forest soils on two rock types (sedimentary and ultrabasic igneous) along an altitudinal gradient (700-2700 m above sea level) where total OM concentrations in the surface mineral horizon progressively increased from 4% to 30%. The ratios of organic carbon to mineral surface area increased from 0.6-3.1 mg m^{-2}, $\%ORG_{untreated}$ from <5% to 100%, and $\%SFA_{occluded}$ from 20 to 75% with increasing altitude on the sedimentary series. While high iron

contents limit our inferences, a similar altitudinal pattern appeared in the ultrabasic series. These altitudinal changes, with low $\%ORG_{untreated}$ and high $\%SFA_{occluded}$ in soils at intermediate OM loadings, supported our hypothesis and implied a strong control of OM loading on the organo-mineral arrangement. Similar OM loading control on the arrangement was found in soils from other geographic and climatic regions (n = 33, including spodic horizons), suggesting global applicability of these relationships.

3.2. Introduction

The organic and mineral constituents that make up soil vary in chemistry, size, and shape. As the concentration of organic matter (OM) in soil increases, the association of these two constituents becomes an important determinant of the extent and chemistry of soil surfaces as well as the geometry of organo-mineral aggregates. The manner in which mineral constituents interact with OM likely affects surface-mediated processes (e.g., sorption, solute/colloid mobilization, and weathering) as well as OM preservation, a critical storage term in the global carbon cycle.

The correlations among OM concentration, fine-mineral abundance, and specific surface area (SFA) found in a wide range of soils and sediments imply an important role of mineral surfaces in OM protection (Mayer, 1994a,b; Keil et al. 1994; Ransom et al. 1998; Kahle et al. 2002). Significant liberation of SFA upon oxidation of OM frequently observed in surface soils (Burford et al. 1964; Kaiser and Guggenberger, 2003) indicates the intimate association of OM with at least some of the mineral surfaces. Sorption of dissolved OM on mineral surfaces has been regarded as an important mechanism of mineral control of soil OM preservation (e.g., Sollins et al., 1996; Baldock and Skjemstad, 2000). Laboratory sorption studies have shown a range of sorptive capacity

depending on mineralogy and surface chemistry – preferential sorption occurs on hydroxylated surfaces such as metal oxides and the edges (as oppose to siloxane planes) of phyllosilicate clays (Schulthess and Huang, 1991). The extent of sorption to account for the OM preservation in field is, however, unclear. In a range of temperate soils and continental shelf sediments, minor fractions of mineral surfaces were organically covered, implying limited sorptive preservation of soil and sedimentary OM. (Mayer, 1999; Mayer and Xing, 2001).

The majority of mineral SFA in many soils and sediments is associated with small mesopores (2- 8 nm, Mayer, 1994a,b) which appear to originate from angled stacking arrangements among clay domains (micro-aggregates of individual clay crystallites, Mayer et al., 2004 and the literature therein). These inter-crystallite (inter-domain) mesopores are small enough to limit the accessibility of hydrolytic enzymes (Zimmerman et al. 2004). A range of soils and sediments, however, have been shown to contain only minor fractions of total OM in the small mesopores, implying that most OM locates external to these pores (Mayer et al. 2004). Why does OM correlate so well with mineral SFA and texture while the proposed mechanisms (sorption, small mesopore) unlikely account for the OM protection? Information on the geometric arrangement of OM with respect to mineral surfaces would help to answer this question.

At low OM concentrations, most mineral surfaces are unlikely affected by OM although the most reactive sites might be. At higher OM concentrations, OM might accumulate via sorption onto all mineral surfaces (essentially "painting"), as particles that don't strongly interact with minerals (e.g., fragmented plant detritus), or as OM that only

incidentally encapsulates minerals (e.g., mucus secretion or growth of amorphous humic material).

How can we test among these possibilities? Gas sorption has been used to assess averaged degrees of OM association with fine mineral particle surfaces (e.g., Feller et al. 1992; Mayer and Xing, 2001). We consider here two variables derived from this approach.

(1) Relative proportion of the fraction of exposed surface area of untreated soil ($SFA_{untreated}$) that is organic ($\%ORG_{untreated}$) can be estimated from a previously developed model using the energetics of N_2 gas adsorption onto solids (Mayer 1999). The model is based on the different enthalpies of gas adsorption onto organic vs. mineral surfaces. The enthalpy term is expressed in the Brunauer-Emmett-Teller (BET) equation (Brunauer et al., 1938) as the so-called C-constant, which ranges from 10-30 for various organic surfaces, to 80-120 for mineral surfaces in the absence of micropores (Mayer, 1999). Thus, a low C-constant is indicative of organic dominance of $SFA_{untreated}$.

(2) The association of OM with mineral surfaces can significantly reduce the SFA of whole soil as is evident from surface area increases upon OM removal and decreases upon sorption of dissolved OM (e.g., Kaiser and Guggenberger, 2003). The fraction of the mineral surfaces that were not accessible to N_2 gas in an untreated sample due to the organic occlusion of mineral particles ($\%SFA_{occluded}$) can be estimated based on the liberation of total mineral surface area ($SFA_{mineral}$) upon OM removal (Mayer and Xing, 2001).

These two variables allow us to distinguish four modes of organo-mineral assemblage and the trajectories that might connect them in a gradient of OM loading.

Here we illustrate four assemblage modes with the same mineral components, differing only in the amount and manner of OM loading (Fig. 3.1).

(I) Dot mode is defined by low $\%ORG_{untreated}$ and low $\%SFA_{occluded}$, and would result from patchy adsorption of dissolved OM, or attachments of organic particles/colloids onto mineral particles.

(II) Paint mode is defined by high $\%ORG_{untreated}$ and low $\%SFA_{occluded}$, and would be expected if monolayer coverage of mineral surfaces occurs (e.g., dissolved OM adsorption onto all mineral surfaces).

(III) Partial encapsulation mode is defined by low $\%ORG_{untreated}$ and high $\%SFA_{occluded}$. In this mode, much of the mineral surfaces are covered by low-SFA organic material, allowing the remaining naked minerals to make up most of measurable surface area.

(VI) Full encapsulation mode is defined by high $\%ORG_{untreated}$ and high $\%SFA_{occluded}$. This mode is expected where all the fine mineral grains are embedded in an amorphous organic matrix.

The OC concentrations in both volume and mass basis likely increase in the order: I < II < III < IV. $\%ORG_{untreated}$ and high $\%SFA_{occluded}$ are independent measurements, yet inter-related. For instance, a mineral sample without any OM must always have zero $\%SFA_{occluded}$ and zero $\%ORG_{untreated}$, and a highly organic sample in the full encapsulation mode must have 100 $\%SFA_{occluded}$ and 100 $\%ORG_{untreated}$ as all the surfaces accessible to gas sorption are organic.

Along a full gradient of soil OM loading, starting and end points presumably correspond to the dot and full-encapsulation modes. The trajectory between these two

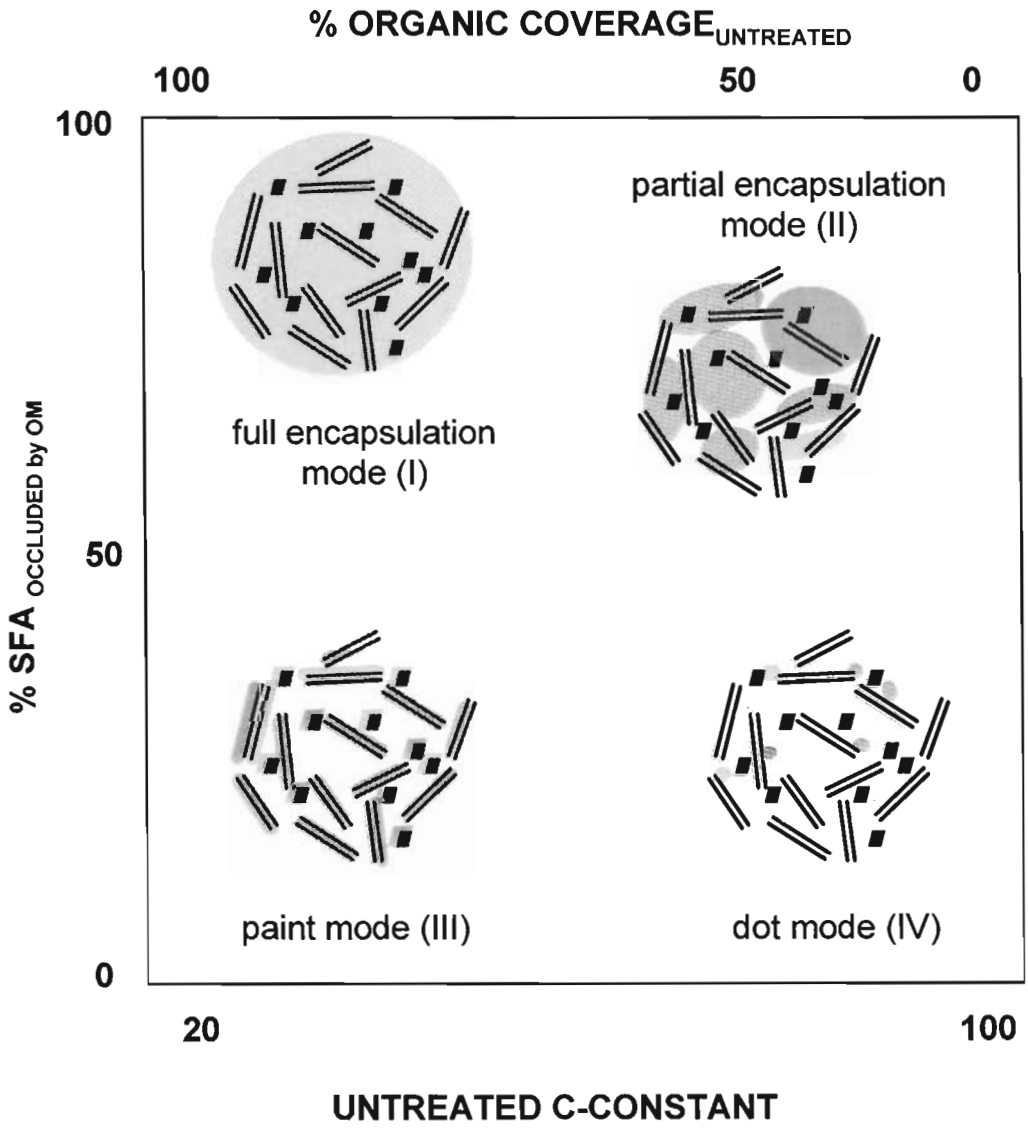

Figure 3.1: Four conceptual models of organo-mineral assemblage. Lines and rectangles represent mineral particles, and orange-colored spheres represent OM. Minerals and OM shown here don't reflect actual relative sizes. Note that mode (II) has slightly lower $\%SFA_{occluded}$ than mode (I), and lower untreated C-constant value than mode (IV)..

points is, however, more difficult to predict. Thus we developed two simple mathematical models of contrasting OM-mineral association mechanisms to assess the possible trajectories (Fig. 3.2).

The occlusion model assumes polymerization of added organic compounds (i.e. stronger OM-OM attraction than between OM and mineral surface) and subsequent occlusion of mineral particles as a function of the volume of OM (V_{OM}). Specifically, we assumed that the fraction of mineral surface occlusion is a function of [V_{OM} / (V_{OM} + $V_{pore\ space}$)], where $V_{pore\ space}$ is the total volume of pore in the bulk soil. In other words, OM is presumed to encapsulate minerals with a probability equivalent to the volume fraction of OM. Mineral and OM densities were assumed to be 2.6 and 1.4 g cm^{-3} (Mayer et al. 2004), respectively. Bulk density of the whole sample was set to decrease from 1.0 to 0.4 g cm^{-3} with the increase in OM content of the sample, and the total pore volume was calculated from the bulk density. The painting model assumes preferential adsorption of added OM to mineral surfaces. Adipic acid was used because the organic coverage of this adsorbate onto mineral surfaces has been established by experimentation (Mayer, 1999). In both models, hypothetical uniform clayey and sandy soils with $SFA_{mineral}$ of 100 and 10 m^2 g^{-1}, respectively, were considered, and C-constant values of samples were assumed to decline as an exponential function of the organic coverage of the samples (see Fig. 4 in Mayer, 1999).

These two models predict two contrasting trajectories (Fig. 3.2). In reality, fine-sized minerals are perhaps more preferentially occluded. Modification of the occlusion model allowing the preferential occlusion of finer particles (assuming that the sample contains both clay- and sand-sized particles) only slightly shifted the curve towards

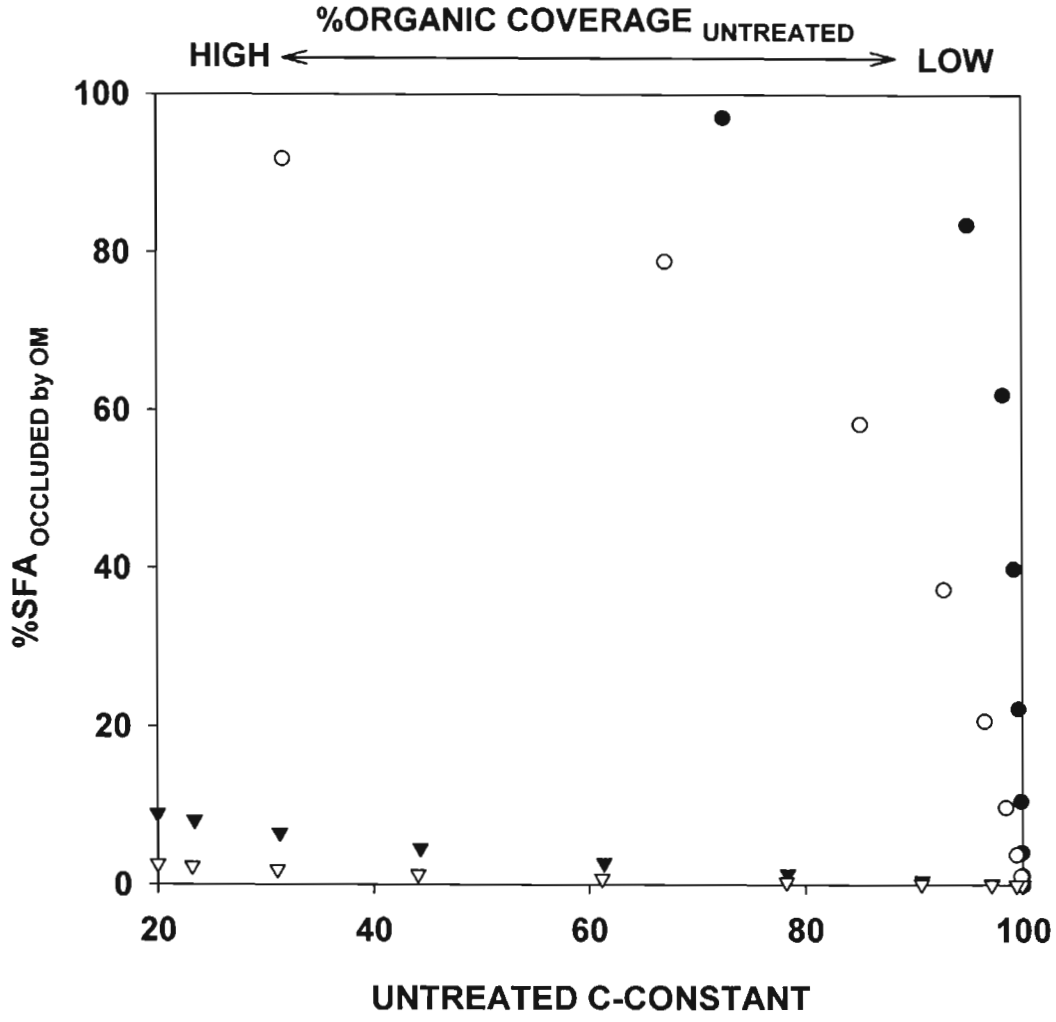

Figure 3.2: Trajectories of OM concentration gradients predicted by the occlusion model (circle) and painting mode (triangle) for two hypothetical samples with contrasting SFA, mineral SFA of 100 m^2 g^{-1} (closed) and 10 m^2 g^{-1} (open). The highest OM concentration for each trajectory is 1.6% for low SFA painting model, 5% for the high SFA painting model, and 58% for both occlusion models. Ten data points on each trajectory represents 10% increments from zero to maximal OC concentrations.

center. While the organo-mineral interactions of natural samples were significantly simplified, these two end-member trajectories shown in this model exercise provide a basis to assess the changes in the organo-mineral arrangements along OM concentration gradients with respect to potential mechanisms of organo-mineral association.

We tested this approach using a series of undisturbed humid tropical forest soils on an altitudinal gradient which has been shown to increase soil OM concentration. The altitude range of 700-2700m above sea level provided a climate gradient with mean annual air temperature progression from 24 to 12 ^{o}C, which serves as a surrogate latitudinal gradient. We tested the hypothesis that, with increasing altitude, organo-mineral assemblage transforms from the dot to partial-encapsulation to full-encapsulation modes, without transitioning through the paint mode because OM affinity to aluminosilicate clays is largely restricted to hydroxylated edges (Schulthess and Huang, 1991). Thus the organic coating of all clay surfaces seems unlikely except at very high OM loading. In other words, this hypothesis predicts a trajectory closer to the occlusion model than the painting one (Fig. 3.2). Two sets of soils developed from contrasting parent rocks (acidic sedimentary and ultrabasic igneous) along the altitudinal gradient were used for this test. A companion study (Chapter 2) assessed the climate and parent material controls on soil OM storage and partitioning into physical fractions using the same set of study sites.

3.3. Materials & Methods

3.3.1. Study area

We studied soils on the eastern and southern slopes of Mt. Kinabalu (4095 m, 6°05'N, 160°33' E), developed on both acidic sedimentary and ultrabasic igneous parent materials, under the primary rain forests protected as the Kinabalu Park. The six selected sites (at ca. 700, 1700, and 2700 m above sea level on the two rock types) are part of a long-term ecological study (e.g., Kitayama, 1992; Aiba and Kitayama, 1999; Kitayama and Aiba, 2002). The climate is humid tropical with weak influences of the Asiatic monsoon. A strong temperature gradient is present along the slope (Table 3.1): mean annual air temperature (MAT) decreases with altitude at a mean lapse rate of 0.0055 °C m^{-1}, with <2 °C intra-annual variations (Kitayama, 1992). Mean annual rainfall is relatively constant (2300-2400 mm yr^{-1}) with altitude, although inter-annual variation can be large (e.g., 1800-3300 mm yr^{-1} during 1996-1999, Kitayama and Aiba, 2002). Air and soil moisture generally increase with altitude due to cooling and more frequent cloud cover at upper altitudes. Under the humid tropical regime, however, MAT exerts strong control on the forest structure and net primary productivity while rainfall or moisture appear to have little control (Kitayama and Aiba, 2002).

The sedimentary rocks in the study area (Trusmadi formation) include Eocene argillite, slates, siltstones, and sandstones (Jacobson, 1970). The ultrabasic igneous rocks consist mostly of peridotite, with various degrees of serpentinization, characterized by high concentrations of MgO, FeO, and heavy metals (Jacobson, 1970). Soil pH of surface mineral horizons was roughly one pH unit higher on the untrabasic rock than on sedimentary rock at each altitude, reflecting the contrasting chemistry and reactivity of

Table 3.1: Climate and soil characteristics of Mt. Kinabalu study sites. S.E. is standard error with five replicates.

		Sedimentary rock series			Ultrabasic rock series		
		elevation (m)					
		700	1700	2700	700	1700	2700
Actual elevation of each site (m)		650	1560	2590	700	1860	2700
Mean annual air temperature (°C) #		23.8	18.8	13.1	23.3	16.9	12.3
Mean annural rainfall (mm)*		2392	2380	2256	2392	2380	2256
pH in deionized water	Mean	3.88	4.13	3.86	4.83	5.45	4.87
	S.E.	0.10	0.11	0.13	0.11	0.10	0.15
pH in $CaCl_2$	Mean	3.48	3.36	3.09	4.01	4.59	4.19
	S.E.	0.03	0.06	0.05	0.09	0.25	0.20
soil OC in A-horizon (%)	Mean	2.98	4.91	14.22	3.03	6.21	8.30
	S.E.	0.43	0.70	1.83	0.28	0.81	0.77
soil N in A-horizon (%)	Mean	0.25	0.28	0.70	0.21	0.31	0.49
	S.E.	0.03	0.05	0.09	0.02	0.04	0.05
soil C:N	Mean	11.7	18.1	20.3	14.8	20.0	16.9
	S.E.	0.4	0.7	0.7	0.8	0.7	0.2
Dithionite-extractable Fe	Mean	33	13	6.2	492	73	48
(mg FeOOH g^{-1} soil)	S.E.#	5.1	5.4	2.3	10	23	2.6
Mineralogy of < 2 μm fraction **		Kaolinite (Gibbsite)	Kaolinite Illite Quartz	Kaolinite Illite	Hematite Goethite	Chlorite Goethite Talc	Chlorite Goethite Illite?
Soil suborder ‡		humic	tropical	tropical	peric	tropical	tropical
Soil order ‡		Ultisol	Alfisol (Incept/Spod)	Inceptisol	Oxisol	Alfisol	Inceptisol

based on the weather station at 2700m and the lapse rate of 0.0055 °C per meter.

* from the weather station at each elevation

** Settling of soil particles was calculated assuming the mineral density of 2.6 g/cc for all sites. Iron rich soils, 700m Ult in particular, contain heavier particles. Thus the isolated materials are likely smaller.

‡ tentative classification of soils at each site according to US Taxonomy (Soil survey staff, 1999)

the two parent materials (Table 3.1). Parent rock above 3000 m is largely granite. All soils were sampled on gentle slope positions (<27°) under closed canopy. Colluvial deposition of the ultrabasic minerals on the sedimentary rock sites appears minimal as a preliminary elemental analysis of surface soils from the sedimentary sites showed little cobalt and nickel indicative of ultrabasic materials (data not shown). Deposition of sedimentary rock onto the sites underlain by the ultrabasic rocks was difficult to assess due to no strong indicator elements.

The margin of former glaciers in the area is unclear. Areas above 1700 m were likely either glaciated or received peri-glacial deposits, whereas the 700-m altitude had no evidence of glacial influence (Jacobson, 1970). Thus the 700-m soils presumably experienced longer weathering due to their older soil surface age compared to the 1700 and 2700-m sites where pedogenesis likely re-started after glaciations. Highly weathered soil characteristics such as heavy texture, red hue, and deep solumn (field observation) as well as advanced clay mineralogy (Table 3.1) found at the 700-m soils, therefore, likely reflect the longer soil development time as well as faster chemical weathering under higher MAT compared to the upper sites. Nevertheless, the interactions of OM and mineral particles in surface mineral soils have likely reached a quasi steady-state at all of our studied sites after the last glaciation because soil OM accretion, as well as A-horizon formation (and hence organo-mineral associations therein), significantly slow down after the initial several centuries of pedogenesis on non-volcanic rocks (Birkeland, 1999; Schlesinger, 1990). Altitudinal gradients on mountain slopes have been used to study climate controls on soil texture-OM relationships and OM dynamics (Harradine and Jenny, 1958; Trumbore et al., 1996).

3.3.2. Soil sampling and handling

After the initial soil survey, five soil samples were collected from 2-20 meters apart, to account for heterogeneity, adjacent to the permanent vegetation plots at the six sites. Surface mineral horizon samples (0-10 cm) were 4-mm sieved and subsets were analyzed for soil pH in deionized water and 0.01N calcium chloride at a soil:solution ratio of 1:5 (g:mL) after 0.5-1.0 hr equilibration. The remaining sieved soils were freeze-dried and kept frozen until analysis. Soil depth profile samples were 2-mm sieved and freeze-dried in the same way.

To expand the breadth of our study of OM-mineral surface relationships, we compiled 9 temperate soils (Alfisols, Mollisols, and Ultisols), 10 A/E-horizons and 16 B-horizons of acid soils (Inceptisols and Spodosols) from the USA, and 1 forested Oxisol from Puerto Rico were also examined. These samples were all 2-mm sieved and freeze-dried or air-dried. The acid soil samples are from Mayer and Xing (2001), and most other samples are from Mayer et al (2004) and Wagai and Mayer (submitted), except for two samples. Those are a cultivated, udic Alfisol from Indiana (0-23cm) and an orchiric Ultisol from Maryland (0-13cm), obtained from a soil archive (USDA, Soil Survey Center, Nebraska).

3.3.3. Soil surface related characterizations

The gas sorption technique (Mayer, 1999) was used to measure the specific surface areas (SFA) of untreated and OM-removed samples, and to estimate the organic matter contribution to the mineral surfaces. Water molecules in samples can cause large

errors in the gas sorption analysis, yet the water-removal treatments may alter soil mineral phases and thus SFA. Thus we first conducted a pilot test of water-removal treatments (helium gas flow at room temperature vs. 150 °C heating under vacuum) for eight samples along the altitudinal gradient using a Quantachrome Monosorb (Quantachrome Corp., Syosset, NY, USA). The samples with $SFA_{untreated}$ >10 m^2 g^{-1} had minor changes in SFA of outgassing temperature (-6 to +17%, n = 4), while those with $SFA_{untreated}$ <10 m^2 g^{-1} had greater change (-41 to +54%, n = 4). Because of no systematic change between the treatments and better reproducibility, we adapted the heating treatment. Five freeze-dried, surface-horizon samples from each site and selected deeper horizon samples were outgassed under vacuum at 150 °C. Gas sorption analysis was conducted using a Quantachrome A-1 Autosorb under a series of N_2 pressures. Surface area values were calculated using the Brunauer-Emmett-Teller (BET) equation (Brunauer et al. 1938), using sorption data at partial pressures of < 0.3. One representative surface sample from each site was also subjected to the gas sorption analysis at higher partial pressure (0.3-1.0) to estimate pore size distribution (ca. 2-200 nm) using the BJH method (Barrett et al., 1951), assuming slit-like geometry for the pores (see Mayer, 1994b and Mayer et al., 2004). After gas sorption analyses, samples were quantitatively transferred to beakers and muffled at 350 °C overnight to remove their OM (discussed later). Upon cooling, the same outgassing and sorption analyses were performed on the muffled samples.

C-constants were estimated from regression analysis of BET plots (Mayer, 1999). Measured C-constants before and after OM removal were converted to enthalpy equivalents, which were used to estimate the fraction of unmuffled soils that is organic

($\%ORG_{untreated}$). This calculation is based on the coverage-enthalpy exponential relationship previously established from sorption experiments with model adsorbants and adsorbates (Mayer, 1999).

The fraction of the total mineral surface area that was not accessible to N_2 gas in the unmuffled soils, due to organic occlusion of the mineral surfaces, was calculated following Mayer and Xing (2001):

$$\%SFA_{occluded} = (SFA_{muffled} - SFA_{untreated}) / SFA_{muffled} \times 100$$

where $SFA_{untreated}$ and $SFA_{muffled}$ refer to the specific surface area of untreated and muffled soil, respectively.

3.3.4. OM removal for mineral surface area estimate

The surface area of mineral components cannot be measured accurately if a soil contains high amounts of amorphous mineral phases (e.g., less crystalline oxides) that are easily altered by OM removal treatments. Dry or wet heating of less-crystalline metal oxide phases results in lowering of SFA due to sintering of smaller pores and/or transformations of mineral phases (Sequi et al. 1983; Widler and Stanjek, 1998; Mayer and Xing, 2001; Kaiser and Guggenberger, 2003). Thus OM removal techniques must compromise between mineral alteration and incomplete OM removal. We used dry muffling at 350 °C overnight, which gave similar $SFA_{mineral}$ results compared to a commonly-used, wet oxidation treatment by hydrogen peroxide among river sediments (Keil et al. 1997). More recently, Kaiser and Guggenberger (2003) modified the sodium hypochlorite (NaOCl) technique of Lavkulich and Wiens (1970) to remove OM, reducing the alteration of less-crystalline iron and aluminum oxides.

Thus we conducted a pilot study using one representative surface soil from each site to compare the muffling and the modified NaOCl techniques, with respect to OM removal efficiency and $SFA_{OM\text{-}removed}$. Soil samples were mixed with 1M NaOCl (pH pre-adjusted to 8 ± 0.1) at a soil:solution ratio of 1:50 at 22-25 °C for 6 hrs. Then solutions were centrifuged at 40000 *g* for 45 min, and the supernatants discarded. The residues were subjected to the same treatment three more times. Frothing was minimal during the last NaOCl treatment. The final residues were rinsed with deionized water, freeze-dried, and analyzed for SFA as described above. The muffling showed significantly better efficiency of OM oxidation than the NaOCl treatment (Table 3.2). Previous study has also shown more complete OM removal by the muffling treatment.

Table 3.2: Comparison of two OM-removal pretreatments.

Elevation	OC in bulk	Efficiency of OM removal by		Intact soil SSA	SSA after NaOCl	SSA after muffling
		NaOCl	muffling			
(m)	(%)	---------- (%) ----------		---------- ($m^2 g^{-1}$) ----------		
Ultrabasic rock series						
700	2.99	79.5	99.1	57.5	55.9	103
1700	4.40	64.4	N.D	10.7	16.8	18.6
2700	9.39	64.8	N.D	6.6	13.4	27.3
Sedimentary rock series						
700	2.76	80.1	97.6	26.4	27.9	32.0
1700	2.24	78.2	N.D	7.3	6.6	10.9
2700	11.57	76.3	N.D	3.7	6.2	12.4

Consistently higher $SFA_{muffled}$ than SFA_{NaOCl} for all of the samples, despite possible reduction of $SFA_{muffled}$ by sintering, imply the presence of organically-occluded, fine mineral particles in the NaOCl residues. Minerals with high SFA (finer size or microporous minerals) tend to bind preferentially to OM (Kaiser and Guggenberger, 2003) and such organo-mineral associates are quite resistant to wet chemical treatment (Pichevin et al. 2004). Thus, we chose the muffling technique to remove OM. Thus $SFA_{muffled}$ was regarded as an approximation of the SFA of mineral components for the soils examined.

3.3.5. Other analyses

To quantify the OC associated with soil minerals, particulate OM (e.g., plant detritus) unassociated with soil minerals was removed from sub-samples by a density separation technique, following Golchin et al. (1994). Samples were mixed with 1.6 g cm^{-3} sodium polytungstate solution and treated with ultrasound (656 J mL^{-1}) using a Fisher-Artek-Dynatech Model 300 sonicator with 19-mm diameter tip after calorimetric calibration of the sonicator. Settled materials in the sodium polytungstate solution after the sonication were rinsed with deionized water and centrifuged repeatedly, and then freeze-dried. Total OC and N in dried bulk samples and density separates were analyzed using a Perkin-Elmer 2400 CHN analyzer (Perkin-Elmer, Norwalk, CT, USA). A pilot test showed the absence of carbonate in our soils.

Pedogenic iron oxide concentration was estimated for 2-4 surface soils from each site by a modified dithionite extraction method. This method eliminated the usual organic complexer and added an acid rinse treatment (Wagai and Mayer, submitted), and showed

similar iron dissolution efficiency as the conventional dithionite-citrate method across a range of mineral soils (98 ± 4%, mean ± SD). This dithionite extraction was performed twice for all of the ultrabasic soils and the 700-m sedimentary soils for total recovery of pedogenic iron oxides.

Mineralogy was determined for the clay-size fraction from a representative surface soil from each site. Clay-size fractions were isolated by the pipette method (Soil Survey Staff, 1996) after OM removal by hydrogen peroxide at 80 °C. The isolated clay fraction was oriented on glass slides as slurries, dried, and subjected to X-ray diffraction, on a Rigaku Miniflex X-ray diffractometer with CuKα radiation and variable slits.

3.4. Results

3.4.1. OM-surface area relationship

Specific surface area of minerals in the soils ($SFA_{muffled}$) was significantly higher at the lowest altitude than at higher altitudes on both rock types, consistent with the more weathered mineralogy (Table 3.3), and thus presumably more abundant fine minerals in the 700-m soils. The high $SFA_{muffled}$ and weathered mineralogy in these soils may reflect both longer weathering time (lack of glaciation) and warmer climate regime (see Method). Surface areas of unmuffled samples ($SFA_{untreated}$) were also higher at lower altitude sites, likely as a result of both higher $SFA_{muffled}$ and less coverage of mineral surfaces with OM (more discussion later).

Organic carbon (OC) and nitrogen (N) concentrations in the surface mineral soils generally increased with increasing altitude on both rock types (Table 3.1). From the low to high altitude, progressively greater proportions of total soil OM consisted of light-

Table 3.3: Soil surface-related characteristics.

		Sedimentary rock series			Ultrabasic rock series		
		Altitude (m)					
		700	1700	2700	700	1700	2700
Untreated soil surface area ($m^2 g^{-1}$)	Mean	25.5	9.3	4.7	59.6	16.8	7.9
	S.E.	2.4	2.4	0.9	3.0	1.4	1.1
Untreated soil C-constant	Mean	80.4	51.3	18.8	87.3	68.9	63.6
	S.E.	4.4	12.6	3.5	1.6	3.6	4.4
Mineral surface area ($m^2 g^{-1}$)	Mean	31.4	17.3	21.6	96.7	29.6	24.3
	S.E.	2.4	4.3	2.9	6.7	2.8	1.5
Muffled C-constant	Mean	107.0	109.9	151.1	69.5	65.7	76.3
	S.E.	1.5	6.0	12.5	3.0	2.4	2.5
% mineral SFA occluded by OM	Mean	19	46	78	38	43	68
	S.E.	2.6	2.8	5.5	2.5	12.4	3.5

density fractions that were not strongly attached to soil minerals (Chapter 2). To better assess the OM-mineral surface relationships, we normalized OC in heavy-density fractions (OC_{HF}) to mineral surface area (OC_{HF}:$SFA_{muffled}$). This loading increased with increasing altitude (decreasing temperature) with a similar slope on both rock types (Fig. 3.3). Similar response of soil OM to an altitudinal gradient has been reported from forest soils in the Sierra Nevada mountains where total soil N concentration was normalized by a texture index (Harradine and Jenny, 1958). Higher OC_{HF} loadings in the sedimentary soils than in ultrabasic soils under comparable MAT (Fig. 3.3) imply a parent rock control on the OM-SFA relationship.

While climate exerted primary control on the OC_{HF} loading (7-10 fold change) among the studied soils, parent material and soil pH appeared to explain some variations in the OC_{HF} loading within certain sites and altitudes. The OC_{HF} loading correlated negatively with soil pH (in water) among the 700-m ultrabasic soils ($p = 0.003$), across the 700-m soils ($p = 0.001$) and across the 1700-m soils ($p = 0.05$, Fig. 3.4a,b). Similarly,

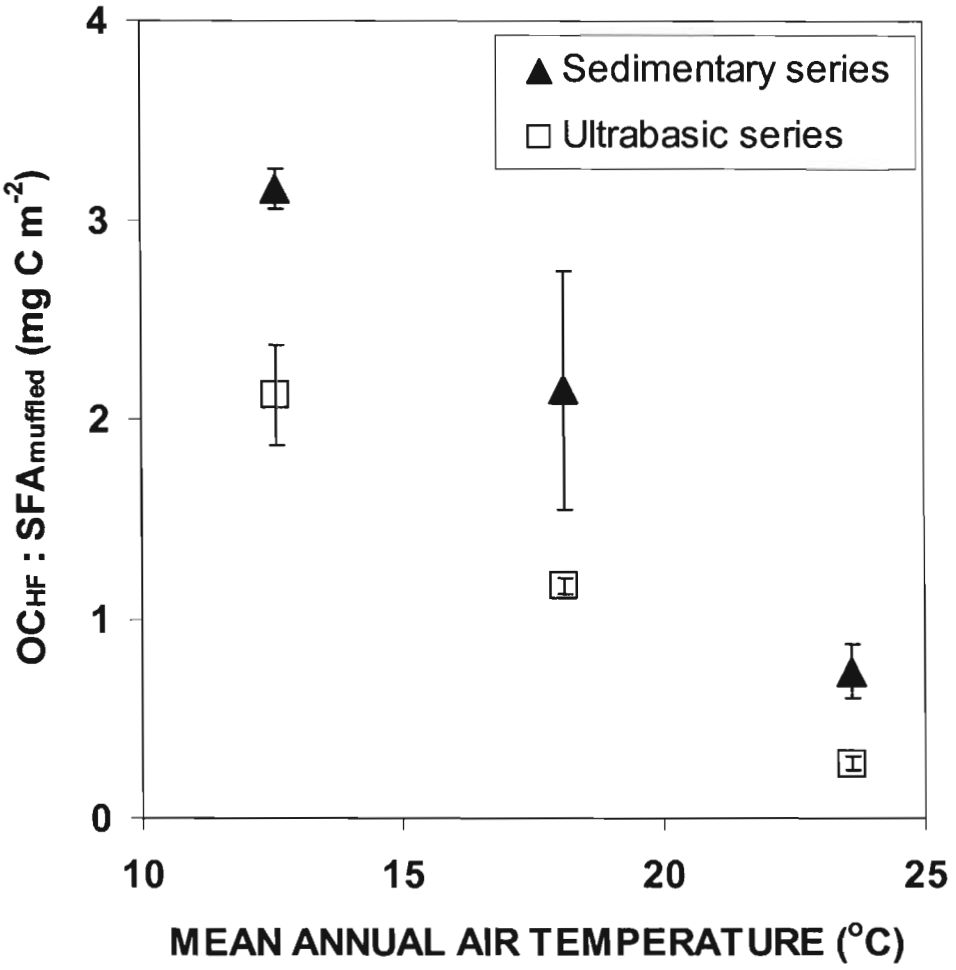

Figure 3.3: Heavy-fraction OC loading normalized by muffled SFA vs. estimated mean annual temperature. Error bar represents standard deviation (n=5).

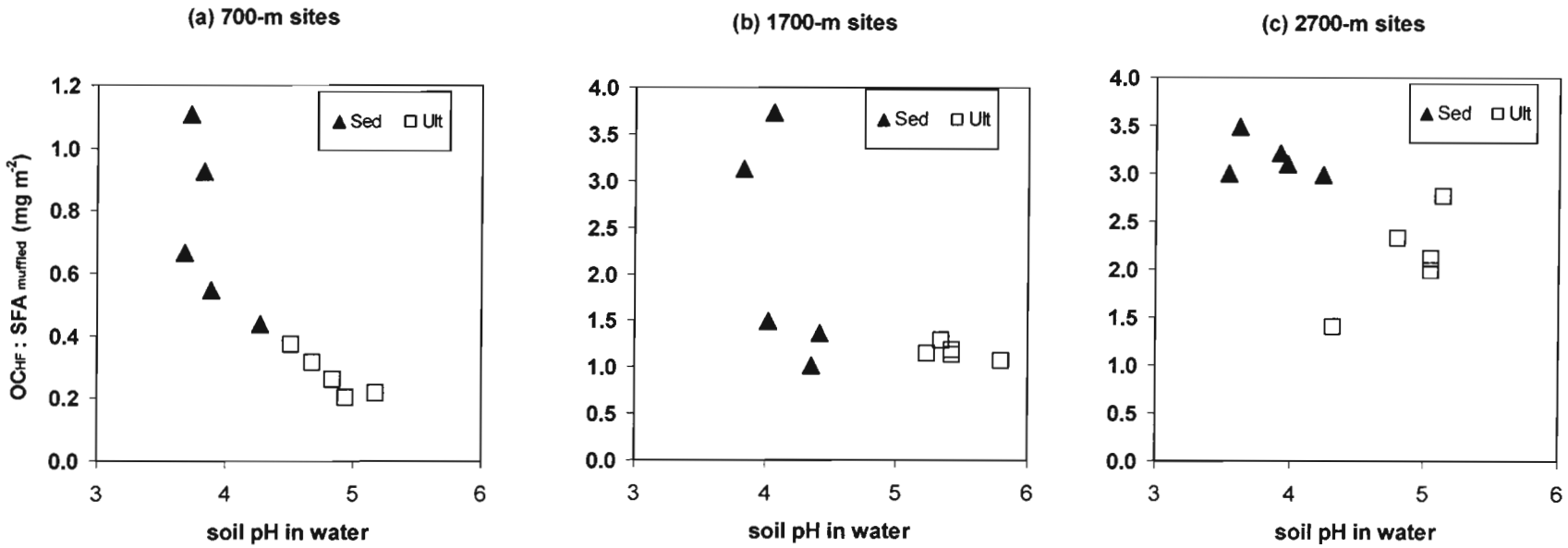

Figure 3.4: Heavy-fraction OC loading (OCHF :SSAmuffled) with respect to soil pH in deionized water for the 700-m sites (a), 1700-m sites (b), and 2700-m sites (c).

among cool temperate acidic soils, SFA-normalized OC_{bulk} loading was negatively correlated with the soil pH (Mayer and Xing, 2001). The observed pH-OC loading patterns may suggest that lower pH promotes OM sorption (e.g., Jardine et al. 1989), coagulation of humic substances (Myneni et al. 1999) or retardation of microbial decay process (Motavalli et al. 1995), resulting in greater OM accumulation relative to $SFA_{muffled}$. Low soil pH also enhances the extent of positively-charged surfaces of both organic and mineral components, and the concentration of multivalent metal cations in soil solution, which may facilitate organo-metal complexation/precipitation onto soil surfaces (e.g., Wagai and Mayer, submitted). In contrast with the 700-1700 m soils, no correlation was found between the narrower range of OC_{HF} loadings and pH across the 2700-m sites (Fig. 3.4c). Furthermore, the OC_{HF} loading was positively correlated with soil pH within the 2700-m ultrabasic soils ($p = 0.05$). Nevertheless, soil pH control on the OC_{HF}:$SFA_{muffled}$ relationship was minor compared to the altitudinal control (Fig. 3.3).

3.4.2. Organic coverage and occlusion of soil surfaces

The C-constants of untreated samples decreased with increasing altitude on both rock series (Fig. 3.5), suggesting that greater fractions of $SFA_{untreated}$ were organic under progressively cooler climate regimes. The sedimentary soils showed a stronger and more linear response to MAT than ultrabasic soils, suggesting a parent rock effect on the organic coverage of soil surfaces. Consistent with the increasing trend in the organic coverage of unmuffled samples, greater fractions of mineral surface were occluded by OM at higher altitude (Fig. 3.6). The observed increase in $\%SFA_{occluded}$ with increasing

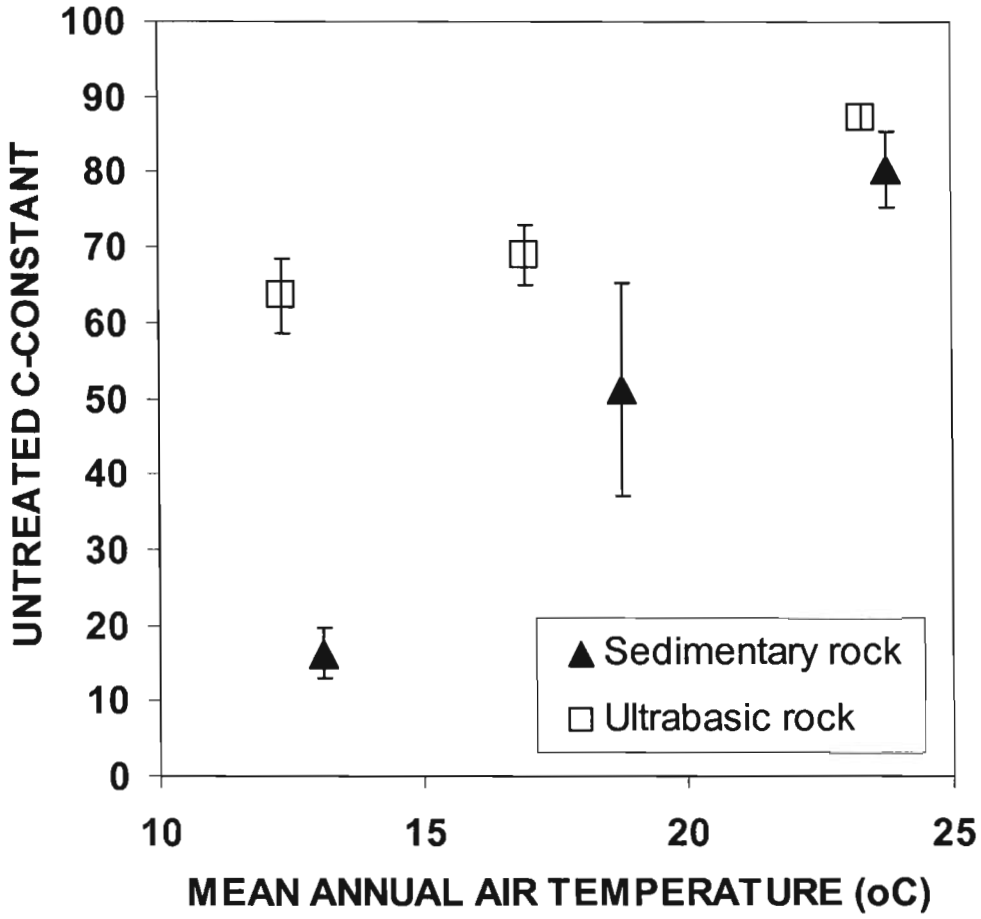

Figure 3.5: The C-constant of untreated soil samples vs. estimated mean annual air temperature for both parent rock series. Error bars represent standard deviation (n = 5).

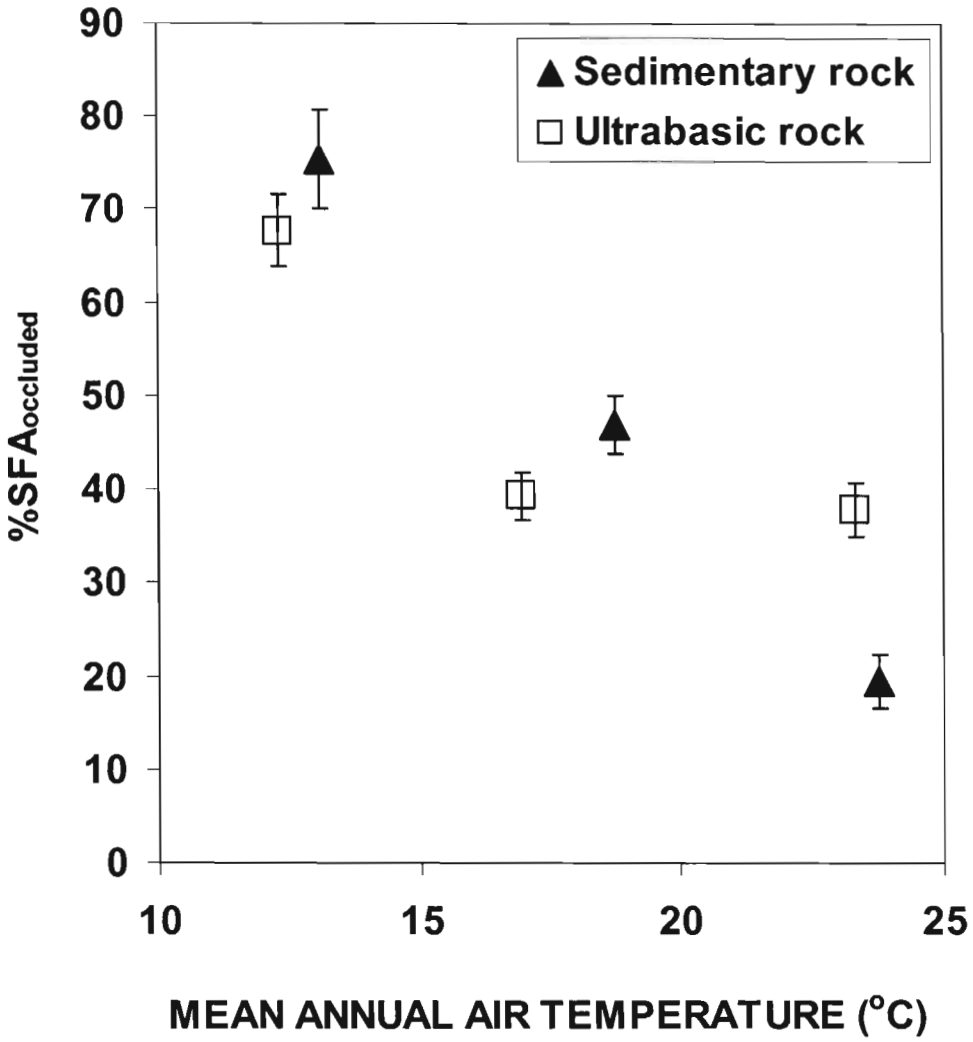

Figure 3.6: The percentage of the mineral surface area that was occluded by OM vs. estimated mean annual air temperature for both parent rock series. Error bar represents standard deviation (n = 5).

altitude (thus soil OM concentration) implies that OM association with soil mineral constituents significantly decreased the total surface area of organo-mineral aggregates (i.e. $SFA_{untreated}$). This SFA drop is presumably due to very low SFA (<1 m^2 g^{-1}) of soil OM (Chiou, 1990) and is consistent with the observations that soil SFA increases upon OM removal and decreases upon sorption of natural dissolved OM (Kaiser and Guggenberger, 2003 and the citations therein).

For the sedimentary soils consisting mainly of aluminosilicates, we estimated the fractional organic coverage of untreated samples ($\%ORG_{untreated}$) based on the increase in the C-constant from untreated to muffled samples (Table 3.3). $\%ORG_{untreated}$ exponentially increased from a few percent to essentially 100% with increasing altitude. Concomitantly, $\%SFA_{muffled}$ linearly increased from 13-26% to 60-90% along the altitudinal gradient (Fig. 3.6).

For the ultrabasic soils, alterations in iron oxide phases upon muffling treatment limited the applicability of our surface characterizations. Muffling treatment caused a drop in C-constant below the level of its unmuffled counterpart (Table 3.3) and thus the equation to estimate $\%ORG_{untreated}$ was not applicable. The reduction in C-constant upon muffling likely resulted from the transformation and sintering of metastable iron oxides whereby high-energy sites (e.g., micropores <2 nm) were reduced with the formation of more stable oxides (Weidler and Stanjek, 1998; Mayer and Xing, 2001). Muffling effect on SFA depends on the phases of iron oxides and temperature – dry heating at ca. 300 °C decreased the SFA of ferrihydrite by 40% while increased that of goethite by 120%, and 600 °C heating of the latter mineral dropped its SFA by 80% (Pritchard and Ormerod, 1976; Weidler and Stanjek, 1998).

Significantly higher $\%SFA_{occluded}$ of the ultrabasic soils than sedimentary soils under the highest MAT (Fig. 3.6) may be attributable to the abundance of very fine-sized minerals of the ultrabasic soils (Table 3.3). Hematite and goethite crystals can be as small as several nanometers (Schwertmann and Taylor, 1989). Finer particles (higher $SFA_{mineral}$) presumably have more sensitive response in $\%SFA_{occluded}$ to the changes in OM accretion (Fig. 3.3). Given the comparable OC_{HF} concentrations, the higher $\%SFA_{occluded}$ of ultrabasic soils at this altitude likely resulted from the contrasting mineralogy and $SFA_{mineral}$ between the two rock types. We cannot, however, rule out the possibility of overestimation of $SFA_{mineral}$ if muffling increased $SFA_{mineral}$, which would increase $\%SFA_{occluded}$ of ultrabasic soils. Proper determination of $SFA_{mineral}$ and $\%ORG_{untreated}$ for metal-oxide rich materials will require more development work.

There are, nevertheless, three lines of findings suggesting an increase in $\%ORG_{untreated}$ with increasing altitude in the ultrabasic series: (1) The untreated C-constants progressively increased up to 80-90 with increasing MAT (Fig. 3.5), values in the range for organic-free pure iron oxide phases (Kaiser and Guggenberger, 2003). Assuming that the C-constants of organic-free mineral components are comparable among all of the ultrabasic soils along the gradient, the pattern of the untreated C-constants are in line with the increase in $\%ORG_{untreated}$ with increasing altitude. (b) The untreated C-constants negatively correlated with OC concentration in the HF ($p = 0.03$, data not shown). Thus, the lower untreated C-constants and higher total OC concentrations at higher altitudes imply greater organic coverage (c) Laboratory sorption of increasing amounts of natural OM onto iron oxide phases caused progressive lowering of C-constants in a similar manner as those onto aluminosilicate clays (Kaiser and

Guggenberger, 2003), supporting the inference of the organic coverage from the C-constant measurements for non-aluminosilicate samples.

If we apply the entire range of reasonable C-constants of naked iron oxides (74-130) to the estimation for $\%ORG_{untreated}$ at the 700-m ultrabsic soils, the organic coverage was <6%. Thus, at the lowest altitude, $\%ORG_{untreated}$ of ultrabasic soils seem similar to those of the 700-m sedimentary soils. Clay-size minerals in these soils are mostly goethite and hematite (Table 3.3).

At lower MAT, the ultrabasic soils showed progressively higher untreated C-constants than their sedimentary counterparts (Fig. 3.5). Significantly higher C-constants in the 2700-m ultrabasic soils imply that more than minor fractions of the untreated soil surfaces were inorganic in contrast with the full organic coverage in the 2700-m sedimentary soils. The ultrabasic soils at the 2700 m contained seven-fold higher concentration of pedogenic iron oxides than the sedimentary soils (Table 3.3), and these oxides have characteristically high SFA and C-constant (discussed above). Thus the likelihood that iron oxide is frequently solubilized and reprecipitated (on pedogenic time scales) implies that relatively small amounts of naked iron oxides can dominate the SFA of whole sample and elevate the untreated C-constant value.

3.4.3.OM associated with small mesopores

Small mesopores (ca. 2-10 nm diameter), that generally account for most of the $SFA_{mineral}$, are small enough to exclude hydrolytic enzymes and, thus, were hypothesized to explain the mineral protection of OM (Mayer, 1994a). Mayer et al (2004), however, showed that only minor fractions of total OM were contained in the small mesopores

across a range of soils and sediments. Their soil samples were all from temperate climates and mostly cultivated soils. In addition, light-density materials (e.g., plant detritus) were not removed. We therefore tested here the possibility that small mesopores may protect significant fractions of OM in the mineral-associated fraction (HF) in these undisturbed tropical soils.

The volume of both <10 nm and 10-200 nm range pores in muffled samples across sites (Fig. 3.7) followed the pattern of $SFA_{muffled}$, in line with the positive correlation of $SFA_{mineral}$ and small mesopore volume commonly observed in soils and sediments (Mayer, 1994a, b). The increase in pore volumes upon muffling was ascribed to OM volatilization (Mayer et al., 2004). The proportions of small mesopore volumes that were attributable to OM filling or covering increased with increasing altitude from 6 to 73% in the ultrabasic series and 17 to 66% in the sedimentary series. These patterns are consistent with the increasing organic coverage (Fig. 3.5) and occlusion (Fig. 3.6) of soils at higher altitudes, and suggest the preferential association of OM with mesoporous parts of mineral surfaces. If the latter inference is true, our results support the laboratory findings where amino acids were preferentially sorbed to the < 3-8 nm pores of alumina and silica microfabrics (Zimmerman et al. 2004).

The organic matter content of small mesopores can be calculated with the assumption that liberation in the mesopore volumes upon muffling results from OM removal. Applying a soil OM density of 1.4 g cm^{-3} (Mayer et al., 2004), small mesopores could account for 10, 5, and 7% of the total OC concentration in the HF for the 700, 1700, and 2700-m sedimentary soils, and 11, 14, 18% for the 700, 1700, and 2700-m ultrabasic soils, respectively. While the $SFA_{mineral}$ and pore size distribution for

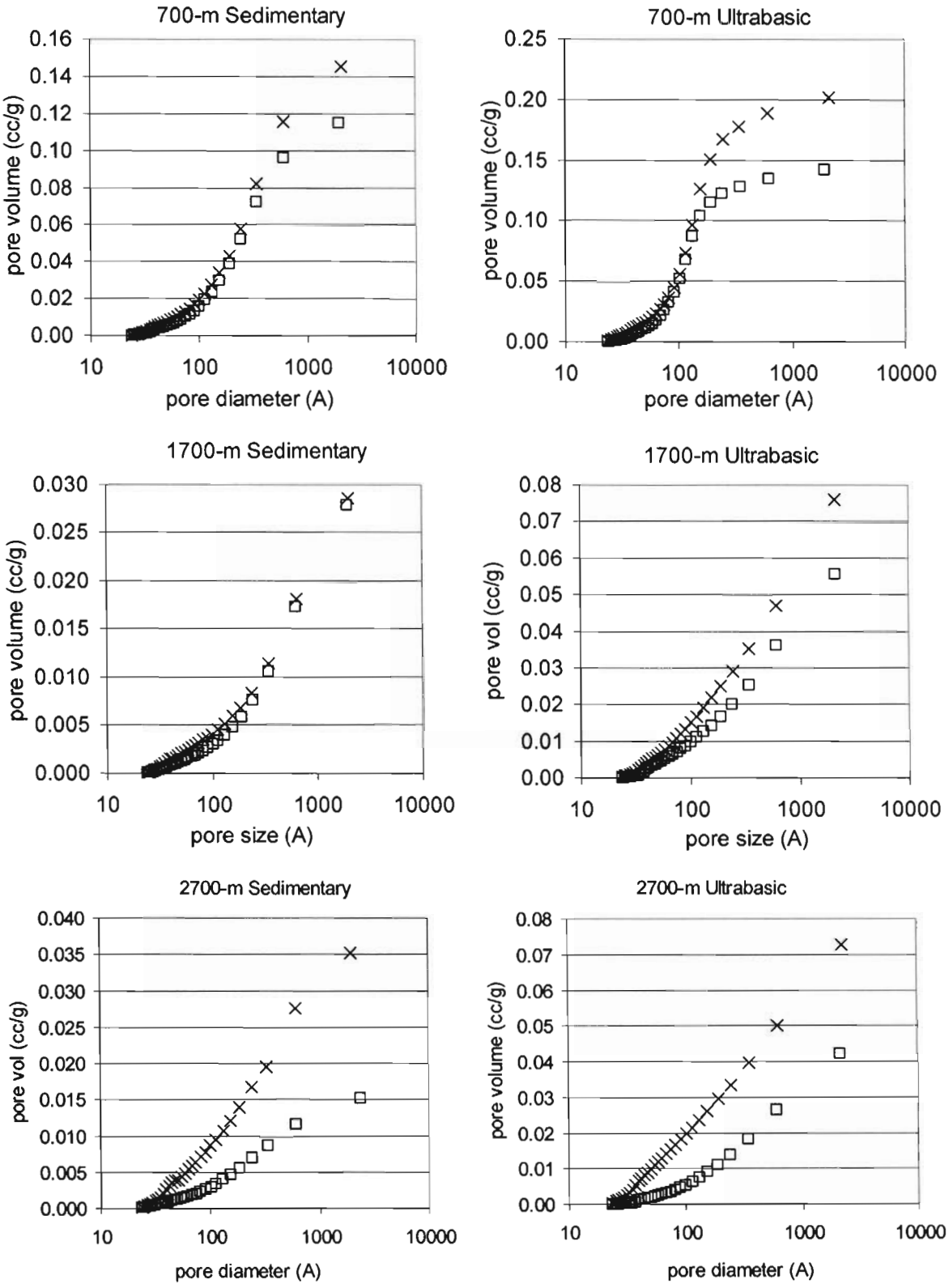

Figure 3.7: Pore-size distribution of a selected surface soil per site before (rectangle) and after the OM removal by muffling (cross).

aluminosilicate-dominant materials were robust against muffling treatment (Mayer et al., 2004), iron oxides may not be, as goethite and hematite have needle and sphere-type geometries in contrast with the platy clay. Thus, the estimate of the mesopore-contained OM in the 700-m ultrabasic soils may be inaccurate. Nevertheless, our results generally confirmed the previous finding that only minor fractions of total OC content, in whole soil or the HF, can be present in the small mesopores capable of excluding enzymes.

3.4.4. Geometry of organo-mineral assemblages

The two surface-related variables (untreated C-constant and $\%SFA_{occluded}$) illustrate changes in organo-mineral arrangements along the altitude gradient (Fig. 3.8). The untreated C-constants generally decreased and $\%SFA_{occluded}$ increased with increasing altitude on both rock types. The trajectory was closer to that predicted from the occlusion model than the one from the painting model, especially for the ultrabasic series (Fig. 3.2), supporting our hypothesis. Clear cases of the full-encapsulation, partial-encapsulation, and dot modes were observed in the 2700-m sedimentary, 2700-m ultrabasic, and 700-m sedimentary soils, respectively. None of the studied samples showed the paint mode, supporting the premise that the majority of clay surfaces (e.g., siloxane planes) are not preferentially covered with OM.

At all three altitudes in the sedimentary series and at the 700-m ultrabasic site, one representative soil pit was selected to examine the changes in the organo-mineral arrangements with soil depth. Shifts in untreated C-constants and $\%SFA_{occluded}$ from the surface to deeper horizon samples in all of the four depth sequences showed similar trajectories of decreasing organic coverage and $\%SFA_{occluded}$ (Fig. 3.9), as the altitudinal

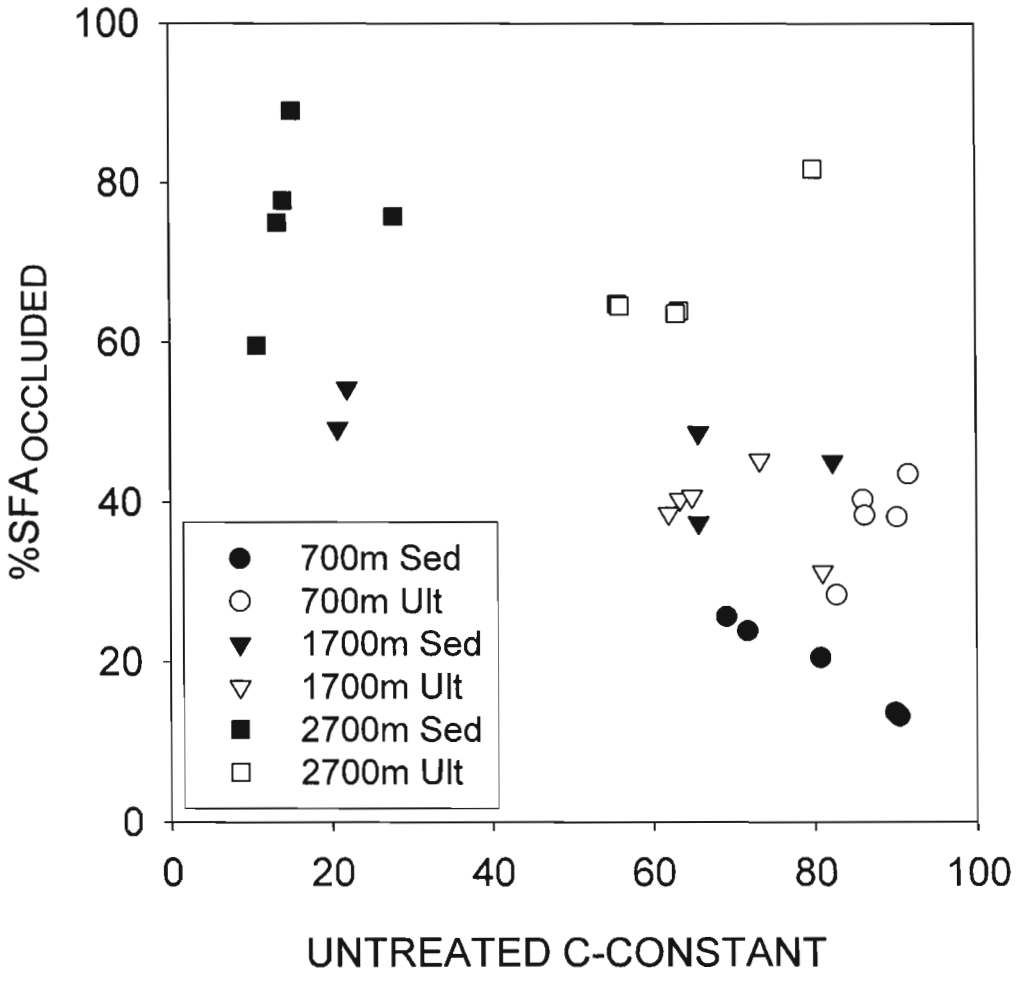

Figure 3.8: The changes in untreated C-constant and % mineral SFA occluded by OM across all six sites (n = 5 per site).The changes in the unmuffled C-constant and % SFA occluded by OM.

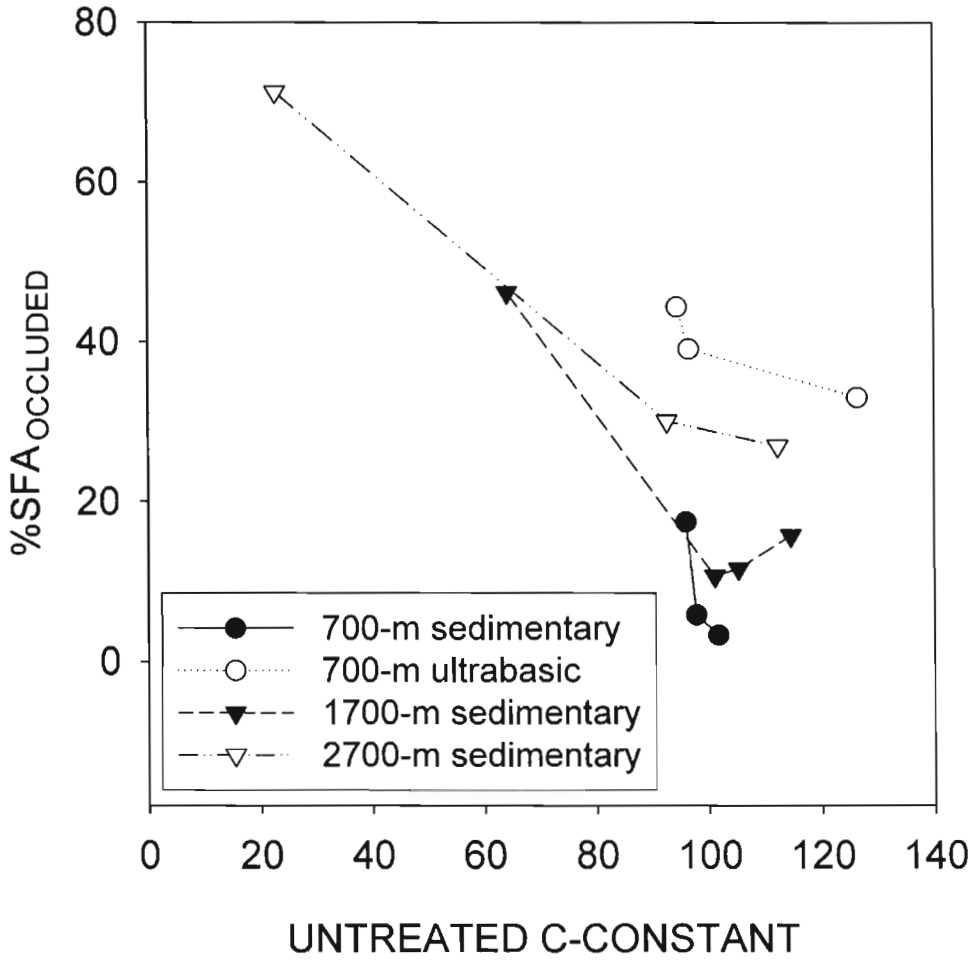

Figure 3.9: The changes untreated C-constant and the fraction of mineral SFA occluded by OM along soil depth profiles. From the upper left to bottom right, soil sample depths are 0-10/ 20-40/ 60-80 cm for the 700-m sedimentary soil, 0-10/ 20-30/ 80-100 cm for the 700-m ultrabasic soil, 0-10/ 10-20/20-40/50-62 cm for the 1700-m sedimentary, and 0-9/10-20/ 20-30 cm for the 2700-m sedimentary soil.

gradient of the surface soils (Fig. 3.8). Fully-encapsulated aggregates in the 2700-m surface sedimentary soil quickly shifted to the dot-type mode in the B-horizon (10-30 cm deep) with concomitant decline in total OC concentration. Overall similarity in the trajectories between the altitude and soil depth gradients, with parallel changes in OM level, implies that the changes in both the organic coverage of untreated soils ($\%ORG_{untreated}$) and $\%SFA_{occluded}$ are driven by the concentration of OM in soil.

3.5. Discussion

3.5.1. Extent of sorptive preservation of soil OM across studied soils

How is the OM in the HF associated with and, possibly, protected by the soil mineral matrix? The potential importance of sorption to account for the bulk of OC in the HF can be assessed by comparing the observed OC_{HF} loading (OC_{HF}:$SFA_{muffled}$ ratio) with the sorptive capacity of pure mineral phases reported from sorption experiments. The experiments examining natural dissolved OM sorption onto mineral phases at field-relevant pH's (pH 4-7) have shown the maximum sorptive capacity of hydrous iron oxide and aluminum oxide phases to be 4.7 and 1.0 mg m^{-2}, respectively (Tipping, 1981; Kaiser et al. 1997) and that of clays (kaolinite and montmorillonite) to be roughly 0.3 mg m^{-2} (Jardine et al. 1999; Chorover and Amistadi, 2001).

The upper two altitudes of sedimentary soils had aluminosilicate clay minerals in the clay-size fraction, and contained <3 % of pedogenic iron oxides (Table 3.3). Thus the maximum sorptive capacity of these soils is likely 0.3-0.5 mg m^{-2} (i.e., a slope of 0.3-0.5 in Fig. 3.10). The OC_{HF} loading in most of these soils was clearly above this capacity, implying a minor role of simple sorptive preservation for bulk OM storage in these soils.

The 700-m sedimentary soils were also dominated by aluminosilicate clays but contained slightly more iron oxide (ca 4%). Assuming equal abundance of pedogenic iron and aluminum oxides in these soils, the maximum sorptive capacity is 0.6 mg m^{-2}. Thus the OC_{HF} loading in these soils was at or slightly above sorption capacity. The organic coverage was, however, < 5% of total soil surfaces in the 700-m sedimentary soils, implying that majority of OM in the HF is likely present as belbs of OM having limited contact with mineral surfaces (see below).

The upper altitude ultrabasic soils had mixed clay mineralogy of aluminosilicate clays and goethite, and cwith <10% of pedogenic iron oxides (Table 3.3). Thus the maximum sorptive capacity of these soils doesn't likely exceed 0.7 mg m^{-2}. The 1700-m and 2700-m ultrabasic soils had OC_{HF} loadings 2.9-4.2 and 5.5-11 times more than the sorptive capacity, respectively, assuming that half of the total mineral surfaces are organically covered. Even assuming full organic coverage of mineral surfaces, OC_{HF} loadings would still be 1.5-5.4 times more than the sorptive range. Thus, major fractions of OC_{HF} in these soils are also likely stored via non-sorptive mechanisms. In contrast, low OC_{HF} loadings of the 700-m ultrabasic soils (Fig. 3.10) were 13-23 fold less than the maximum sorptive capacity of these iron-rich soils (49% iron oxides, Table 3.3). $\%ORG_{untreated}$ in these soils were considered to be < 5%, in which case the mineral surface that was in contact with OM ($SFA_{mineral\text{-}OM}$) would be < 3.7-5.7 m^2 g^{-1}, and OC_{HF}:$SFA_{mineral\text{-}OM}$ would become 4.0-7.4 mg m^{-2}, roughly the maximum sorptive capacity of goethite (Tipping, 1981; Kaiser et al. 1997). Thus, only in the 700-m ultrabasic soils might direct sorptive preservation play a major role in bulk OM storage. Repeated dithionite plus acid extractions released up to 80% of the OC_{HF} from the

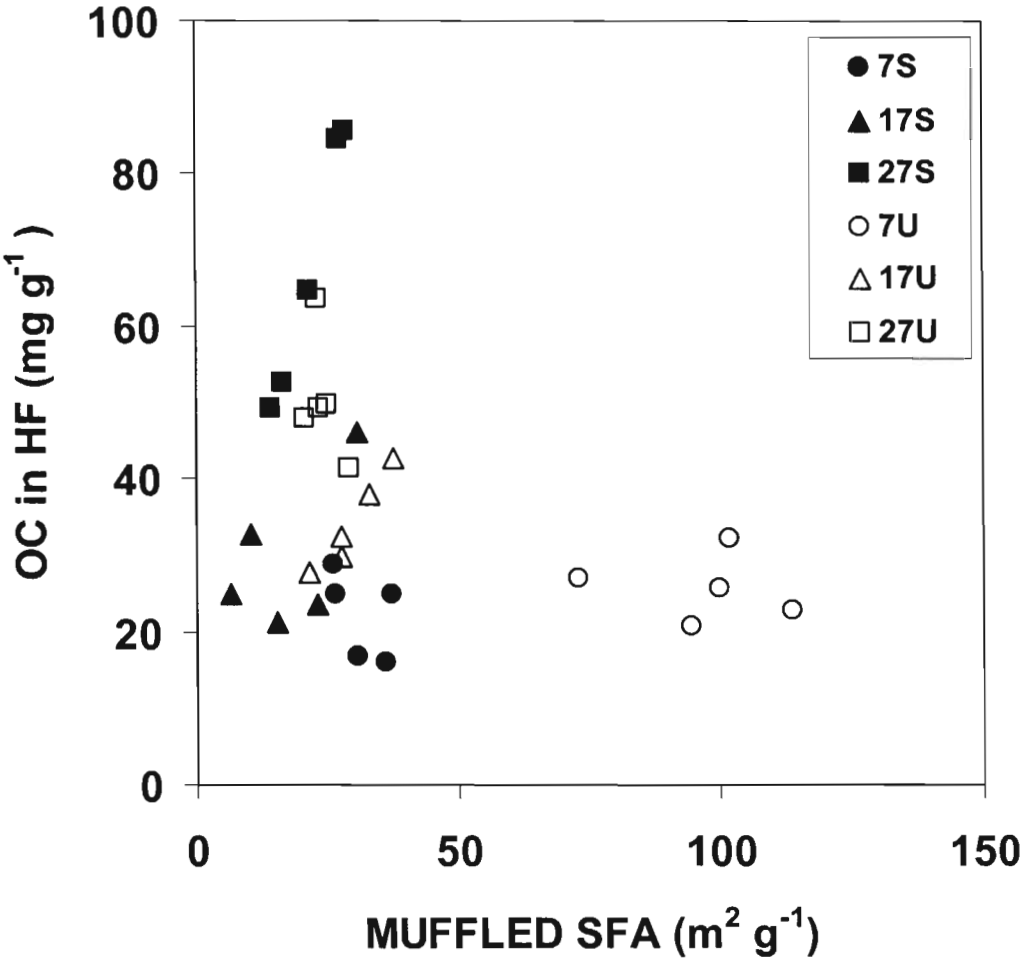

Figure 3.10: The specific surface area of muffled samples with respect to the OC concentration in the heavy-density fraction.

700-m ultrabasic soil, but only 15-30% of the OC in HF from the rest of Mt. Kinabalu soils (Wagai and Mayer, submitted), corroborating the importance of sorptive storage only in the 700-m ultrabasic soils consisting mostly with iron oxides.

While iron and aluminum oxides have high sorptive capacities, these metal concentrations found in many surface soils and their physical fractions appeared to have limited surface areas to account for bulk of soil OM (Wagai and Mayer, submitted). For most surface soils, direct sorption appear to protect only a limited fraction of OM in the bulk or HF, and the importance of this mechanism may be limited to subsurface horizons (Kaiser and Gubbenberger, 2003).

3.5.2. Possible non-sorptive mineral controls on OM preservation

The $SFA_{muffled}$ was positively correlated with the OC_{HF} within the 1700-m ultrabasic soils and 2700-m sedimentary soils (Fig. 3.10). What are the non-sorptive mechanisms that allow $SFA_{mineral}$ or texture to enhance the OM preservation under such high OC_{HF}:$SFA_{muffled}$ ratios? The 1700-m soils appear to fit with the partial encapsulation mode (Fig. 3.8). One variation of this mode is extensive coating of globular "humic" OM by oriented clays (e.g., Fig. 14-7, Emerson et al. 1986). This mode could physically protect the coated OM from enzymatic attack, and is consistent with limited $SFA_{muffled}$ to sorptively protect the OM in HF. Even in the 2700-m sedimentary soils, high SFA-to-volume ratio phyllosilicate clays may reduce the accessibility of hydrolytic enzymes or microbes themselves to labile substrates, depending on the size of "throats" present in the organo-mineral assemblages (Mayer et al., 2004). Besides the direct physical control of minerals, $SFA_{muffled}$ may also indirectly affect soil OM concentrations. For instance, high

$SFA_{muffled}$ may correspond to better soil nutrient status (e.g., base cation retention), which can enhance OM inputs to soil (Oades, 1988).

Widely observed OC-texture correlations have led to the concept of "capacity" and "saturation" of soils to store OC (e.g., Hassink, 1996; Six et al., 2002) and incorporation of texture control on OC turnover in simulation models (e.g., Parton et al. 1987). Yet the mechanistic reasons for the OC-texture relationship remain unresolved, leaving uncertainty in our prediction of soil OM responses to future environmental perturbations. In this study, we conclude that two of the proposed mechanisms of mineral-controlled OM preservation, sorption and mesopore protection, didn't account for major fractions of the OC storage in our soil samples except for the 700-m ultrabasic soils, in accordance with other recent studies (Guggenberger and Kaiser, 2003; Mayer et al., 2004). Then does the OM-surface area relationship provide any useful information?

The low range of OC_{HF}:$SFA_{muffled}$ (0.20-1.1 mg m^{-2}) observed in the 700-m soils (Fig. 3.3) likely resulted from the high microbial degradation of OM and high $SFA_{untreated}$ with little organic coverage under higher MAT. This low OC loading range appears to represent a refractory background OC level below which OM decay becomes very slow, presumably due to mineral protection, and then the OC loadings above this level may represent the OC masses less protected by the mineral matrix. The following observations are consistent with this view: (a) The OC:$SFA_{mineral}$ ratios in many marine sediments have been shown to decrease with depth and level off at around 0.5-1 mg m^{-2} where OM appears very resistant to further decay (Mayer, 1994a). (b) Weathered tropical soils consisting of a range of mineralogy also showed OC_{total}:$SFA_{mineral}$ ratios of 0.5-1.0 mg m^{-2} (Feller et al. 1992). These low loadings and limited SFA liberations upon OM

removal in their soils are also consistent with the dot-mode arrangement. (c) Seven loess-derived temperate soils showed quite constant $OC:SFA_{mineral}$ ratios of 0.7-0.8 mg m^{-2} in 0.2-2.0 μm fractions and 0.2-0.3 mg m^{-2} in the <0.2 μm fractions (Kahle et al., 2003). Similarly, most < 2-μm size fractions of temperate acid soils, particularly those without fertilizer or manure inputs, had $OC:SFA_{mineral}$ ratios ranging from 0.3 to 1.2 (Kiem and Kögel-Knabner, 2002). (d) All C-horizon samples and many B-horizons among a range of temperate acid soils had $OC:SFA_{muffled}$ <1 mg m^{-2} (Mayer and Xing, 2001). Organic carbon found in deeper soils and sediments as well as finer soil aggregates generally turns over more slowly (Hedges and Oades, 1997). Therefore 0.2-1.0 mg m^{-2} appears to be a common refractory background range across a wide range of soils and sediments, implying similar mineral protection mechanisms operative in low OC and/or high $SFA_{mineral}$ conditions.

3.5.3. Nature of organic matter in the organo-mineral aggregates

The high OC_{HF} loadings of the 1700-2700 m sedimentary and ultrabasic soils, in excess of the estimated sorptive capacities of respective soil mineral phases, are consistent with the geometry of the organo-mineral arrangements (the full or partial encapsulation modes) independently deduced from $\%SFA_{occluded}$ and $\%ORG_{untreated}$ measurements (Fig. 3.2 and 3.8). Even in the 700-m sedimentary soils, where the dot mode fits well, sorptive preservation appeared limited when accounting for the limited $\%ORG_{untreated}$. In addition, the majority of OC_{HF} was located outside of the small mesopores in the mineral matrix. Organic matter in the HFs of all of the studied surface soils (with a possible exception of the 700-m ultrabasic soils) must therefore be present as belb-like forms external to <10 nm pores in the mineral matrix.

Predominance of globular OM across the altitudinal (OM accretion) gradient suggests that extra OM grows from OM nucleation points (the dots) and encapsulates fine mineral particles, rather than accumulating around the mineral particles in thin, paint-like layers. In other words, the organic covering or occlusion of mineral surfaces appears as a by-product of OM ingrowth rather than resulting from the strong affinity of OM to mineral surfaces. Weak forces such as van der Waals force, hydrophobic interaction, and hydrogen bonding become strong between macromolecules due to their additive effect (Sposito, 1989). Cation bridging between anionic organic function groups may also facilitate the globular OM formation.

Apparent growth of globular OM and encapsulation of fine minerals were not accompanied by a large compositional changes in the OM_{HF} along the altitudinal gradient. Carbon-to-nitrogen ratios in the HFs (11-17) were more close to those of microbial biomass (5-8, Paul and Clark, 1996) than to those in the light-density fractions (26-56) isolated from the same soils along the gradient (Chapter 2), implying that the OM growth in the HFs is related to microbial transformation of plant detritus. Genesis as well as the geometry of humified, discrete OM present in association with mineral matrices are rarely studied (Myneni et al., 1999) and merit further investigation.

Lack of the paint-type mode across all the samples examined (Fig. 3.8 and 3.9) is consistent with the idea that OM sorption takes place largely at aluminous clay edges (Schulthess and Huang, 1991) and micropores from metal oxides (Kaiser and Guggenberger, 2003), rather than on siloxane planes that account for most of the mineral surfaces and small mesopores. In laboratory sorption experiments, Kaiser and Guggenberger (2003) showed a limited reduction in $SFA_{mineral}$ (15-40%) and untreated C-

constant (20-50%) at the highest OM loading among a range of silicate and metal oxide phases, further supporting this idea. These reactive surface zones may act as nucleation points from which OM grows in size via OM-OM interactions. Positive correlation of OC with less-crystalline iron and aluminum oxides found in soils with low OC loadings such as weathered tropical soils (Hughes, 1982; Shang and Tiessen, 1998) are consistent with this idea. These reactive zones would preferentially adsorb OM (Kaiser and Guggenberger, 2003) and the adsorbed OM are likely well-stabilized and thus have older ^{14}C age (Eusterhues et al., 2003).

3.5.4. Global implication of OM-mineral surface relationship

Observed patterns in the organic coverage and occlusion of mineral surfaces along the altitudinal gradient (Fig. 3.5 and 3.6) were largely attributable to the changes in the soil OM concentration. Soil OC concentrations in the HF significantly correlated with untreated C-constant ($R^2 = 0.32\text{-}45$, $p < 0.05$) and $\%SFA_{occluded}$ ($R^2 = 0.52\text{-}73$, $p < 0.001$) across the altitude gradient for both rock series. This OM influence can be viewed by adding a third axis, SFA-normalized OC_{HF} loading, in the plane of C-constant-$\%SFA_{occluded}$. The concomitant increases in $\%ORG_{untreated}$, $\%SFA_{occluded}$, and OC_{HF} loading found among the Kinabalu soils (Fig. 3.11) appears to be applicable to the soils of different region, soil type, and climate (Fig. 3.12). For these non-Kinabalu soils, the data on soil OC_{HF} were not available and total OC loading (OC_{Total}:$SFA_{muffled}$) were plotted instead. Nevertheless, the two-dimensional trajectory for the non-Kinabalu surface horizons was also closer to the occlusion model pathway rather than the painting model pathway, supporting the generality of our inference from the Kinabalu samples. Three B-horizon samples from the temperate acid soils had anomalously higher C-

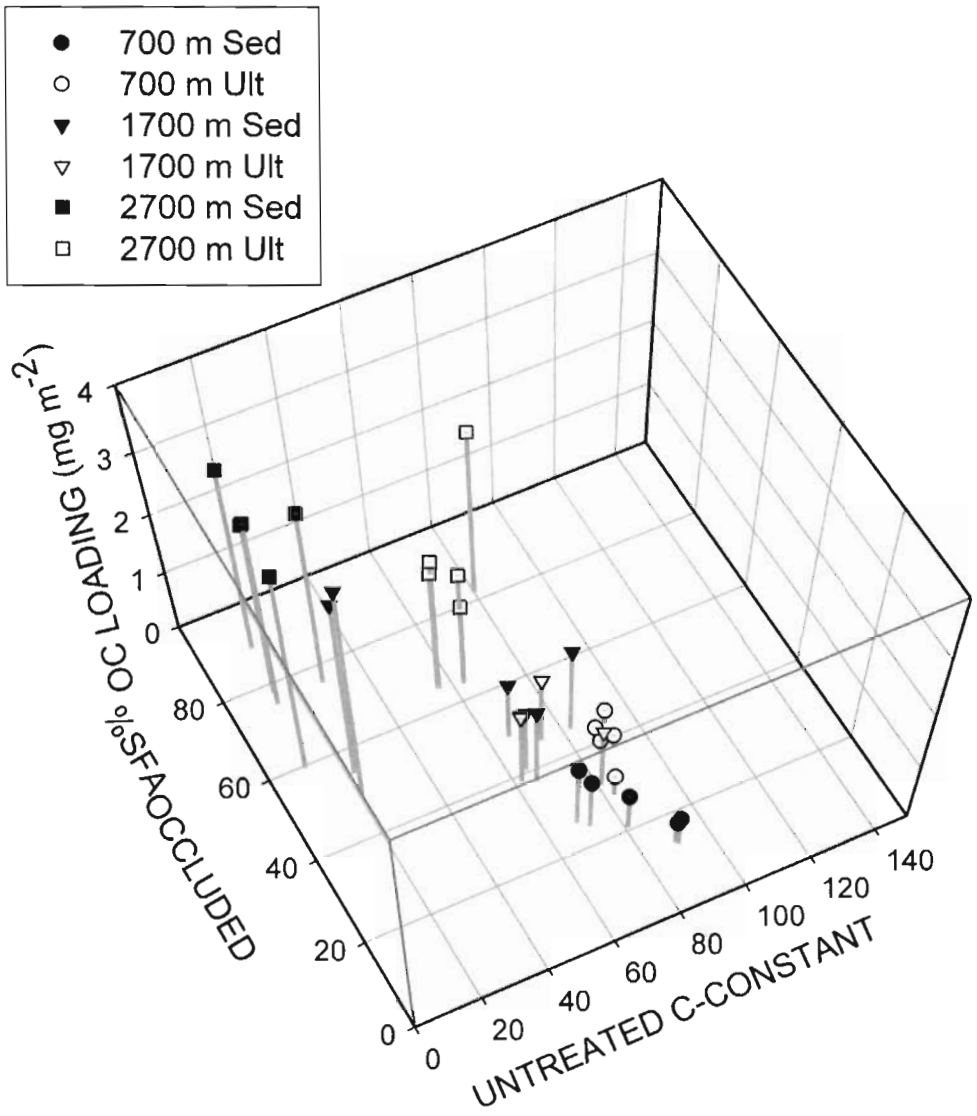

Figure 3.11: The changes in untreated C-constant, $\%SFA_{occluded}$, and OC_{HF}:$SFA_{muffled}$ ratio in the heavy-deinsity fractions across all six sites.

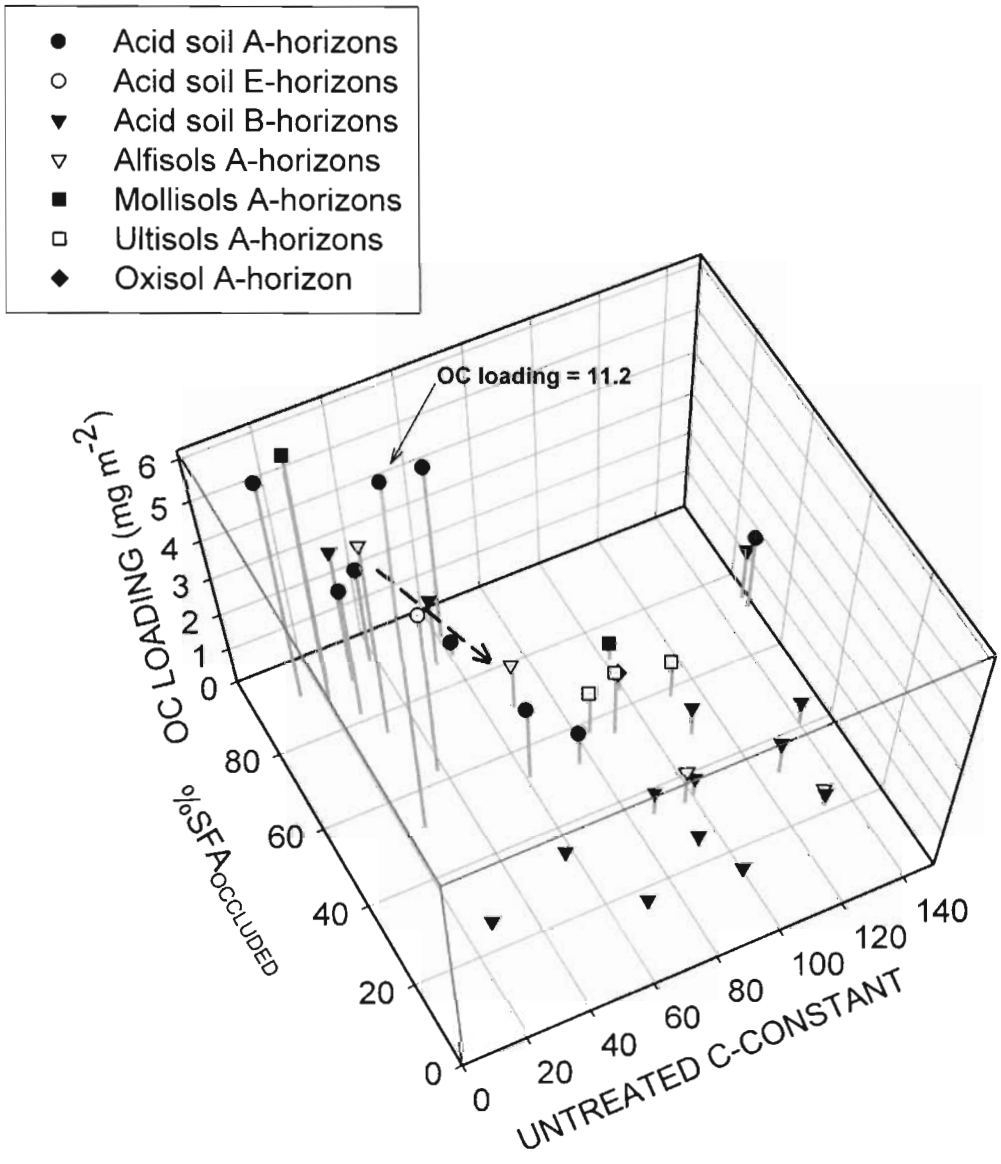

Figure 3.12: The changes in untreated intact C-constant, $\%SFA_{occluded}$, and OC_{Total}:$SFA_{muffled}$ ratio across all non-Kinabalu soils.

constants of 150-210, presumably due to microporous metal oxides (Mayer and Xing, 2001), and thus were omitted. The metal oxide content in soils may be responsible for the wide variation in the C-constant of these B-horizon samples. Two of the acid soil B-horizon samples were positioned closer to the paint mode region than any of the Kinabalu samples, suggesting the possible importance of paint-mode type OM preservation in acid-leached B-horizons. Cultivation effect on the organo-mineral assemblage appeared to follow the same general trajectory. From uncultivated to cultivated Alfisol samples (Albia series), the aggregates appear to shift from the full encapsulation towards the dot-mode region (dotted line in Fig. 3.12).

The overall similarity in the trajectory between the Kinabalu and non-Kinabalu samples suggest that the changes in the OC loading beyond certain level (e.g., 0.5-1.5 mg m^{-2}) may lead to significant responses in soil surface-mediated reactions. Below this range of OC loading, OM decay is likely limited by the protective effects of extensive, naked mineral matrix (discussed above). Our results would imply that long-term changes in OM inputs and/or oxidation via processes such as (de)forestation, (no) tillage, or climate change would proceed through changes in occlusion or encapsulation.

Chapter 4 - The significance of hydrous iron oxides for organic carbon storage in a range of mineral soils

4.1. Abstract

Predictive capability for the long-term storage of soil organic carbon (OC) is limited by insufficient understanding of the processes and factors that control mineral protection of soil OC. For decades, hydrous iron oxides (FeOx) have been thought as one of the main soil mineral components that stabilize significant amounts of OC, based on iron-carbon correlations found across many field soils and their physical fractions, abundance of sorptive surfaces of FeOx, and ease of FeOx-organic matter microaggregate formation. The basis of the correlations is, however, unclear because no direct information is available on the mass of OC that is associated with iron. We therefore directly quantified the OC that can be released from FeOx phases using a selective FeOx dissolution technique for 34 mineral soil samples representative of most world soil types. Iron extractability by our modified dithionite technique (eliminating organic chelators, plus weak acid rinse) was comparable to the conventional dithionite-citrate extraction. The difference in dissolved OC between the dithionite and control extractions represents the potentially-soluble OC bound to reducible Fe phases. Iron-bound OC, thus defined, averaged 11% of total soil OC (range: 0-37%), indicating a minor role of reducible FeOx for bulk soil OC storage for virtually all the samples examined. The mass ratios of OC to iron (OC:Fe) of the extracted phases in most samples were consistent with those reported from sorption experiments, and positively related to the specific surface area of reducible FeOx phases. Sorption of OC onto FeOx is thus a plausible mechanism for organo-iron

associations in these samples. The limited contribution of sorptively-stabilized OC to bulk OC storage is therefore limited by the amount of FeOx. Some low pH, organic-rich samples (e.g., spodic horizons) showed OC:Fe ratios above those found in sorption experiments, implying the presence of organo-iron complexes. We conclude most OC in our samples must be stored via mechanisms other than simple sorptive associations with FeOx, and consider organo-metal complexation and ternary associations (clay-FeOx-organic matter) as possible alternative mechanisms. OC:Fe ratios provide a context to examine the linkage in organo-iron association between soil and aquatic systems.

4.2. Introduction

Soil organic matter (SOM) represents an important carbon reservoir in the global carbon cycle and serves as a basis for sustainable land management (e.g., Tiessen et al., 1994). Soil minerals exert strong controls on SOM storage and dynamics (e.g., Torn et al., 1997). Yet our mechanistic understanding of the mineral protection of SOM remains poor largely because multiple mineralogical factors often co-vary with SOM properties, making it difficult to isolate specific mineralogical effects on SOM (Sollins et al., 1996; Oades, 1988; Baldock and Skjemstad, 2000). Uncertainty in current models to predict the response of SOM pool to climate and land-use changes stems in part from limited understanding of organo-mineral interactions (Parfitt et al., 1997; Krull et al., 2003).

While aluminosilicate minerals dominate the earth's surface, iron oxides, hydroxides, and oxyhydroxides (FeOx) are ubiquitous due to their high stability even at small sizes - down to several nanometers (Schwertmann and Taylor, 1989), ease of redox change, and consequent mobility. FeOx have extensive and reactive surfaces, thereby

significantly controlling surface-mediated reactions such as adsorption of organic acids and phosphate (Stumm and Morgan, 1996). Along with the redox coupling of the iron cycle with those of nitrogen and organic carbon (e.g., Schwertmann et al., 1986; Davidson et al., 2003), FeOx greatly influences biogeochemical processes in aquatic ecosystems (Young et al., 1991; Stumm and Sulzberger, 1992).

For decades, FeOx have been regarded as one of the major mineral components that stabilize significant fractions of SOM. Despite the presence of various amounts of mineral-free OC (plant detritus and charred materials) in soils, field studies across a wide range of soils have shown that organic carbon (OC) concentrations, in bulk soils and their physical fractions, correlate very well with the concentrations of reducible FeOx phases (Tiessen et al., 1984; Evans and Wilson, 1985; Skjemstad et al., 1989; Kaiser and Guggenberger, 2000) and/or poorly-crystalline FeOx and their aluminum analogs, AlOx (Hughes, 1982, Johnson and Todd, 1983; Adams and Kassim, 1984; Shang and Tiessen, 1998). More recent studies correlating OC turnover rates with FeOx and AlOx concentrations further support the inference of OC protection by FeOx and AlOx (Torn et al., 1997; Masiello et al., *in press*). Little information is available, however, to examine causality in these correlations or the actual mechanisms of organo-iron associations perhaps responsible for these correlations. Three mechanisms are generally considered.

FeOx promotes microaggregate formation as a cementing agent, particularly in highly weathered soils. Intimate associations of FeOx crystals with organic matter in weathered soils have been shown by microscopy (Santos et al., 1989; Vrdoljak and Sposito, 2002) and by combinations of physical separations and chemical extractions (Shang and Tiessen, 1998). Both OC and extractable phases of FeOx positively correlate

with aggregate stability in field soils (Duiker et al., 2003; Krishna Murti and Huang, 1987). Physical protection of OC via FeOx-participated aggregation is, however, difficult to quantify or distinguish from the following chemical mechanisms of organo-iron associations.

Dissociated functional groups on organic matter can complex Fe(III) ions, and occur in soils where a high supply of humic material allows competition with growth of FeOx (Schwertmann et al., 1986). High stability of organo-metal complexes against microbial degradation has been shown by bioassay experiments using synthetic organo-Fe and organo-Al complexes (e.g., Boudot et al., 1989). These complexes play a major role in Spodosol formation (e.g., Buol et al., 1989; Lundström et al., 2000). Direct evidence of organo-Fe(III) complexes in natural environment appears to be restricted to acidic, organic-rich environments such as peaty soils (Schwertmann and Murad, 1988) and colloids in organic-rich river water (Allard et al., 2004). More recently, the importance of organo-metal complexation in a wider range of soils was suggested based on the correlation of soil OC stock with pyrophosphate-extractable Al concentration (Masiello et al. in press; Percival et al., 2000) and with the extractable Fe concentration (Masiello et al. *in press*). Furthermore, pyrophosphate-extractable phases of aluminum appear to retard the OC turnover in soils (Tate, 1992; Veldkemp, 1994; Masiello et al., *in press*). Pyrophosphate is, however, not selective; it peptizes soil colloids and dissolves metals from AlOx and FeOx phases (McKeague and Schuppli, 1982; Kaiser and Zech, 1996) as well as complexes with other metals such as calcium. Furthermore, portions of SOM are soluble at the high pH of this extractant (e.g., Stevenson, 1994). Thus the

specific mechanisms as well as the significance of organo-metal complexation for SOM storage and dynamics remain elusive.

Sorption of dissolved OC onto mineral surfaces has been considered as one of the major mechanisms of SOM stabilization (Oades, 1988; Sollins et al., 1996; Baldock and Skjemstad, 2000). FeOx phases generally have high surface areas (Borggaard, 1982), and laboratory experiments have shown them to strongly adsorb natural organic matter (e.g., Tipping, 1981; Kaiser et al., 1997) and to reduce biodegradation of sorbed OC (Jones and Edwards, 1998). Based on the OC-Fe correlations found in field soils (cited above) and the demonstrated reactivity of FeOx, sorption is often presumed to account for the protective association between bulk OC and FeOx (Kaiser and Guggenberger, 2000; Kaiser et al., 2002; Kiem and Kögel-Knabner, 2002; Eusterhues et al., 2003; Wiseman and Püttmann, 2004). The ratios of bulk OC to extractable iron that can be inferred from correlations, however, are usually higher than have been observed in laboratory sorption experiments. Sorption experiments showed the maximum sorptive capacity of various FeOx phases to be 0.02-0.22 g-OC g-Fe^{-1} (Tipping, 1981; Kaiser et al., 1997). If we calculate OC:Fe ratios for field soils from the OC-Fe correlations (cited above), values are 7-24 fold higher, suggesting far greater masses of organic matter in these field soils than the amount FeOx could hold via a simple sorption mechanism.

Clearly more direct assessment of the amounts of OC bound to FeOx phases would help ascertain the basis for these correlations. We developed a modified dithionite method to reduce FeOx selectively, eliminating the usual organic chelator, and directly quantified the OC released upon Fe(III) reduction. Dithionite is considered to have little impact on other soil mineral phases (Borggaard, 1982). Assuming that previously

dissolved OC adsorbed onto FeOx surfaces becomes soluble upon the dissolution of adsorbant, this method extracts the OC directly bound to FeOx via a sorption mechanism. Dissolution of OC from organo-Fe(III) complexes by dithionite extraction is less clear but likely. The formation of organo-Fe(III) complexes presumably requires dissolved forms of OC, and dithionite extraction almost fully dissolved organically-complexed Fe from a drained peat soil (Schwertmann and Murad, 1988). While dithionite effectively disperses Fe-cemented microaggregates (discussed above) (Pinheiro-Dick and Schwertmann, 1996), insoluble organic matter (e.g., plant detritus) in these aggregates will not be accounted for in the dithionite-extractable phase. Therefore the OC extractable by our dithionite method represents the potentially-soluble OC that is bound to reducible Fe phases via sorption and, to some extent, complexation mechanisms, and will hereafter be called Fe-bound OC.

We focus here on this Fe-bound OC fraction, testing the hypothesis that the Fe-bound OC accounts for only a minor fraction of total OC. We tested this hypothesis for 34 mineral soil horizons, including soil orders that account for most soil OC storage of the world (Eswaran et al., 1993). We also examined, to a limited extent, organo-aluminum associations released by the dithionite and weak acid extractions.

4.3. Materials & Methods

4.3.1. Sample source and storage

Mineral horizons relatively enriched with OC were sampled from a range of soil types and geographic areas under non-arid climate regimes (Table 4.1). Deeper samples

Table 4.1: Sample source information and soil characteristics.

Sample ID	Soil Taxonomy sub-order / order		Location	Vegetation	Altitude (m)	Horizon: Depth (cm)	Total OC (mg g^{-1})	Total N (mg g^{-1})	C/N	OC in HF [c] (mg g^{-1})	pH in H_2O
Ent	orthic	Entisol	Hawaii Island	native forest	<500	A: 0-2	165	10	17	N.A.	5.4
Inc-1E	udic	Inceptisol	Massachusetts	N.A.	<500	E: 6-12	29.5	0.8	39	N.A.	4.5
Inc-1Bw	subsurface horizon of Inc-1E					Bw: 12-22	30.3	1.2	25	N.A.	4.0
Inc-2	aquic	Inceptisol	Massachusetts	cultivated	<500	Ap: 0-18	28.9	2.4	12	N.A.	5.0
Inc-3	umbric	Inceptisol	Washington	forest, conif	625	A: 0-10	45.7	1.1	42	N.A.	5.3
Inc-4	andic	Inceptisol	Oregon	forest, conif	180	A: 0-10	105	6.0	17	N.A.	5.2
Inc-5	tropical	Inceptisol[a]	Kinabalu, Malaysia	native forest	2700	A: 0-10	93.9	3.3	28	60.2	4.5
Inc-6	trop/udic	Incept/Alf	Kinabalu, Malaysia	native forest	1700	A: 0-10	22.4	1.3	17	14.5	4.6
Inc-7	tropical	Inceptisol	Kinabalu, Malaysia	native forest	2700	A: 0-10	126	6.6	19	62.8	4.9
Alf-1	udic	Alfisol	New Jersey	uncultivated	<500	A: 0-6	79.7	5.1	16	N.A.	4.3
Alf-2	udic	Alfisol	New Jersey	cultivated	<500	Ap: 0-13	10.1	1.1	9	N.A.	6.0
Alf-3	aquic	Alfisol	Mississippi	cultivated	<500	Ap: 0-8	14.1	1.5	10	N.A.	6.0
Alf-4	udic	Alfisola	Kinabalu, Malaysia	native forest	1700	A: 0-10	43.1	2.3	19	33.0	5.3
Mol-1	ustic	Mollisol	North Dakota	N.A.	<500	A: 0-5	23.8	2.2	11	N.A.	5.8
Mol-2	udic	Mollisol	Indiana	N.A.	<500	Ap: 0-28	26.3	2.2	12	N.A.	5.7
Ult-1	udic	Ultisol	Virginia	cultivated	<500	Ap: 0-20	44.8	3.2	14	N.A.	5.2
Ult-2	udic	Ultisol	Maryland	cultivated	<500	Ap: 0-13	41.6	3.6	12	N.A.	4.9
Ult-3	udic	Ultisol	Virginia	cultivated	<500	Ap: 0-20	60.9	5.4	11	N.A.	6.2
Ult-4	humic	Ultisol	Kinabalu, Malaysia	native forest	700	A: 0-10	27.6	2.2	13	20.3	4.4
Ox-1	udic	Oxisol	Puerto Rico	native forest	<500	A: 0-5	66.2	3.7	18	N.A.	5.2
Ox-2	udic/ustic	Oxisol	Puerto Rico	native forest	<500	A: 0-5	64.7	4.5	14	N.A.	5.6
Ox-3	orthic	Oxisol	Para˜na, Brazil	cultivated	<500	A: 0-2	38.5	3.3	12	N.A.	6.2
Ox-4	peric	Oxisola	Kinabalu, Malaysia	native forest	700	Ac: 0-10	29.9	2.4	12	25.7	4.8
Spd-1E	orthic	Spodosol	Massachusetts	N.A.	<500	E: 10-15	15.7	0.6	26	N.A.	4.7
Spd-1Bhs	subsurface horizon of Spd-1E					Bhs: 15-18	72.6	3.5	21	N.A.	4.2
Spd-2B1	orthic	Spodosol	Maine	forest, decid	<500	B1: 0-5[b]	60.9	2.6	23	48.7[d]	4.5
Spd-2B2	subsurface horizon of Spd-2B1					B2: 5-25[b]	39.3	1.9	21	35.4[d]	4.6
Spd-3B1	humic	Spodosol	Maine	forest, conif	<500	B1: 0-5[b]	86.8	3.8	23	69.4[d]	4.7
Spd-3B2	subsurface horizon of Spd-3B1					B2: 5-25[b]	92.1	3.9	24	82.9[d]	4.9
Ando	udic	Andisol	Hawaii Island	native forest	500	A: 0-2	151	10	15	N.A.	5.1

[a] developed on ultrabasic parent materials

[b] top 0-5 and 5-25cm from the bottom of overlaying E-horizon.

[c] HF refers to heavy-density fraction isolated from bulk soils by 1.6 g cm^{-3} heavy liquid (see Method for detail)

[d] density separation data from adjacent soils (*Parker et al.*, 2002).

were also taken from two weathered tropical soils for the comparison with surface samples. Soil samples were either air-dried at room temperature or freeze-dried, passed through a 2-mm sieve, and stored at room temperature (for air-dried samples) or in a freezer (for freeze-dried samples) for less than three years. Alfisols, Mollisols, and Ultisols from the US were obtained from a soil archive (USDA, Soil Survey Center, Nebraska).

4.3.2. FeOx reduction method development

Our FeOx extraction is based on the original dithionite method (Deb, 1950) from which evolved the commonly used approach of incorporating an organic complexing agent and pH buffer to minimize the precipitation of iron sulfide (Mehra and Jackson, 1960). Mitchell and MacKenzie (1954) and Mitchell et al. (1971) conducted a fully inorganic dithionite extraction, reporting data that were inconclusive with respect to the effect of pH on iron extractability.

We thus conducted a pilot study by manipulating the pH of the dithionite-extraction system using three soils of contrasting mineralogy. To lower pH, the "x1 HCl" treatment received 0.096-mmol hydrochloric acid (HCl), and "x2 HCl" had 0.192-mmol HCl into a mixture of 14-mL deionized water (Milli-Q), 60-mg soil, and 120-mg of sodium dithionite. The "no buffer" treatment had no HCl, and the "neutral" treatment received 0.120-mmol sodium bicarbonate into the same mixture. A soil-to-solution ratio of 4.3 mg mL^{-1} and sodium dithionite concentration of 0.049M were used for all extractions. All dithionite extractions were done at ~23 °C for 16 hours on a slow rotational shaker (Labquake, Barnstead Thermolyne) to ensure good mixing, followed by centrifugation (40000 g, 0.7 hour). After removing the supernatant, residues were

extracted with 0.05M HCl for 1 hour to recover any iron and associated OC precipitated during the dithionite extraction. We compared the Fe recoveries from these treatments with those using the conventional dithionite-citrate extraction method (Loeppert and Inskeep, 1996). Sodium dithionite reagent (Fisher Scientific, laboratory grade) contained OC at the level of 0.30% by mass. This OC was accounted for by subtracting the OC concentrations in dithionite controls (dithionite plus water without soil) in each set of extractions in the pilot and following standard dithionite extractions.

In contrast to previous studies that suggested greater iron precipitation at lower pH (e.g., Mehra and Jackson, 1960), we found little or negative effect of pH neutralization on the iron recovery (Table 4.2). Slightly higher OC recovery from the "neutral" treatment likely results from alkaline-induced dissolution. The "no buffer" treatment consistently showed the highest or second highest iron recovery among the three contrasting soils tested, and thus was adapted as the standard extraction procedure.

4.3.3. Standard extraction procedures

The dithionite extraction and subsequent acid rinse conditions were the same as the "no buffer" treatment in the pilot study. The soil-to-solution ratio (mg mL^{-1}) of the dithionite extraction was 4.3 for Fe-rich soils and 7.1 for Fe-poor soils. Special care was taken to use fresh sodium dithionite which was mixed with pre-weighed soil plus deionized water immediately after weighing, double-sealing each tube with Parafilm (within 15 s) to minimize dithionite auto-oxidation and to maximize reductive dissolution of FeOx (Gan et al., 1992), and minimizing the headspace in extracting tubes.

Table 4.2: Pilot test of dithionite extractions with solution pH manipulation.

Treatment	pH of extract after 16-hr extr	Dith-extr Fe ($mg\ g^{-1}$)	HCl-extr Fe [a] ($mg\ g^{-1}$)	Dith+HCl extr Fe ($mg\ g^{-1}$)	Dith+HCl relative to DC-extr [b] Fe (%)	Dith-extr OC ($mg\ g^{-1}$)	HCl-extr OC [a] ($mg\ g^{-1}$)	Dith+HCl extr OC ($mg\ g^{-1}$)
Oxisol (goethite, hematite-rich A-horizon. Mt. Kinabalu at 700m)								
no buffer	6.7	117	68	185	75	6.7	5.9	12.6
x1 HCl	4.6	42	3.8	46	19	7.5	1.0	8.7
x2 HCl	3.7	60	1.9	62	25	7.1	0.70	8.1
neutral	7.1	83	56	138	56	7.4	3.9	11.5
Ultisol (kaolinitic A-horizon, Mt. Kinabalu at 700m)								
no buffer	6.2	21	3.0	25	94	3.0	3.3	6.4
x1 HCl	4.1	27	0.50	27	104	5.0	1.5	6.6
x2 HCl	3.5	17	0.40	17	65	5.9	0.60	6.5
neutral	7.0	14	4.6	19	72	5.7	1.8	7.4
Spodosol (Bhs-horizon from Massachusetts, USA)								
no buffer	4.4	20	2.8	23	98	15	6.9	22
x1 HCl	3.5	20	0.60	21	90	19	2.8	21
x2 HCl	3.2	20	1.0	21	91	21	2.8	24
neutral	7.0	16	5.8	21	90	20	4.0	24

[a] HCl-extractable Fe and OC were measured after 0.05M HCl extraction of dithionite residues.
[b] DC-extr. = standard dithionite-citrate extraction (Loeppert and Inskeep, 1996).

The pH of dithionite extracts was measured immediately after the 16-hour extraction and centrifugation step.

A single dithionite extraction was usually sufficient to bleach soils, which indicates near complete dissolution of reducible FeOx phases. The samples with less-bleached appearance after initial dithionite extraction were subjected to repeated dithionite and acid extractions, which released very little Fe from all but the Oxisols that still had red/brown colors (see text below). A few samples high in FeOx had a black precipitate with sulfide odor, presumably implying FeS precipitation during the dithionite

extraction. Repeated 1-hour acid rinsing (0.05M HCl) of selected dithionite residues confirmed the recovery of most precipitated FeS by a single acid rinse.

Iron extraction efficiency of our method was averaged 98 ± 4% (mean ± SD) of the dithionite-citrate method (Loeppert and Inskeep, 1996) for all the soils studied (Table 4.3). Filtration of the centrifuged extracts by 0.45-μm polycarbonate membrane showed no change in Fe and OC concentrations relative to the supernatants after the centrifugation in a pilot study. Our supernatants likely did not contain colloidal particles, based on the lack of peptizer (e.g., pyrophosphate), presence of salt, and high-speed centrifugation (e.g., Loeppert and Inskeep, 1996; Skjemstad et al., 1989). For five randomly-chosen samples, OC recoveries (the sum of OC dissolved by the dithionite and acid extractions, plus residual OC) were 107 ± 12.8% of total OC concentrations of bulk samples. The precision of the OC and Fe measurements in dithionite and acid extractions was assessed from the replicates of 17 randomly-chosen samples by normalizing the means of all pairs. The coefficient of variation was <6.4% for all analyses except for the acid-extractable Fe alone which had 16.7%. The coefficient of variation for the sum of dithionite and acid extractable Fe was, however, low (6.4%).

OC dissolution is sensitive to solute composition and pH of the system. Not all of the OC dissolved by our dithionite and acid extractions is attributable as Fe-bound OC because some of the OC in soils are soluble in water and exchangeable by oxysulfur anions. Therefore, control extractions of all samples were performed for 16 hours using a 0.049M sodium sulfate solution, after adjusting the pH with HCl to the level found at the end of the dithionite extraction for each sample. The difference in dissolved OC released between dithionite extractions and control extractions (Δ OC = $DOC_{dithionite}$ + DOC_{HCl} –

$DOC_{control} - DOC_{control\text{-}HCl}$) was regarded as Fe-bound OC. Similarly, the difference in dissolved Fe (Δ Fe = $Fe_{dithionite} + Fe_{HCl} - Fe_{control} - Fe_{control\text{-}HCl}$) was regarded as the amount of reducible Fe.

The final pH of the controls were similar to those of the dithionite extracts (Table 4.3). Five samples had >1 pH unit lower in the sulfate control extracts. Lower pH generally causes less OC dissolution. Thus the lower pH of controls likely led to more liberal estimate of Fe-bound OC for these samples. Sulfate and subsequent acid treatments released up to 23 mg g^{-1} of OC representing 12-73% of the OC extracted by the dithionite plus acid treatments (Table 4.3), illustrating the importance of parallel control extractions to accurately estimate the amount of OC attributable to the association with reducible iron. One E-horizon sample of a Spodosol released slightly more OC from the control than from dithionite extractions, which likely result from the low OC concentrations in both extracts.

Concentrations of Fe, Al, Si, and Mn in dithionite, sulfate, and HCl extracts were measured by an inductively-coupled plasma spectrometer (ICP, Thermo Jarrell-Ash Model 975, MA, USA) and those of OC were measured using a Shimadzu TOC 5000 (Kyoto, Japan).

4.3.4. Density separation of selected soils

To quantify the OC associated with soil minerals, particulate organic materials that are little associated with soil minerals were removed from bulk soil for selected samples by a density separation technique, following Golchin et al. (1994). Samples were mixed with 1.6 g cm^{-3} sodium polytungstate solution and treated with ultrasound (656 J mL^{-1}) using a Fisher-Artek-Dynatech Model 300 sonicator with 19-mm diameter tip.

Table 4.3: Results from the dithionite plus weak acid and control (sulfate plus weak acid) extractions.

Sample ID	Dith. pH	Sulfate pH	DC-extr Fe[a]	Dith+HCl extr Fe	Sulf+HCl extr Fe	ΔFe[b]	Dith+HCl extr OC	Sulf+HCl extr OC	ΔOC[b]	ΔOC / ΔFe	Total Fe[c]	Dith+HCl extr Al	Sulf+HCl extr Al
			---------- (mg g^{-1}) ----------							(g:g)	------- (mg g^{-1}) -------		
Ent	6.2	5.0	7.6	8.8	0.94	7.8	11	2.3	9.0	1.2	30	2.2	2.1
Inc-1E	3.8	3.7	8.0	8.5	0.53	7.9	3.1	2.0	1.0	0.13	33	1.6	1.1
Inc-1Bw	4.1	3.1	41	48	2.2	46	12	5.8	6.6	0.14	76	8.4	2.4
Inc-2	4.0	3.5	15	9.0	0.59	8.4	4.9	3.4	1.5	0.18	34	2.3	1.0
Inc-3	3.7	4.6	20	16	0.88	15	4.1	3.0	1.1	0.07	35	7.6	5.6
Inc-4	3.7	4.1	39	40	0.70	39	16	7.3	8.6	0.22	62	16	9.7
Inc-5	3.5	3.7	27	25	1.8	24	10	3.8	6.4	0.27	58	2.8	1.3
Inc-6	4.2	3.9	12	9.7	1.1	8.5	3.9	2.0	1.8	0.22	15	1.3	0.64
Inc-7	3.5	3.6	1.2	1.2	0.14	1.1	9.8	2.7	7.0	6.56	6.8	0.51	0.45
Alf-1	4.1	3.5	9.5	9.2	0.43	8.7	9.2	5.3	3.9	0.45	20	3.9	2.4
Alf-2	4.4	4.3	10	9.7	0.30	9.4	1.7	1.1	0.6	0.06	25	2.4	B.D
Alf-3	3.9	3.9	20	14	1.6	12	2.0	0.7	1.3	0.11	32	1.8	0.80
Alf-4	3.8	3.6	33	32	0.63	31	4.8	1.6	3.2	0.10	67	3.4	0.4
Mol-1	4.0	3.9	8.0	9.5	0.11	9.4	2.0	0.9	1.1	0.12	19	1.0	0.34
Mol-2	4.4	4.4	8.5	12	0.13	12	2.3	1.4	0.9	0.08	22	2.3	0.93
Ult-1	3.4	3.5	25	24	0.31	24	5.3	3.2	2.0	0.08	47	7.8	3.6
Ult-2	3.8	3.8	24	20	1.0	19	8.0	3.4	4.6	0.25	46	2.8	1.4
Ult-3	3.0	3.4	32	33	0.31	33	4.4	3.2	1.2	0.04	66	8.6	3.8
Ult-4	6.2	5.4	26	25	0.43	24	6.4	2.0	4.3	0.18	32	4.9	1.4
Ox-1	5.5	4.2	145	107	0.18	106	8.0	3.0	5.0	0.05	251	8.4	1.5
Ox-2	6.1	4.8	132	195	0.10	194	6.7	1.1	5.6	0.03	253	14	N.D.
Ox-3	3.3	3.5	134	108	0.10	107	2.1	1.1	1.0	0.01	184	4.4	0.85
Ox-4	6.7	6.0	245	185	0.12	185	13	1.5	11	0.06	388	11	0.14
Spd-1E	3.1	3.1	1.0	1.5	0.02	1.5	0.4	0.7	-0.3	N.D.	4.7	0.16	0.17
Spd-1Bhs	4.4	4.2	24	23	1.9	21	22	6.4	16	0.74	28	4.8	2.5
Spd-2B1	4.3	4.4	25	23	2.0	21	22	12	10	0.48	32	7.9	5.6
Spd-2B2	4.5	3.9	21	20	1.5	19	14	6.9	7.6	0.40	54	6.4	4.4
Spd-3B1	4.6	4.3	31	32	1.7	30	39	17	22	0.73	40	16	9.6
Spd-3B2	4.6	4.5	19	20	0.62	20	43	23	20	1.0	45	22	16
Ando	6.2	4.2	179	142	1.7	141	28	6.9	19	0.14	206	20	5.2

Dith = dithionite. Sulf = sulfate. DC = dithionite-citrate. N.D. = not determined. B.D. = below detection.

[a] DC-extr. Fe = iron extracted by the standard dithionite-citrate technique (see Methods).

[b] Δ OC = Fe-bound OC = $OC_{dithionite} + OC_{HCl} - OC_{control} - OC_{control\text{-}HCl}$.
Δ Fe = reducible Fe = $Fe_{dithionite} + Fe_{HCl} - Fe_{control} - Fe_{control\text{-}HCl}$.

[c] Total Fe includes pedogenic FeOx and structural iron in primary and secondary minerals.

Settled materials in the sodium polytungstate solution after the sonication were rinsed with deionized water and centrifuged repeatedly, and then freeze-dried for total OC and N analysis.

4.3.5. Surface area analysis

To estimate the specific surface area of the FeOx phases dissolved by the dithionite treatment, soil sample surface area was measured by the N_2 gas sorption technique (Mayer, 1999) before and after the dithionite plus acid treatments. Five soil samples were randomly chosen from fine-textured samples to achieve accurate surface area measurement. Bulk samples and their dithionite residues were outgassed under vacuum at room temperature to remove water. The gas sorption analysis was conducted using a Quantachrome A-1 Autosorb (Quantachrome Corp., Syosset, NY, USA) under a series of N_2 pressures. Surface area values were determined from the Brunauer-Emmett-Teller (BET) equation (Brunauer et al., 1938). Specific surface area of reducible FeOx phases (SSA_{FeOx}) was estimated based on Borggaard (1982):

$$SSA_{FeOx} = (SSA_{bulk} - SSA_{dithionite+HCl\ residue}) / [\text{dissolved Fe}]_{dithionite+HCl} \times (AW_{Fe} / MW_{FeOOH}).$$

For $SSA_{dithionite+HCl\ residue}$, we corrected for the weight change during the dithionite and subsequent acid extractions using the sum of dissolved organic matter (assuming

50% OC), Fe, Al, Si, and Mn. Dissolved Fe was assumed to derive from goethite (FeOOH) with a molecular weight of 88.85.

4.3.6. Other analyses

Dried bulk soil samples (2-mm sieved) were measured for soil pH in deionized water after 1-hour equilibration. Total OC and N in dried samples were analyzed using a Perkin-Elmer 2400 CHN analyzer (Perkin-Elmer, Norwalk, CT, USA) after removal of carbonate by fuming with hydrochloric acid (Mayer, 1994). Total Fe concentrations were measured by ICP after dissolution by a sodium peroxide fusion method (detection limit = 0.05%, ALS Chemex, Sparks, NV, USA).

4.4. Results and Discussion

4.4.1. Fe-bound OC

The net mass of solubilized OC attributable to Fe(III) reduction (Δ OC) ranged from 0.4 to 43 mg g^{-1} (Table 4.3). The fraction of total soil OC explained by Fe-bound OC was always low (<25%) except for one FeOx-rich Oxisol (37%, Figure 4.1). Thus direct association of OC to reducible iron had only a minor role in bulk OC storage for virtually all the soil samples examined here, supporting our hypothesis.

These conclusions assume that a single dithionite extraction was sufficient to remove all the reducible iron from the samples. Repeated dithionite extractions for selected samples showed almost complete extraction by the single treatment (see Methods) except for highly weathered Oxisols. For the two Oxisols tested, OC release significantly dropped while iron dissolution rate continued strongly over three extractions

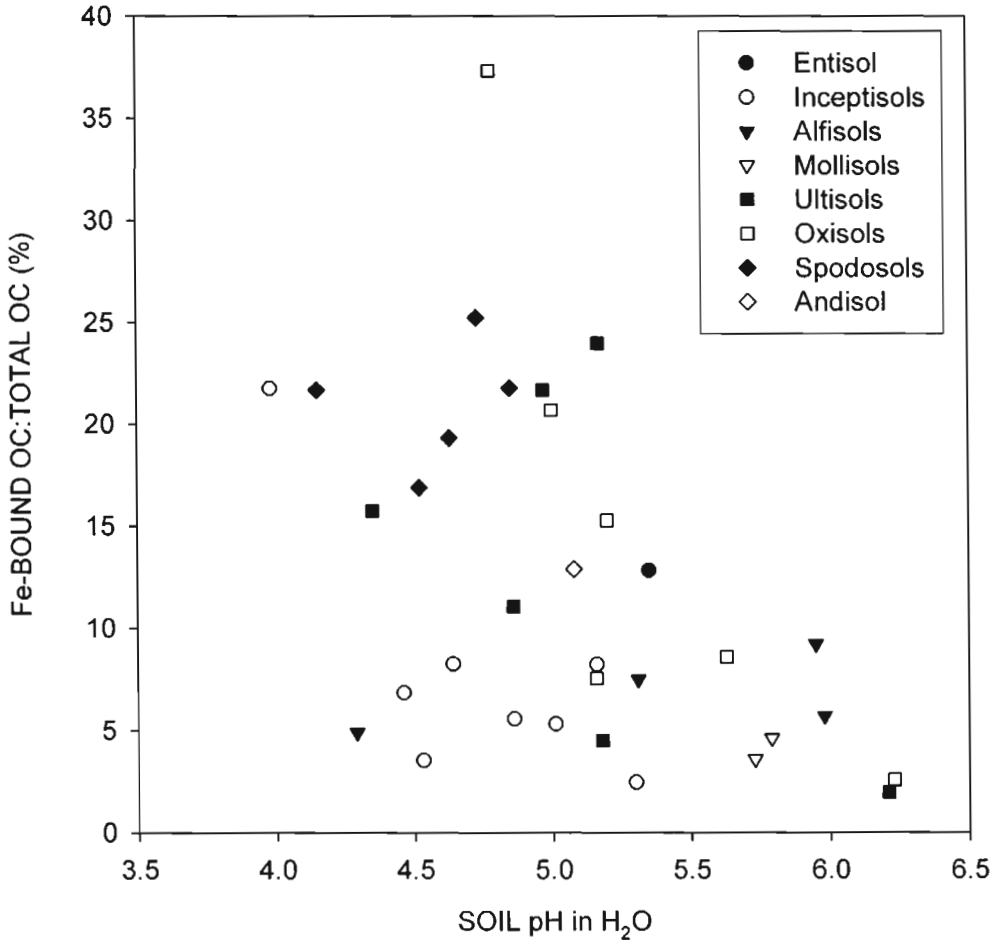

Figure 4.1: Fraction of total OC that was attributable to Fe association against soil pH in deionized water.

(Table 4.4), suggesting that the most easily reducible Fe phase (i.e., first extract) was enriched in OC. The Puerto Rican Oxisol released only a minor fraction of bulk OC during the three extractions. The Kinabalu Oxisol, however, released half of the bulk OC (Table 4.4), suggesting that the most easily reducible Fe phase (i.e., first extract) was enriched in OC. The Puerto Rican Oxisol released only a minor fraction of bulk OC during the three extractions. The Kinabalu Oxisol, however, released half of the bulk OC and may have yielded more with further extractions. The high proportion of Fe-bound OC in the Kinabalu Oxisol is reasonable as it consists of essentially pure FeOx. For the rest of the Oxisols, total iron concentrations were used to extrapolate a potential upper limit for Fe-bound OC. If we assume that all of this iron was in an FeOx form and had a similar OC:Fe ratio as the single dithionite-extractable fraction, still only a minor fraction of TOC (4-18%) could be bound to these iron phases. Thus only in the Kinabalu Oxisol sample was dithionite-reducible or total Fe able to account for more than a minor fraction (~50%) of the bulk soil OC.

Bulk soil includes mineral-free particulate OC as well as mineral-associated OC. Does the Fe-bound OC account for a major fraction of mineral-associated OC, the fraction of SOM likely representing long-term storage (e.g., Baisden et al., 2002)? After correcting total OC for the light-density fraction (plant detritus and possibly charred material), still only 10-32% of mineral-associated OC was accounted for as Fe-bound OC for the 12 samples, excluding the Kinabalu Oxisol, for which density separation data are available (Table 4.1). The light fractions typically have much higher C:N ratios (25-70)

Table 4.4: Repeated dithionite and acid extractions of two Oxisol samples.

	Dith-extr Fe	HCl-extr Fe	Dith-extr OC	HCl-extr OC	Dith+HCl extr OC	Sulfate+HCl extr OC	Δ OC	Δ OC rel. to TOC
	---------- (mg g^{-1}) ----------							(%)
Puerto Rican Oxisol (Ox-1)								
1st extraction[a]	70	20	4.1	3.4	7.5	3.0	4.5	6.8
2nd extraction	69	15	0.72	2.5	3.2	1.3[b]	1.9	2.9
3rd extraction	37	7.1	0.16	0.82	1.0	0.39[b]	0.59	0.9
sum	176	42	4.9	6.7	11.7	4.7	7.0	10.6
Kinabalu ultrabasic Oxisol (Ox-4)								
1st extraction[a]	103	48	5.2	4.5	9.8	1.5	8.3	28
2nd extraction	101	33	0.64	3.4	4.0	0.6[b]	3.4	11
3rd extraction	45	7.6	1.8	2.1	3.9	0.6[b]	3.3	11
sum	249	88	7.7	10.0	17.7	2.6	15.0	50

[a] The difference in the OC and Fe concentrations in the first extractions and those in the corresponding samples in Table 3 derive from subsampling and/or analytical errors.

[b] Control extractions (sulfate and HCl) were not conducted for the residues from the second and third dithionite extractions. Sulfate plus HCl extractable OC was assumed to be proportional to the first extractions as follows:
$[\text{sulfate+HCl-extr OC}]_{2\text{nd extr.}} = [\text{dithionite+HCl-extr OC}]_{2\text{nd extr.}} * [\text{sulfate+HCl-extr OC}]_{1\text{st extr.}} / [\text{dithionite+HCl-extr OC}]_{1\text{st}}$
$[\text{sulfate+HCl-extr OC}]_{3\text{rd extr.}} = [\text{dithionite+HCl-extr OC}]_{3\text{rd extr.}} * [\text{sulfate+HCl-extr OC}]_{1\text{st extr.}} / [\text{dithionite+HCl-extr OC}]_{1\text{st}}$

than mineral-associated fractions (10-20) and account for a minor fraction of total OC except in some allophanic or organic soils. Most of the samples for which density separation data are unavailable had relatively low C:N ratios, and those with high C:N (> 25) contained <4% of total OC in association with iron. Thus our conclusions likely apply to the mineral-associated OC for all of our samples except for the Kinabalu Oxisol.

The highest contributions of Fe-bound OC were found in low pH soils (Figure 4.1). This trend appeared strong for Oxisol and Ultisol samples. The OC-enriched, subsurface horizons of acid soils (all spodic horizons and the most acidic Inceptisol sample) showed consistently high, Fe-bound OC relative to total OC. The solubility of FeOx phases increases with decreasing pH below 6-7 (Stumm and Morgan, 1996),

implying that dissolved Fe increases in importantce for organo-iron association relative to solid FeOx phases (discussed below). While our sample number is quite limited, our results also suggest a possible linkage between organo-iron associations and soil development. Fe-bound OC accounted for higher fraction of total OC only in the highly-weathered or strongly-leached end-member soils where base elements are largely leached via acidification, an important pedogenic process under humid regimes (Chesworth, 1992).

4.4.2. Soil depth series

Soil OC storage generally decreases with depth, but greater fractions of total OC are likely stabilized by minerals in subsurface horizons (e.g., Kaiser et al., 2002; Eusterhues et al., 2003). Thus we selected three soil types with high pedogenic FeOx to examine Fe-bound OC at depth. From the surface to 1-m depth of the Kinabalu Oxisol, progressively smaller fractions of total OC were released by a single dithionite extraction with depth (Table 4.5). The actual amount of Fe-bound OC at depth in this Oxisol is unclear, however, because repeated dithionite extractions were not performed.

On the other hand, a single dithionite treatment was sufficient to fully dissolve pedogenic FeOx from a kaolinitic Kinabalu Ultisol which showed increasing contribution of Fe-bound OC to total OC with increasing depth (Table 4.5). Yet the contribution was still minor (24% of the total OC). While eluviated horizons of an Inceptisol and Spodosol contained little Fe-bound OC, their underlying horizons with high accumulation of illuviated iron contained much more, accounting for 22-24% of the total OC (Table 4.3). The other B horizons of Spodosols also consistently showed relatively high contributions

Table 4.5: Soil depth trends in the dithionite and sulfate control extractions.

Soil sample depth (cm)	Soil pH in H_2O	Dith+HCl extr Fe	Sulfate+HCl extr Fe	Dith+HCl extr OC	Sulfate+HCl extr OC	Δ OC	Δ OC rel. to TOC (%)	Δ OC / Δ Fe (g:g)
		---------- (mg g^{-1}) ----------						
	Kinabalu ultrabasic Oxisol (Ox-4)							
0-10	4.8	185	0.12	12.6	1.5	11.2	34	0.06
20-40	5.0	212	0.17[a]	2.3	0.28	2.0	21	0.01[b]
80-100	5.2	257	0.21[a]	0.48	0.08	0.40	15	<0.01[b]
	Kinabalu sedimentary Ultisol (Ult-4)							
0-10	4.4	25	0.43	6.4	2.0	4.3	16	0.18
20-40	5.0	26	0.45[a]	3.1	0.96	2.2	22	0.09[b]
60-80	5.2	29	0.52[a]	1.8	0.55	1.3	24	0.04[b]

[a] Iron concentrations in the sulfate and subsequent acid extractions were not measured but assumed to be proportional to the ratio of dithionite+HCl to sulfate+HCl extractable Fe at the top horizon as follows:
$[\text{sulfate+HCl-extr Fe}]_{x\text{-}y\,cm} = [\text{dith+HCl-extr Fe}]_{x\text{-}y\,cm} * [\text{sulfate+HCl-extr Fe}]_{0\text{-}10cm} / [\text{dith+HCl-extr Fe}]_{0\text{-}10cm}$

[b] Δ OC:Δ Fe ratios for deeper samples used estimated Fe values for the sulfate+HCl extractions. This iron estimation unlikely causes significant changes in the OC:Fe ratios due to much greater Fe values from the dithionite extraction (see text).

of Fe-bound OC (19-25%), with deeper sections of illuvial horizons having slightly less (Table 4.3). These results are consistent with well-known importance of extractable phases of Fe and Al in subsurface OM accumulation in podzolic soils (Buol et al., 1989).

4.4.3. OC:Fe ratios and the nature of the association

The ratios of OC to iron in the extracts (Δ OC: Δ Fe in Table 4.3) provide insight into the potential nature of the organo-iron associations if compared to these ratios from reported sorption experiments. The maximum sorption of natural organic matter (OM) onto FeOx phases at pH 4-7 reported in the literature is 0.22 g-OC g-Fe^{-1} (K. Kaiser, *personal comm.*) where freshly-precipitated ferrihydrite with a specific surface area of 224 m^2 g^{-1} FeOx was used as the adsorbent and dissolved OM from a temparate forest O-horizon as the adsorbate. Sorptive capacity of mineral phases generally increases with decreasing pH (e.g., Schulthess and Huang, 1991). At lower pH, however, certain adsorbents such as metal oxides become unstable and metals dissolve to form metal-orgnanic complexes. Thus it becomes difficult to distinguish OC sorption onto FeOx surfaces from the precipitation of dissolved iron complexed with OC (more discussion later). Here I simply used a constant maximum sorptive capacity as an inititial approximation. This sorption capacity corresponds to a volumetric ratio of 1.0 OM:FeOx assuming that OM is 50% C, the density of soil OM is 1.4 g cm^{-3} (Mayer et al., 2004), and FeOx consists of FeOOH with a density of 4.0 g cm^{-3}. In other words, laboratory experiments indicate that FeOx phases can adsorb only up to approximately their own volume in organic matter. This point will be discussed later.

All of our soils but the Spodosols, the Entisol, and one each of the Alfisols and Inceptisols showed OC:Fe ratios below this maximum sorption capacity (Figure 4.2). Sorption of OM onto FeOx is thus a plausible mechanism for the association between these two phases for these samples, consistent with inferences drawn from correlation studies (Kaiser and Guggenberger, 2000; Kaiser et al., 2002; Kiem and Kögel-Knabner, 2002; Eusterhues et al., 2003; Wiseman and Püttmann, 2004). The limited contribution of this sorption mechanism to bulk OC storage in our soil samples (Figure 4.1) is thus limited by the amount of FeOx, a point that is emphasized by the dominant role of FeOx in OM storage in the surface horizon of Kinabalu Oxisol composed of essentially pure FeOx.

With increasing depth of the Kinabalu Oxisol and Ultisol up to one meter, OC:Fe ratios appear to decrease and remain well below the sorption capacity (Table 4.5). The OC:Fe ratios from the deeper horizons were calculated with the assumption that the ratio of $Fe_{dith+HCl}$ to $Fe_{sulfate+HCl}$ is constant with depth for each soil. The latter ratio for all the surface horizons of Oxisols and Ultisols determined was high (20-2000, Table 3), and thus even a 10-fold overestimation in $Fe_{sulfate+HCl}$ concentration would not increase the delta OC:Fe values above the sorption capacity for both soils. While Fe-bound OC in the Kinabalu Oxisol may be underestimated (discussion above), sorptively-stabilized OC onto FeOx appears to play a minor role in bulk OC storage at all studied depths of the Kinabalu Ultisol.

All of the spodic horizons, the Entisol, an uncultivated Alfisol and a tropical-forest Inceptisol had OC:Fe ratios higher than have been found in sorption experiments (Figure 4.2). Therefore, some of the dithionite-extractable OC must be associated with Fe

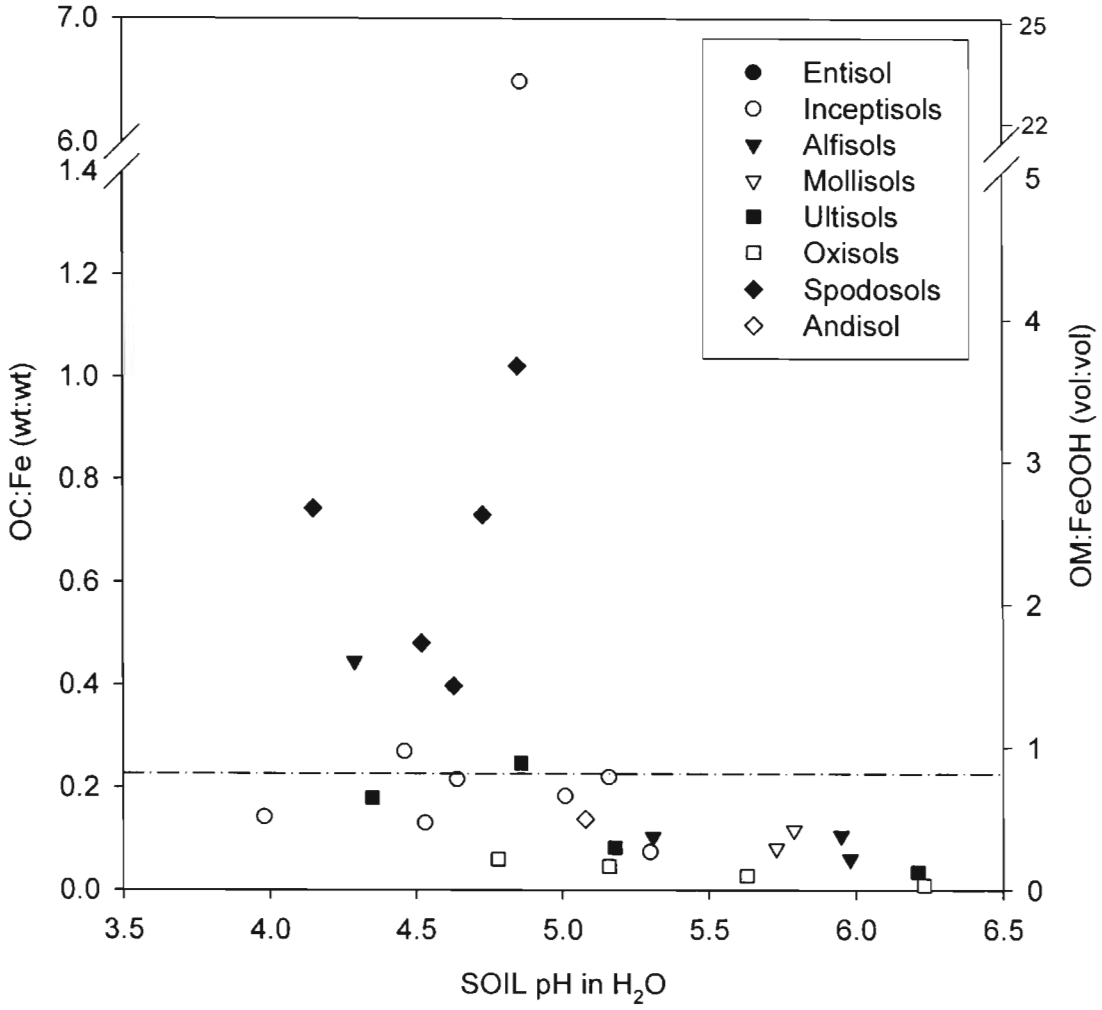

Figure 4.2: The mass ratio of OC to Fe (left axis) and volumetric ratio of organic matter to FeOx (right axis) of the material attributable to organo-iron associations with respect to soil pH in deionized water. These ratios were calculated from ΔOC and ΔFe in Table 4.3. The horizontal line represents the maximum sorptive capacity of FeOx phases: 0.22 g-OC g-Fe^{-1} = 1.3 mm^3 OM (mm^3 FeOOH)$^{-1}$ from sorption experiments (K. Kiser, *personal comm.*).

via non-sorptive mechanisms that allow greater masses of OC binding per unit mass of Fe(III). These soil samples with high ratios all had lower pH (Figure 4.2), consistent with the calculations that lower pH favors complexation of Fe with organic matter while higher pH favors adsorptive association between FeOx and organic materials (Tipping et al., 2002). Field observations from a range of surface soils (Skjemstad et al., 1989) and suspended river materials (Allard et al., 2004) support pH control of this trend in organo-iron association mechanisms. Complexation may protect organic matter via a mechanism analogous to metal tanning, in which monomers and oligomers of metals, especially trivalent metals, form extensive cross-links among organic molecules that prevent enzymatic attack on the organic moieties. Both iron and aluminum have been used in commercial tannages.

The range and variation in OC:Fe ratios for organo-Fe complexes occurring in field soils are not clear despite the extensive studies on this topic, particularly for podzolic soils. Theoretical OC:Fe ratios for organo-metal complexes have been calculated to be at least 1.3-2.2 (wt:wt), based on assumptions on charge balance and organo-metal stoichiometry (Oades, 1989, and references therein). These minima are 6-10 fold higher than the maximum sorption ratio. Using dissolved OM from a forest floor, experimental addition of dissolved iron showed a removal of >75% of dissolved iron from aqueous phase as organo-Fe precipitates at the OC:Fe ratio <7 (wt:wt) at pH 3.5-4.5 (Nierop et al., 2002). Equilibrium model calculations, however, indicate the possible presence of inorganic FeOx phases in the precipitated material at this pH range (Nierop et al., 2002), making it difficult to assess the actual OC:Fe ratios of complex associations. Nevertheless, it appears possible that precipitated organo-Fe complexes can have OC:Fe

ratios below the maximum sorption capacity. Thus, while our OC:Fe ratios above the maximum sorption capacity imply the presence of organo-Fe complexes, those below the sorption capacity do not necessarily indicate the presence of FeOx-sorbed OC. Sorptively-stabilized OC may thus represent even lower fractions of the total OC than shown in Figure 4.1.

Most of the low pH (< 4.5) samples with OC:Fe ratios below the maximum sorption capacity (Figure 4.2) had low total OC concentration (< 30 mg g^{-1}), suggesting that organic supply limits organo-Fe complex formation. All of the samples with high OC:Fe ratios were found in soils with higher OC concentrations (Figure 4.3). Thus our results support the conceptual model that iron shifts from FeOx to organo-Fe complexes with increasing OC supply (Schwertmann et al., 1986). In general, the supply of either OC (organic acids), dissolved Fe, or oxygen likely limit complex formation (Skjemstad et al., 1989). Under humid regimes, high SOM concentration often results from inefficient microbial decomposition due to cooler climate, which promotes organic acidity. Low pH, in turn, retards microbial degradation of OC (e.g., Motavalli et al., 1995), making it difficult to assess the causality between high OC and low pH. Nevertheless, both low pH and high total OC concentration appear to be prerequisites for organo-Fe(III) complex formation among the studied soil samples.

Our measurements of OC:Fe ratios directly from organo-iron associates in soils provide a way to compare the nature of organo-mineral associations across systems. The ratios of total OC to dithionite-extractable Fe for iron-rich precipitates in spring water and small streams ranged from 0.03 to 0.19 (Carlson and Schwertmann, 1980 and 1981;

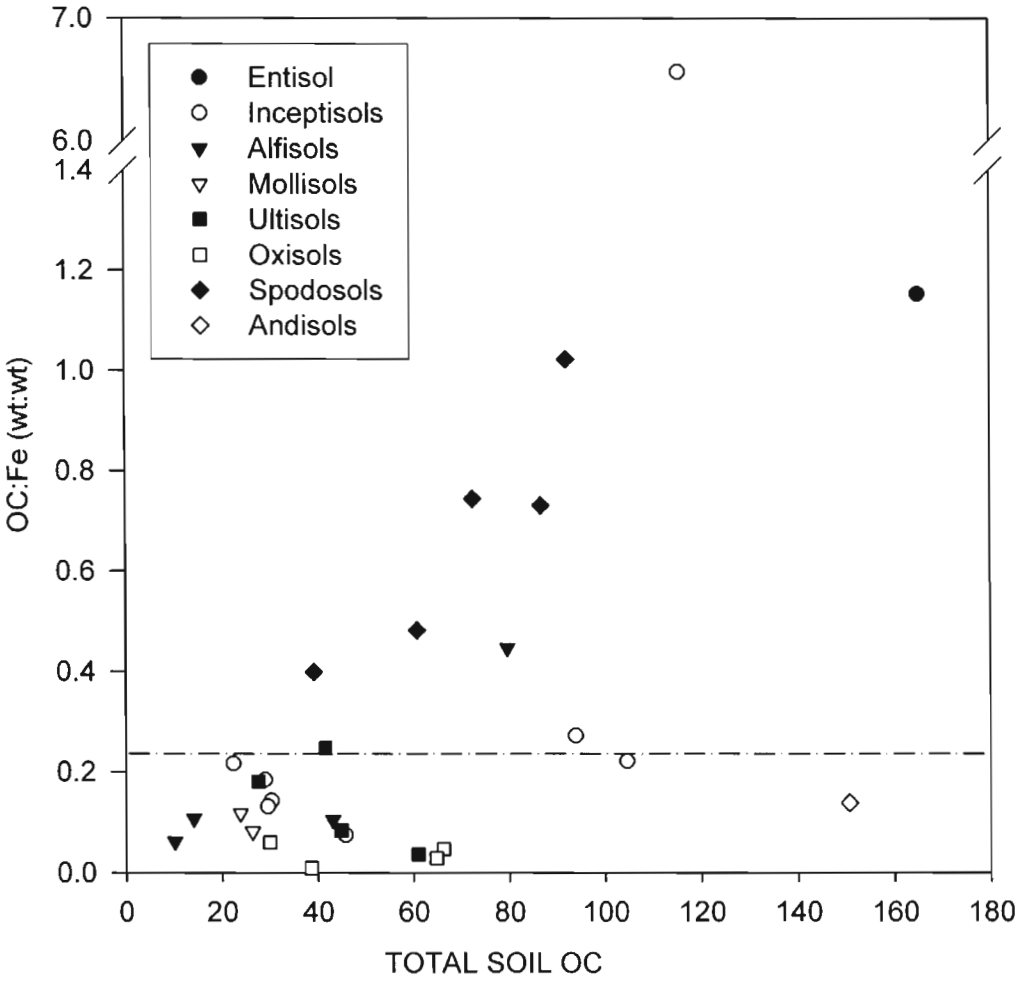

Figure 4.3: The mass ratio of OC to Fe of the material attributable to attributable to organo-iron associations against total soil OC concentration. The horizontal line represents the maximum sorption capacity of iron oxide phases (see Fig. 4.2).

Rhoton et al., 2002), consistent with sorption. In the Amazon river systems, Allard et al. (2004) found an abundance of organo-Fe(III) complexes only in acidic, organic-rich water, which reflected the dominance of podzolic soil types in the catchments. Thus both sorptive and complex associations exist in aquatic systems as well as in soils.

4.4.4. Surface characteristics of reducible FeOx and OM loading

We also examined the organo-iron associations in the context of the surface area provided by the reducible FeOx phases and the loading of OC onto these surfaces. We rejected data from two out of the five samples studied because the differences in specific surface area (SFA) before and after the dithionite plus acid treatments were statistically insignificant. Borggaard (1982) estimated the SFA of FeOx phases extracted by dithionite-citrate-bicarbonate (DCB) and organic chelator (EDTA) from temperate and weathered tropical soils. Crystalline and poorly-crystalline FeOx phases had mean SFA of 84 and 519 m^2 g-$FeOx^{-1}$, respectively, assuming FeOx consists of FeOOH (Borggaard, 1982). We found a low SFA of 88 m^2 g-$FeOx^{-1}$ for reducible FeOx in the Kinabalu Oxisol, which consists mainly of goethite and hematite, consistent with crystalline FeOx (Borggaard, 1982). The Kinabalu Ultisol (kaolinitic) and Bw horizon of the acidic Inceptisol had much smaller concentrations of reducible FeOx with higher SFA (123-281 m^2 g-$FeOx^{-1}$), implying less-crystalline FeOx phases. In fact, citrate alone extracted virtually all the dithionite-extractable Fe from the Kinabalu Ultisol (data not shown), indicating a poorly-crystalline nature for the reducible FeOx phases.

The OC loading onto the reducible FeOx surfaces ranged from 0.35 to 0.73 mg OC $(m^2\ FeOx)^{-1}$ and the samples that released higher OC:Fe ratio materials appeared to

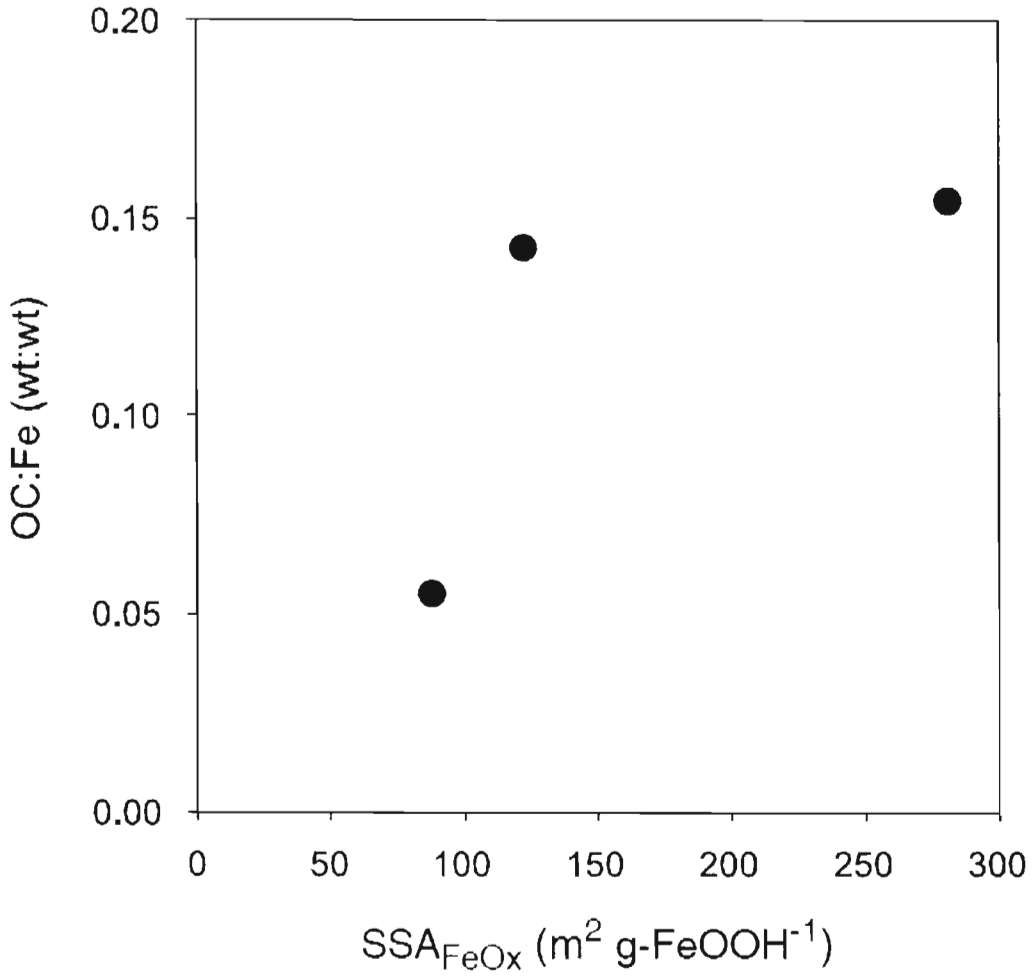

Figure 4.4: The mass ratio of OC to Fe of the material attributed to organo-iron associations with respect to the specific surface area of reducible FeOx phases for the three samples (Inc-Bw, Ult-4, and Ox-4 in Table 4.1 and 4.3).

have higher SFA_{FeOx} (Figure 4.4), implying that smaller-sized or more porous FeOx phases have higher OC sorption capacities. While this generalization is not strong based on three data points, our results are consistent with the experiments demonstrating higher $OC:SFA_{FeOx}$ ratios for ferrihydrite than for goethite sorption (Tipping, 1981; Kaiser et al., 1997), and strong sorptive affinity of microporous FeOx for dissolved OC (Kaiser and Guggenberger, 2003).

4.4.5. Aluminous phases

AlOx and amorphous aluminosilicate phases provide other reactive adsorbants for SOM, and are often considered with FeOx phases (e.g., Torn et al., 1997; Kaiser and Guggenberger, 2000). Lack of specific inorganic extractants, analogous to dithionite for iron, prevented us from similarly testing their potential role in SOM preservation. Co-dissolution of aluminum upon the reductive dissolution of FeOx phases, on molar basis, accounted for 20.4 ± 15.2% of reducible metal oxide phases for all the samples and 36.5 ± 15.9% for spodic horizons (Table 4.3). Similar levels of aluminum substitution in FeOx, particularly in goethite, have been reported (Schwertmann, 1988). Allophanic and imogolitic material, occasionally important in spodic horizons, was minimally present or not extractable by our treatments in our spodic samples, as the silica dissolution was low.

The acid rinsing treatments were done at pH = 1.3, at which significant dissolution of AlOx is expected. The acid-dissolution of Al from sulfate-extraction residues correlated very strongly with OC dissolution across all of our samples ($[OC]_{control\text{-}HCl} = 1.60*[Al]_{control\text{-}HCl} - 0.23$. $R^2 = 0.87$, $p < 0.001$). This correlation suggests a potential importance of organo-aluminum association in our soil samples. Similarly, in

spodic horizons of Australia, weak acid extractions (0.01-0.5M HCl) led to a significant co-dissolution of OC and Al but not Fe (Skjemstad et al., 1992), which was mainly attributed to the hydrolysis of organo-Al complexes (Skjemstad, 1992). We assumed that all the acid-extracted OC was bound to aluminum to assess the possible extent of sorptive OC preservation by the acid-labile AlOx phases in the same way that we examined for the OC-Fe relationship for reducible iron phases. The ratios of OC:Al in our acid extracts mostly exceeded the maximum sorptive capacity of amorphous AlOx phases from sorption experiments, 0.82 g-OC g-Al^{-1} (Kaiser et al., 1997) (Figure 4.5). Similar to the relationship between the OC:Fe ratio of dithionite-reducible phases with pH (Figure 4.2), lower soil pH generally corresponded to higher OC:Al ratio (Figure 4.5). The solubility of AlOx phases and activity of Al^{3+} are greater at lower pH (Stumm and Morgan, 1996). Together with the fact that low pH generally corresponds to high SOM and supply of organic acids (e.g., Figure 4.2 and 4.3), the observed OC:Al ratios above the maximum sorption range suggest organo-aluminum complexes.

For all of our samples except for the spodic horizons, the acid-labile OC accounted for < 4% of the total OC. For the spodic horizon samples, in contrast, 5-35% of the total OC was explained by the acid-labile phase, in accordance with the well-known importance of organo-aluminum associations in spodic horizons (Skjemstad, 1992; Lundström et al., 2000). Among the spodic horizons, the molar OC:Al ratios of the acid-extractable phases (5.2 ± 1.2) were similar to the molar OC:Fe ratios of dithionite-reducible phases (3.2 ± 1.2), and these ratios were consistently greater than those of the maximum molar sorptive capacities of FeOx (1.0) and AlOx phases (1.8), respectively, from sorption experiments. These results further support the overall importance of

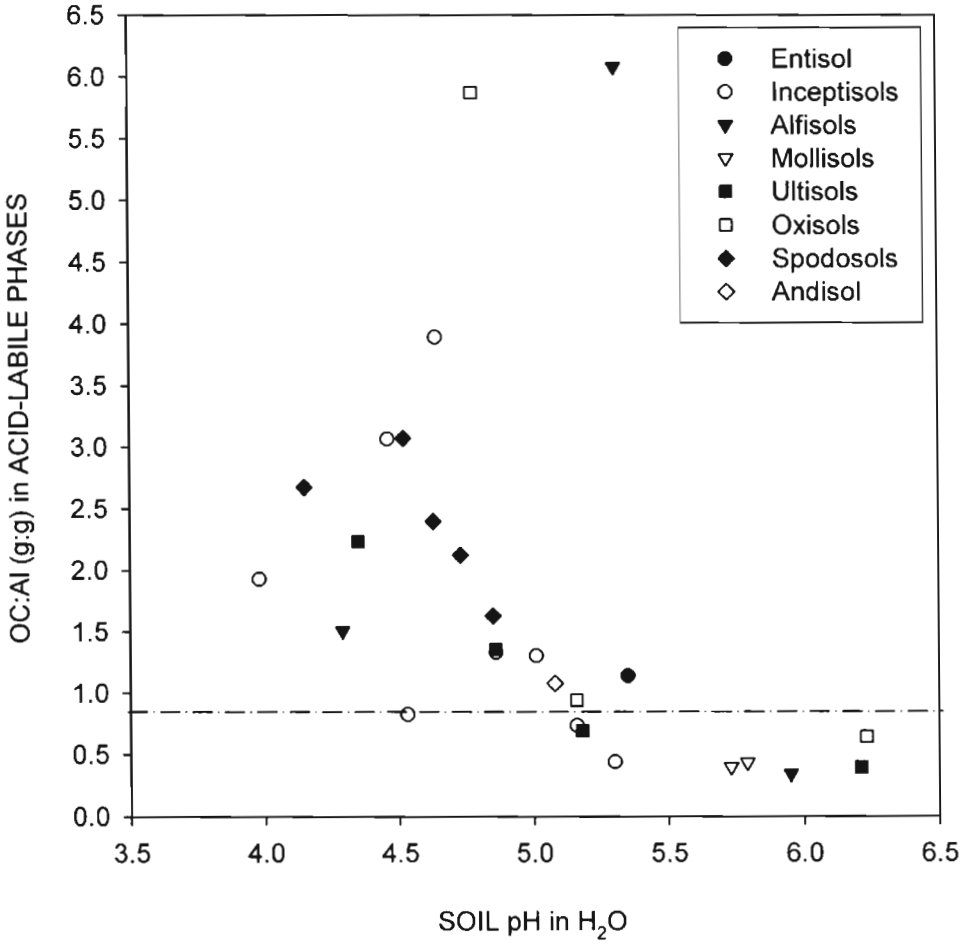

Figure 4.5: The mass ratio of OC to Al of the material extracted by the acid rinse treatment of sulfate-control residue from each sample with respect to bulk soil pH in distilled water. The horizontal line represents the maximum sorptive capacity of AlOx phases (0.82 g-OC g-Al^{-1}) from sorption experiments (Kaiser et al., 1997).

organo-metal complexes in spodic horizons. The relative affinity of dissolved metals to OC can be controlled by many factors such as the type of organic acids, OC:metal ratio, pH, and redox condition (e.g., Skjemstad et al., 1989; Nierop et al., 2002). The relative significance of Fe and Al in organo-metal complexation, or in SOM storage, is beyond the scope of our study. Nevertheless, the observed correlation and their high OC:Al ratios of acid-labile phases (Figure 4.5) as well as findings from other studies including non-spodic soils (e.g., Shang and Tiessen, 1998; Percival et al., 2000; Masiello et al., *in press*) suggest the importance of organo-aluminum association, particularly via complexation, for SOM storage and dynamics.

4.4.6. Implications for OC:Fe correlations in soils

We calculated the volumetric ratios of organic matter (OM) to FeOx and AlOx for soils in the literature where OC-metal correlations were reported, based on the assumptions used earlier, to gain insight into the geometric relationship between OM and metal oxide phases. Adsorbates are generally smaller than adsorbants. The volumetric ratios of OM:FeOx and OM:AlOx calculated from the reported sorption experiments (Tipping, 1981; Kaiser et al., 1997) were <1.0, indicating that organic adsorbates likely have no greater volume than the FeOx and AlOx adsorbants. These ratios, calculated from correlation slopes, for virtually all the reported soils and their physical fractions indicate organic matter volumes that are many times greater than the FeOx and AlOx adsorbants (Table 4.6). Only in one heavy fraction of an Ultisol (Spycher and Young, 1979) were the OM:FeOx ratios close to the sorptive capacity. These patterns imply generality of our conclusion that simple OC adsorption to FeOx phases accounts for only

a minor fraction of bulk OC storage. Guggenberger and Kaiser (2003) suggested the limited sorptive capacities of some temperate acid soils to store bulk OC based on the extrapolation of the sorption maxima measured using field soil horizons. To the extent that OC sorption is largely controlled by the amount of extractable FeOx and AlOx phases in these soils (Kaiser and Guggenberger, 2000), their findings are consistent with our conclusion.

Combining FeOx and AlOx, the ratios of OM to metal oxides decreased, yet still only a few volcanic and spodic soils showed ratios consistent with sorptive preservation (Table 4.6). For the rest of the soils, we need to consider more complex mechanisms, besides simple sorption to metal oxide phases, to enable the storage of a several-fold greater volume of OM per unit volume of metal oxides. Extractable FeOx and AlOx phases in soil matrices are often found as coatings of phyllosilicate clays, and are effective aggregation agents for these clays (Pinheiro-Dick and Schwertmann, 1996). In fact, ternary OM-FeOx-clay associations have been considered important for soil microaggregate formation (Krishna Murti and Huang, 1987; Oades, 1984; Vrdoljak and Sposito, 2002) and OM stabilization in weathered soil (Shang and Tiessen, 1998). Despite the significantly lower sorptive capacity of phyllosilicate clays compared to FeOx and AlOx phases, clay minerals are planar and have high surface-to-volume ratios, effective traits to physically reduce enzyme and oxygen accessibility to OM. Thus the combination of highly-reactive metal oxides with less sorptive yet extensive clays may physically protect large volumes of insoluble OM. Commonly-found covariations of OC-texture (Burke et al., 1989; Homann et al., 1998; Telles et al., 2003), Fe-texture (e.g., Birkeland, 1999), and OC-Fe and Al (discussed above) across a wide range of soils are

Table 4.6: The volumetric ratios of organic matter (OM)-to-metal oxides in bulk soils and their physical or chemical fractions reported in the literature. The ratios where positive correlations were found between OC and metal concentrations are shown in bolds.

General soil type	Horizon or depth	N	Physical fraction of soil analyzed [a]	Extractant used for metal [b]	Ratio of OM to FeOx [c] (vol:vol)	Ratio of OM to AlOx [d] (vol:vol)	Ratio of OM to FeOx+AlOx (vol:vol)	Data source
Eight soil orders	A-B	168	bulk	DC	**3.7**	15	2.9	Tiessen et al. [1984]
Nine soil orders	A	122	bulk	oxalate	5.0-110[e]	**2.8-49**	2.4-16	Percival et al. [2000]
			bulk	pyrophos.	5.0-110[e]	**7.3-74**	3.4-18	Percival et al., [2000]
A range of NE Australian soils	A	36	bulk	DC	3.3	**16.0**	2.7	Skjemstad et al. [1989]
			bulk	oxalate	17.5	**12.0**	7.2	Skjemstad et al. [1989]
			bulk	pyrophos.	64.0	**32.0**	22.0	Skjemstad et al. [1989]
Soils from Oregon	A	3	<2μm, heavier frac.	acid-labile	0.7-7.1	0.9-3.3	0.5-2.3	Spycher and Young [1979]
Three soil orders from California	top 1m	7	bulk	DC	**9-73**	**10-374**	**8-44**	Masiello et al. [in press]
			bulk	pyrophos.	**32-50**	**7-19**	**6-13**	Masiello et al. [in press]
Five soil orders, Hawaii	top 1m	35	bulk	oxalate	NA	NA	**0.4-3.3** [f]	Torn et al. [1997]
A range of Andisols	A	25	pyrophos.	pyrophos.	**4.6-11** [f]	**1.5-3.5** [f]	**1.1-2.6** [f]	Wada [1995]
Acidic temperate soils	A-B	59	sonic., >1.6 g cm^{-3}	DCB	**5.7-14**	NA	NA	Kaiser and Guggenberger [2000]
Acidic temperate soils	A-C	14	>1.6 g cm^{-3}	oxalate, DCB	**19, 11**	NA	NA	Kaiser et al. [2002]
Acidic temperate soils	A	12	size fractions	oxalate, DCB	**5.4, 6.8**	NA	NA	Kiem and Kögel-Knabner [2002]
Two acidic forest soils	A-C	6	bulk	DCB	**6.0-6.3** [g]	NA	NA	Eusterhues et al. [2003]
Spodosols	B	54	pyrophos.	pyrophos.	**22**	**4.4**	**3.7**	Evans and Wilson [1985]
			pyrophos.	DCB	**5.4**	**2.1**	**1.6**	Evans and Wilson [1985]
Spodosols	B	28	pyrophos. in <2μm	pyrophos	**2.2**	NA	NA	Adams and Kassim [1984]
	B	28	bulk	oxalate	**3.6**	NA	NA	Adams and Kassim [1984]
Weathered tropical soils	A	13	sonic, <2μm	oxalate	**18-103**	**5-52**	**4-35**	Hughes [1982]
Weathered tropical soils	A	2	2-50μm [h]	oxalate	**82-123**	**34-42**	**24-31**	Shang and Tiessen [1998]
			2-50μm [h]	DCB	7.0-7.6	13-27	4.6-5.9	Shang and Tiessen [1998]
Mollisol (Haploboroll)	Ah	1	size & density frac.[i]	oxalate, DCB	6.5-211	20-1000+	5.5-333	Turchenek and Oades [1979]

NA = data not available

[a] sonic = sonication of soil prior to physical separation. pyrophos. = pyrophosphate-extractable OC was measured.

[b] DC = dithionite-citrate. DCB = dithionite-citrate-bicarbonate. Pyrophos. = pyrophosphate.

[c] The maximum sorptive capacity of FeOx phases was 1.0 (vol:vol) based on K. Kaiser (*personal comm.*). see text for the calculation.

[d] $Al(OH)_3$ with the density of 2.4 g cm^{-3} was used for the volume calculation of AlOx.
Then the maximum sorptive capacity of AlOx (*Kaiser et al.*, 1997) was 0.95 (vol:vol).

[e] Fe was reported only for dithionite-citrate extraction, not for oxalate or pyrophosphate extractions.

[f] Fe and Al were assumed to account for half of the extractable Fe plus Al concentrations reported in these studies.

[g] HF-soluble OC was used to estimate the volume of OM associated with FeOx.

[h] 3-4 density fractions of 20-50 μm size aggregates separated from two soils.

[i] density fractions only >2.1 g cm^{-3} were reported here.

consistent with this idea. If true, then multiple mechanisms are likely responsible for the OC-Fe correlations, with the organo-metal complexation particularly important for low pH, organic-rich soils and the ternary OM-FeOx-clay associations for other soils. In other words, FeOx may be critical for bulk OC storage, but not via a direct sorption mechanism.

The correlations between standing stocks of bulk organic matter and iron must, therefore, be explained by mechanisms other than simple, binary sorptive associations. The quantitative significance of the metal-complexed OC (particularly as organo-Al complex) and geometric relationships of OM with respect to metal oxide phases and other mineral constituents are among the unanswered key questions.

Composition of the OC bound to reducible Fe is another important question which we did not investigate. While Fe-bound OC accounted for only a minor fraction of bulk OC (Figure 4.1), it may significantly affect the turnover time of bulk OC if this OC is particularly recalcitrant or labile. Data on the quality of Fe-bound OC is limited in the literature. The only direct information was reported by Skjemstad et al. (1992) where the >1000 Dalton organic fraction was isolated from two spodic horizons by an organic-free dithionite treatment similar to our method. Subsequent ^{13}C-NMR analysis revealed the dominance of aliphatic groups with some carbohydrate and carboxylic groups, resembling the spectra of acid-soluble materials (fulvic acid). The amount of dithionite-extractable OC was not quantified in their study but likely accounted for a minor fraction of bulk OC because organo-aluminum complex presumably dominated the bulk OC in these samples (*Skjemsted et al.*, 1992a). Based on the difference in ^{13}C-NMR spectra between bulk samples and those residues after DCB treatment, indirect evidence suggests

possible enrichments in aliphatic, aromatic, and/or carboxylic groups in Fe-bound OC fraction, although this OC fraction likely included some alkaline-soluble OC unbound to iron (*Schulten and Leinweber*, 1995). *Kleber et al.* (2004) suggested the protection of carbohydrate-rich material by reactive surfaces of FeOx phases in finer aggregates of temperate arable soils based on a correlation approach. On the other hand, experimental studies demonstrated the stronger affinity of organic compounds rich in aromatic and carboxylic groups for sorption (McKnight et al., 1992; Kaiser et al., 1997) and those rich in aromatic group for complexation/flocculation (Skjemstad et al., 1992b). Clearly more research is needed to substantiate the composition of Fe-bound organic matter in soils.

While only minor fractions of bulk OC were released from the studied soil samples, reductive dissolution of Fe(III) may have a significant impact on biogeochemical cycling in certain terrestrial and aquatic systems. OC:Fe ratios of suspended materials from the lower Mississippi river (unpublished data – using our current method) ranged from 0.10 to 0.17, consistent with sorptive association, and in good agreement with OC:Fe ratios of iron precipitates recovered by acid dissolution from the secondary streams of the upper Mississippi river (0.10-0.19, Rhoton et al., 2002). These ranges agreed well with the ratios we found for Alfisols and Mollisols from the Mississippi basin (0.08-0.12) as well as the other temperate soils we examined (Table 4.3), consistent with erosion of surface soils into the river. These ratios decreased to <0.03 for marine sediment cores at the mouth of the Mississippi River (unpublished data), implying loss of sorbed OC upon reduction of FeOx during burial. About two thirds of riverine particulate OC from this large river system is lost between delivery and burial (Keil et al., 1997), and this FeOx-reduction induced OC loss may account for up to

20-30% of this loss. Assuming that observed low OC:Fe ratios indicate sorptive OC-Fe associations, we infer that the extent of sorptive association of OC with FeOx is controlled by the FeOx abundance in most soils and fresh surface water, and by redox cycling in sediments. To the extent that dithionite extraction mimics the redox changes occurring in natural environment (e.g., flooding of soils, surface soil runoff, burial of suspended material into sediments), our method may simulate the OC mobilization deriving from these redox changes.

REFERENCES

Aiba, S. and Kitayama, K. 1999. Species composition, structure and species diversity of rain forests in a matrix of altitudes and substrates on Mt. Kinabalu, Borneo. *Plant Ecol.* 140, 139-157.

Adams, W. A. and Kassim, J. K. 1984. Iron oxyhydroxides in soils developed from Lower Palaeozoic sedimentary rocks in mid-Wales and implications for some pedogenic processes. *J. Soil Sci,* 35, 117-126.

Adu, J. K. and Oades, J. M. 1978. Physical factors influencing decomposition of organic materials in soil aggregates. *Soil Biol. Biochem.* 10, 109-115.

Allard, T., Menguy, N., Salomon, J., Calligaro, T., Weber, T., Calas, G., and Benedetti, M. F. 2004. Revealing forms of iron in river-borne material from major tropical rivers of the Amazon Basin (Brazil). *Geochim. Cosmochim. Acta,* 68, 3079-3094.

Baisden, W. T., Amundson, R, Cook, A. C., and Brenner, D. L. 2002. The turnover and storage of C and N in five density fractions from California annual grassland surface soil. *Global Biogeochem. Cyc.*16, 1117-1132.

Baldock, J. A. and Skjemstad, J. O. 2000. Role of the soil matrix and minerals in protecting natural organic materials against biological attack. *Org. Geochem.* 31, 697-710.

Bird, M.I., Chivas, A.R. and Head, J. A. 1996. Latitudinal gradient in carbon turnover times in forest soils. *Nature,* 381, 143-146.

Birkeland, P. W. 1999. *Soils and Geomorphology*, 3rd ed., Oxford Univ. Press, New York. 430. pp.

Borggaard, O. K. 1982. Influence of iron oxides on the surface area of soil. *J. Soil Sci.* 33, 443-449.

Boudot, J.-P., Bel Hadj, B. A., Steiman, R., and Seigle-Murandi, F. 1989. Biodegradation of synthetic organo-metallic complexes of iron and aluminum with selected metal to carbon ratios. *Soil Bio. Biochem.* 21, 961-966.

Brady, N. C. 1990. The nature and properties of soils. 10th ed., Macmillan, New York.

Brunauer S., Emmett, P. H., and Teller, E. 1938. Absorption of gases in multimolecular layers. *J. Am. Chem. Soc.* 60, 309-319.

Buol, S. W., Hole, F. D., and McCracken, R. D. 1989. *Soil genesis and classification*, 2nd ed., Iowa State Univ. Press, Ames, Iowa, 446 pp.

Buol, S.W., Sanchez, P. A., Kimble, J. M. and Weed, S. B. 1990. Predicted impact of climate warming on soil properties and use. In *Impact of Carbon Dioxide, Trace*

Gases, and Climate Change on Global Agriculture (ed. B. A. Kimball, et al.) ASA Special Publication 53, pp. 71-82. Am. Soc. Agron., Madison, Wisconsin.

Burford, J. R., Deshpande, T. L., Greenland, D. J., and Quirk, J. P. 1964. Influence organic materials on the determination of the specific surface areas of soils. *J. Soil Sci.* 15, 192-201.

Burke I. C., Yonker, C. M., Parton, W. J., Cole, C. V., Flach, K., Schimel, D. S. 1989. Texture, climate, and cultivation effects on soil organic matter content in U.S. grassland soils. *Soil Sci. Soc. Am. J.* 53, 800-805.

Burke, I. C., Kaye, J. P., Bird, S. P., Hall, S. A., McCulley, R. L. and Sommerville, G. L. 2003. Evaluation and testing models of terrestrial biogeochemistry: the role of temperature in controlling decomposition. In *Models in Ecosystem Science* (ed. C.D. Canham et al.) pp. 225-253, Princeton Univ. Press, Princeton, New Jersey.

Carson, L. and Schwertmann, U. 1980. Natural occurrence of feroxyhite (δ-FeOOH), *Clays Clay Min.* 28, 272-280.

Carson, L. and Schwertmann, U. 1981. Natural ferrihydrites in surface deposits from Finland and their association with silica. *Geochim. Cosmochim. Acta*, 45, 421-429.

Chesworth, W. 1992. Weathering systems. In *Weathering, Soils, and Paleosols* (ed. I. P. Martini and W. Chesworth) pp. 19-40, Elsevier, New York.

Chiou, C. T. 1990. The surface area of soil organic matter. *Env. Sci. Tech.* 24, 1164-1166.

Chorover, J. and Amistadi, M. K. 2001. Reaction of forest floor organic matter at goethite, birnessite and smectite surfaces. *Geochim. Cosmochim. Acta*, 65, 95-109.

Christensen B. T. 1992. Physical fractionation of soil and organic matter in primary particle size and density separates. In *Advances in Soil Science*, vol. 20, Springer-Verlag, pp 1-89, New York.

Christensen, B. T. 1996. Matching measurable soil organic matter fractions with conceptual pools in simulation models of carbon turnover: revision of model structure. In *Evaluation of soil organic matter models* (ed. D. S. Powlson, P. Smith, and J. U. Smith. Springer-Verlag, Berlin Heidelberg.

Davidson, E. A., Trumbore, S. E., Amundson, R. 2000. Biogeochemistry - Soil warming and organic carbon content. Nature, 408, 789-790.

Davidson, E. A., Chorover, J. and Dail, D. B. 2003. A mechanism of abiotic immobilization of nitrate in forest ecosystems: ferrous wheel hypothesis. *Global Change Biol.* 9, 228-236.

Deb, B. C. 1950. The estimations of free iron oxide in soils and clays and their removal. *J. Soil Sci.* 1, 212-220.

Duiker, S. W., Rhoton, F. E. Torrent, J. Smeck, N. E. and Lal, R. 2003. Iron (hydr)oxide crystallinity effects on soil aggregation. *Soil Sci. Soc. Am. J.* 67, 606-611.

Emerson, W. W., Foster, R. C. and Oades, J. M. 1986. Organo-mineral complexes in relation to soil aggregation and structure. In *Interactions of soil minerals with natural organics and microbes* (eds P. M. Huang and M. Schnitzer). SSSA Special Pub, no. 17, pp. 521-548, Madison, Wisconsin, Soil Sci. Soc. Am.

Epstein, H. E., Burke, I. C., and Lauenroth, W. K. 2002. Regional patterns of decomposition and primary production rates in the U.S. Great Plains. *Ecology,* 83, 320-327.

Eswaran, H., Van Den Berg, E., and Reich, P. 1993. Organic carbon in soils of the world. *Soil Sci. Soc. Am. J.* 57, 192-194.

Eusterhues, K., Rumpel, C, Kleber, M. and Kögel-Knabner, I. 2003. Stabilisation of soil organic matter by interactions with minerals as revealed by mineral dissolution and oxidative degradation. *Org. Geochem.* 34, 1591-1600

Evans, L. J., and Wilson, W. G. 1985. Extractable Fe, Al, Si, and C in B horizons of podzolic and brunisolic soils from Ontario. *Can. J. Soil Sci.* 65, 489-496.

Feller, C. and Beare, M. H. 1997. Physical control of soil organic matter dynamics in the tropics. *Geoderma,* 79, 69-116.

Fernandez, I. J., Rustad, L. E., and Lawrence, G. B. 1993. Estimating total soil mass, nutrient content, and trace metals in soils under a low elevation spruce-fir forest. *Can. J. Soil Sci,* 73, 317-328.

Gan, H., Stucki, J. W., and Bailey, G. W. 1992. Reduction of structural iron in ferruginous smectite of free radicals. *Clays Clay Min.*, 40, 659-665, 1992.

Giardina, C. P. and Ryan M. G. 2000. Evidence that decomposition rates of organic carbon in mineral soil do not vary with temperature. *Nature,* 404, 858-861.

Golchin, A., Oades, J. M., Skjemstad, J. O. and Clarke, P. 1994. Study of free and occluded particulate organic matter in soils by solid-state ^{13}C CP/MAS NMR spectroscopy and scanning electron microscopy. *Aust. J. Soil Res.* 32, 285-309.

Golchin, A., Baldock, J. A., and Oades, J. M. 1997. A model linking organic matter decomposition, chemistry, and aggregate dynamics. In *Soil Processes and The Carbon Cycle* (ed. R. Lal, J. M. Kimble, R. F. Follett and B. A. Stewart.) Advances in Soil Science. CRC Press, pp 245-280, Boca Raton, Florida.

Gonzalez, G. and Seastedt, T. R. 2001. Soil fauna and plant litter decomposition in tropical and subalpine forests. *Ecology* 82, 955-964.

Gregorich, E. G., Kachanoski, R. G., and Voroney, R. P. 1989. Carbon mineralization in soil size fractions after various amounts of aggregate disruption. *J. Soil Sci.* 40, 649-659.

Guggenberger, G., and Kaiser, K. 2003. Dissolved organic matter in soil: challenging the paradigm of sorptive preservation. *Geoderma,* 293-310.

Haile-Mariam, S., Cheng, W., Johnsonc, D. W., Balld, J. T., and Paul, E. A. 2000. Use of carbon-13 and carbon-14 to measure the effects of carbon dioxide and nitrogen fertilization on carbon dynamics in ponderosa pine. *Soil Sci. Soc. Am. J.* 64, 1984-1993.

Hall, S. J., Asner, G. P. and Kitayama, K. 2004. Substrate, climate, and land use controls over soil N dynamics and N-oxide emissions in Borneo. *Biogeochem.* 70, 27-58.

Harradine, F. and Jenny, H. 1958. Influence of parent material and climate on texture and nitrogen and carbon contents of soils. *Soil Sci.* 85, 235-243.

Hassink, J. 1996. Preservation of plant residues in soils differing in unsaturated protective capacity. *Soil Sci. Soc. Am. J.* 60, 487-491.

Hedges, J. I. and Oades, J. M. 1997. Comparative organic geochemistries of soils and marine sediments. *Org. Geochem.* 27, 319-361.

Homann, P. S., Sollins, P., Chappell, H. N., and Stangenberger, A. G. 1995. Soil organic carbon in a mountainous, forested region: relation to site characteristics. *Soil Sci. Soc. Am. J.* 59, 1468-1475.

Homann, P. S., Sollins, P., Fiorella, M., Thorson, T., and Kern, J. S. 1998. Regional soil organic carbon storage estimates for western Oregon by multiple approaches, *Soil Sci. Soc. Am. J.*, 62, 789-796.

Hughes, J. C. 1982. High gradient magnetic separation of some soil clays from Nigeria, Brazil and Colombia. I. The interrelationships of iron and aluminum extracted by acid ammonium oxalate and carbon. *J. Soil Sci.,* 33, 509-519.

Jacobson, G. 1970. *Gunong Kinabalu Area, Sabah, Malaysia.* Geological Survery Malaysia, Kuching, Sarawak, 111 pp.

Jardine, P. M., Weber, N. L. and McCarthy, J. F. 1989. Mechanisms of dissolved organic carbon adsorption on soil. *Soil Sci. Soc. Am. J.* 53, 1378-1385.

Jenny, H. 1941. *Factors of soil formation.* McGraw Hill, New York, 281 pp.

Jenny, H. 1980. *The soil resources: Origin and behavior*. Springer-Verlag, New York, 377 pp.

Johnson, D. W., and Todd, D. E. 1983. Relationship among iron, aluminium, carbon and sulphate in a variety of forest soils. *Soil Sci. Soc. Am. J.* 47, 792-800.

Jones, D. L. and Edwards, A. C. 1998. Influence of sorption on the biological utilization of two simple carbon substrates, *Soil Bio. Biochem.*, 30, 1895-1902.

Kaiser, K. and Zech, W. 1996. Defects in estimation of aluminum in humus complexes of podzolic soils by pyrophosphate extraction, *Soil Sci.*, 161, 452-458.

Kaiser, K. Guggenberger, G., Haumaier, L. and Zech, W. 1997. Dissolved organic matter sorption on subsoil and minerals studied by ^{13}C-NMR and DRIFT spectroscopy. *Eur. J. Soil Sci.*, 48, 301-310.

Kaiser, K. and Guggenberger, G. 2000. The role of SOM sorption to mineral surfaces in the preservation of organic matter in soils. *Org. Geochem.* 31, 711-725.

Kaiser, K., K. Eusterhues, C. Rumpel, G. Guggenberger, and I, Kögel-Knabner, Stabilization of organic matter by soil minerals – investigations of density and particle-size fractions from two acid forest soils, *J. Plant Nutr. Soil Sci.*, 165, 451-459, 2002.

Kaiser, K. and Guggenberger, G. 2003. Mineral surfaces and soil organic matter. *Eur. J. Soil Sci.*, 54, 219-236.

Katterer, T., Reichstein, M. and Andren, O. 1998. Temperature dependence of organic matter decomposition: a critical review using literature data analyzed with different models. *Bio. Fert. Soils*, 27, 258-262.

Keil, R. G., Montluçon, D. B. Prahl, F. G., and Hedges, J. I. 1994. Sorptive preservation of labile organic matter in marine sediments. *Nature,* 370, 549-552.

Keil, R. G., Mayer, L. M., Quay, P. D., Richey, J. E. and Hedges, J. I. 1997. Losses of organic matter from riverine particles in deltas, *Geochim. Cosmochim. Acta,* 61, 1507-1511.

Kiem, R. and Kögel-Knabner, I. 2002. Refractory organic carbon in particle-size fractions of arable soils II: organic carbon in relation to mineral surface area and iron oxides in fractions < 6 μm. *Org. Geochem.* 33, 1699-1713.

Kirschbaum, M. U. F. 2000. Will changes in soil organic carbon act as a positive or negative feedback on global warming? *Biogeochem.* 27, 753-760.

Kitayama, K. 1992. Altitudinal transect study of the vegetation on Mount Kinabalu, Borneo. *Vegetatio,* 102, 149-171.

Kitayama K., Aiba, S., Majalap-Lee, N. and Ohsawa, M. 1998. Soil nitrogen mineralization rates of rain forests in a matrix of altitudes and geological substrates on Mount Kinabalu, Borneo. *Ecol. Res.* 13, 301-317.

Kitayama, K. and Aiba, S. 2002. Ecosystem structure and productivity of tropical rainforests along altitudinal gradients under contrasting soil P pools on Mount Kinabalu, Borneo. *J. Ecol.* 90: 37-51.

Kitayama, K., Suzuki, S, Hori, M., Takyu, M., Aiba, S., Majalap-Lee, N. and Kikuzawa, K. 2004. On the relationships between leaf-litter lignin and net primary productivity in tropical rain forests. *Oecologia,* 140, 335-339. (DOI: 10.1007/s00442-004-1590-7)

Kleber, M., C. Mertz, S. Zikeli, H. Kniker, and R. Jahn. 2004. Changes in surface reactivity and organic matter composition of clay subfractions with duration of fertilizer deprivation. *Eur. J. Soil Sci.*, 55, 381-391.

Knicker, H. and Lu¨demann, H.-D. 1995. ^{15}N and ^{13}C-CPMAS and solution NMR studies of ^{15}N enriched plant material during 600 days of microbial degradation. *Org. Geochem.* 23, 329– 341.

Kölbl, A. and Kögel-Knabner, I. 2004. Content and composition of free and occluded particulate organic matter in a differently textured arable Cambisol as revealed by solid-state ^{13}C NMR spectroscopy. J. Plant Nutr. Soil Sci. 167, 45-53, (DOI: 10.1002/jpln.200321185)

Krisna Murti, G. S. R., and Huang, P. M. 1987. Influence of constituents on the stability of mechanical separates of soils representing major taxonomic orders. *Appl. Clay Sci.* 2, 299-308.

Krull, E. S., Baldock, J. A., and Skjemstad, J. O. 2003. Importance of mechanisms and processes of the stabilization of soil organic matter for modeling carbon turnover, *Funct.Plant Biol.* 30, 207-222.

Lavkulich, L. M. and Wiens, J. H. 1970. Comparison of organic matter destruction by hydrogen peroxide and sodium hypochlorite and its effects on selected mineral constituents. *Soil Sci. Soc. Am. J.* 34, 755-758.

Liski, J., Ilvesniemi, H., Makela, A. and Westman, C. J. 1999. CO_2 emissions from soil in response to climatic warming are overestimated - The decomposition of old soil organic matter is tolerant of temperature. *Ambio* 28, 171-174.

Loeppert, R. H., and Inskeep, W. P. 1996. Iron. In *Methods of Soil Analysis. Part 3, Chemical Methods,* (ed. D. L. Sparks). Soil Sci. Soc. Am. Book Series, 5, pp. 639-664, Madison, Wisconsin.

Lundström, U. S., et al. 2000. Advances in understanding the podzolization process resulting from a multidisciplinary study of three coniferous forest soils in the Nordic Countries. *Geoderma*, *94*, 335-353.

Martin, J. P., Ervin, J. O., and Shepherd, R. A. 1966. Decomposition of the iron, aluminum, zinc, and copper salts or complexes of some microbial and plant polysaccharides in soil. *Soil Sci. Soc. Am. J. Proc.*30, 196-200.

Masiello, C. A., Chadwick, O. A., Southon, J., Torn, M. S., and Harden, J. W. in press. Mechanisms of carbon storage in grassland soils. *Glob. Biogeochem. Cycles.*

Mayer, L. M. 1994a. Surface area control of organic carbon accumulation in continental shelf sediments. *Geochim. Cosmochim. Acta,* 58, 1271-1284.

Mayer, L. M. 1994b. Relationships between mineral surfaces and organic carbon concentrations in soils and sediments, *Chem.l Geol.* 114, 347-363.

Mayer, L. M. 1999. Extent of coverage of mineral surfaces by organic matter in marine sediments. *Geochim. Cosmochim. Acta,* 63, 207-215.

Mayer, L. M. and Xing, B. 2000. Organic carbon-surface area-clay relationships in acid soils. *Soil Sci. Soc. Am. J.* 65, 250-258.

Mayer, L. M., Schick, L. L., Hardy, K., Wagai, R. and McCarthy, J. 2004. Organic matter content of small mesopores in sediments and soils. *Geochim. Cosmochim. Acta* 68, 3863-3872.

McKeague, J. A. and Schuppli, P. A. 1982. Changes in concentration of iron and aluminum in pyrophosphate extracts of soil and composition of sediment resulting from ultracentrifugation in relation to spodic horizon criteria. *Soil Sci.,* 134, 265-270.

McKnight, D. M., Bencala, K. E., Zellweger, G. W., Aiken, G. R., Feder, G. L., and Thorn, K. A. 1992. Sorption of dissolved organic carbon by hydrous aluminum and iron oxides occurring at the confluence of Deer Creek with the Snake River, Summit County, Colorado. *Envir. Sci. Tech.* 26, 1388-1396.

Mehra, O. P. and Jackson, M. L. 1960. Iron oxide removal from soils and clays by a dithionite-citrate system buffered with sodium bicarbonate. *Clays Clay Min.* 7, 317-327.

Mitchell, B. D. and MacKenzie, R. G. 1954. Removal of free iron oxide from clays. *Soil Sci.,* 77, 173-184.

Mitchell, B. D., Smith, B. F. L., and Endredy, A. S. 1971. The effect of buffered sodium dithionite solution and ultrasonic agitation of soil clays. *Isr. J. Chem.* 9, 45-52.

Motavalli, P. P., Palm, C. A., Parton, W. J., Elliott, E. T., and Frey, S. S. 1995. Soil pH and organic C dynamics in tropical forest soils: evidence from laboratory and simulation studies, *Soil Bio. Biochem.* 27, 1589-1559.

Myneni S. C. B., Brown, J., Martinez, G. A. and Meyer-Ilse, W. 1999. Imaging of humic substance macromolecular structures in water and soils. *Science*, 286, 1335-1337.

Neff J. C., Townsend, A.R., Gleixner, G., Lehman, S., Turnbull, J. and Bowman, W. 2002. Variable effects of nitrogen additions on the stability and turnover of soil carbon. *Nature*, 419, 915-917.

Nierop, K. G. J., Jansen, B., and Verstraten, J. M. 2002. Dissolved organic matter, aluminium and iron interactions: precipitation induced by metal/carbon ratio, pH and competition, *Sci. Total Environ.* 300, 201-211.

North, P. F. 1976. Towards an absolute measurement of soil structural stability using ultrasound. *J. Soil Sci.* 27, 451-459.

Oades, J. M. 1984. Soil organic matter and structural stability: mechanisms and implications for management. *Plant Soil*, 76, 319-337.

Oades, J. M. 1988. The retention of organic matter in soils. *Biogeochem.* 5, 35-70.

Oades, J. M., 1989. An Introduction to Organic Matter in Mineral Soils. In *Minerals in Soil Environments* (ed. J. B. Dixon, and S. B. Weed) pp. 89-159, Soil Sci. Soc. Am., Madison, Wisconsin.

Parfitt, R. L., Theng, B. K. G., Whitton, J. S. and Shepherd, T. G. 1997. Effects of clay minerals and land use on organic matter pools. *Geoderma*, 75, 1-12.

Parker, J. L., Fernandez, I. J., Rustad, L. E. and Norton, S. A. 2002. Soil organic matter fractions in experimental forested watersheds. *Water, Air, Soil Poll.* 138, 101-121.

Parton, W. J., Schimel, D. S., Cole, C. V. and Ojima, D. S. 1987. Analysis of factors controlling soil organic matter levels in Great Plains grasslands. *Soil Sci. Soc. Am. J.* 51, 1173-1179.

Paul, E. A. and Clark, F. E. 1996. Soil microbiology and biochemistry. 2nd ed., Academic Press, Dan Diego, California.

Paul, E. A., Follett, R. F., Leavitt S. W., Halvorson, A., Peterson, G. A., and Lyon, D. J. 1997. Radiocarbon dating for determination of soil organic matter pool sizes and dynamics. *Soil Sci. Soc. Am. J.* 61, 1058–1067.

Percival, H. J., Parfitt, R. L., and Scott, N. A. 2000. Factors controlling soil carbon levels in New Zealand grasslands: Is clay content important? *Soil Sci. Soc. Am. J.* 64, 1623-1630.

Pinheiro-Dick, D., and Schwertmann, U. 1996. Microaggregates from Oxisols and Inceptisols: dispersion through selective dissolution and physicochemical treatments. *Geoderma*, 74, 49-63.

Post, W. M., Emanuel, W. R., Zinke, P. J., and Stangerberger, A. G. 1982. Soil carbon pools and world life zones. *Nature*, 298, 156-159.

Pritchard, D. T. and Ormerod, E. C. 1976. The effect of heating on the surface area of iron oxide. *Clay Min.* 11, 327-329.

Rhoton, F. E., Bigham, J. M., and Lindbo, D. L. 2002. Properties of iron oxides in streams draining the loess uplands of Mississippi. *Appl. Geochem.* 17, 409-419.

Saggar, S., Parshotam, A., Sparling, G. P., Feltham, C. W. and Hart, P. B. S. 1996. ^{13}C-labelled ryegrass turnover and residence times in soils varying in clay content and mineralogy. *Soil Bio. Biochem.* 28, 1677-1686.

Santos, M. C. D., Mermut, A. R., and Ribeiro, M. R. 1989. Submicroscopy of clay micro aggregates in an Oxisol from Pernambuco, Brazil. *Soil Sci. Soc. Am. J*, 53, 1895-1901.

Schlesinger, W. H. 1991. *Biogeochemistry: an analysis of global change.* 2nd ed., Academic Press, New York, 588 pp.

Schlesinger, W.H. and Lichter, J. 2001. Limited carbon storage in soil and litter of experimental forest plots under elevated atmospheric CO2. Nature, 411, 466-469.

Schimel, D. S., Braswell, B. H., Holland, E. A., McKeown, R., Ojima, D. S., Painter, T. H., Parton, W. J., and Townsend, A. R. 1994. Climatic, edaphic, and biotic controls over storage and turnover of carbon in soils. *Global Biogeochem. Cycles,* 8, 279-293.

Schimel, J. P. and Bennett, J. 2004. Nitrogen mineralization: challenges of a changing paradigm. *Ecol.* 85, 591–602.

Schulten, H.R. and Leinweber, P. 1995. Dithionite-citrate-bicarbonate-extractable organic matter in particle-size fractions of a Haplaquoll. *Soil Sci. Soc. Am. J.* 59, 1019-1027.

Schulthess, C. P. and Huang, C. P. 1991. Humic and fulvic acid adsorption by silicon and aluminum oxide surfaces on clay minerals. *Soil Sci. Soc. Am. J.* 55, 34-42.

Schwertmann, U., Kodama, H., and Fischer, W. R., 1986. Mutual interactions between organics and iron oxides. In *Interactions of Soil Minerals with Natural Organics and Microbes* (ed. P. M. Huang, and M. Schnitzer) Soil Sci. Soc. Am. Spec. Pub. 17, pp. 223–250, Madison, Wisconsin.

Schwertmann, U. and Murad, E. 1988. The nature of an iron oxide-organic iron association in a peaty environment. *Clay Min.* 23, 291–299.

Schwertmann, U. 1988. Occurrence and formation of iron oxides in various pedoenvironments. In *Iron in Soils and Clay Minerals* (ed. J. W. Stucki *et al.*) pp. 267–308, Reidel, Dordrech.

Schwertmann, U. and Taylor, R. M. 1989. Iron oxides. In *Minerals in Soil Environments* (ed. J. B. Dixon, and S. B. Weed) pp. 379-438, Soil Sci. Soc. Am., Madison, Wisconsin.

Shang, C. and Tiessen, H. 1998. Organic matter stabilization in two semiarid tropical soils: size, density, and magnetic separations. *Soil Sci. Soc. Am. J.* 62, 1247-2157.

Sims, Z. R. and Nielsen, G. A. 1986. Organic carbon in Montana soils as related to clay content and climate. *Soil Sci. Soc. Am. J.* 50, 1269-1271.

Six, J., Conant, R. T., Paul, E. A. and Paustian, K. 2002. Stabilization mechanisms of soil organic matter: implications for C-saturation of soils. *Plant Soil* 241, 155-176.

Skjemstad, J. O. 1992. Genesis of Podzols on coastal dunes in southern Queensland. III: The role of aluminum-organic complexes in profile development. *Aust. J. Soil Res. 30*, 645-665.

Skjemstad, J. O., Bushby, H. V. A., and Hansen, R. W. 1989. Extractable Fe in the surface horizons of a range of soils from Queensland. *Aust. J. Soil Res.* 28, 259-266.

Skjemstad, J. O., Fitzpatric, R. W., Zarcinas, B. A., and Thompson, C. H. 1992a. Genesis of podzols on coastal dunes in southern Queensland. II: Geochemistry and forms of elements as deduced from various soil extraction procedures. *Aust. J. Soil Res. 30*, 615-644.

Skjemstad, J. O., Waters, A. G., Hanna, J. V., Oades, J. M. 1992b. Genesis of podzols on coastal dunes in southern Queensland. IV: Nature of the organic fraction as seen by ^{13}C nuclear magnetic resonance spectroscopy. *Aust. J. Soil Res.* 30, 667-681.

Soil Survey Staff. 1996. Soil survey laboratory methods manual. Soil Survey Investigation Report no. 42. version 3.0. USDA, National Soil Survey Center, Nebraska.

Soil Survey Staff. 1999. Soil Taxonomy. 2nd ed., USDA, Natural Resources Conservation Service, Nebraska.

Sollins, P., Homann, P. and Caldwell, B. A. 1996. Stabilization and destabilization of soil organic matter: mechanisms and controls. *Geoderma*, 74, 65-105.

Sposito, G. 1989. *The chemistry of soils*. Oxford Univ. Press, New York. 277 pp.

Spycher, G. and J. L. Young. 1979. Water-dipersible soil organic-mineral particles: II. Inorganic amorphous and crystalline phases in density fractions of clay-size particles. *Soil Sci. Soc. Am. J.* 43, 328-332.

Spycher, G., Sollins, P. and Rose, S. 1983. Carbon and nitrogen in the light fraction of a forest soil: vertical distribution and seasonal patterns. *Soil Sci.* 135, 79-87.

Stevenson, F. J. 1994. *Humus Chemistry: Genesis, Composition, Reactions*, 2nd ed., Wiley, New York.

Stumm, W. and Sulzberger, B. 1992. The cycling of iron in natural environments: Considerations based on laboratory studies of heterogeneous redox processes, *Geochim. Cosmochim. Acta,* 56, 3233–3257.

Stumm, W. and Morgan, J. J. 1996. *Aquatic Chemistry: chemical equilibria and rates in natural waters*, 3rd ed., Wiley-Interscience, New York.

Tate, K. R. 1992. Assessment, based on a climosequence of soil in tussock grasslands, of soil carbon storage and release in response to global warming. *J. Soil Sci.* 43, 697-707.

Telles, E. D. C., de Camargo, P. B., Martinelli, L. A., Trumbore, S. E., da Costa, E. A., Santos, J., Higuchi, N., and Oliverira, R. C. 2003. Influence of soil texture on carbon dynamics and storage potential in tropical forest soils of Amazonia, *Global Biogeochem. Cycles,* 17. (DOI:10.1029/2002GB001953).

Tiessen, H., Cuevas, E., and Chacon, P. 1994. The role of soil organic matter in sustaining soil fertility. *Nature,* 371, 783-785.

Tiessen, H., Stewart, J. W. B., and Cole, C. V. 1984. Pathways of phosphorous transformations in soils of differing pedogenesis. *Soil Sci. Soc. Am. J.* 48, 853-858.

Tipping, E. 1981. The adsorption of aquatic humic substances by iron oxides. *Geochim. Cosmochim. Acta* **45,** 191-199.

Tipping, E., Rey-Castro, C., Bryan, S. E., and Hamilton-Taylor, J. 2002. Al(III) and Fe(III) binding by humic substances in freshwaters, and implications for trace metal speciation. *Geochim. Cosmochim. Acta,* 66, 3211-3224.

Torn, M. S., Trumbore, S. E., Chadwick, O. A., Vitousek, P. M., and Hendricks, D. M. 1997. Mineral control of soil organic carbon storage and turnover. *Nature*, *389*, 170-173.

Townsend, A. R., Vitousek, P. M. and Trumbore, S. E. 1995. Soil carbon dynamics along gradients in temperature and land-use on the island of Hawaii. *Ecol.* 76,721-733.

Truchenek, L. W. and Oades, J. M. 1979. Fractionation of organo-mineral complexes by sedimentation and density techniques. *Geoderma,* 21, 311-344.

Trumbore, S. E., Chadwick. O. A. and Amundson, R. 1996. Rapid exchange of soil carbon and atmospheric CO_2 driven by temperature change. *Science,* 272, 393-396.

Veldkemp E. 1994. Organic carbon turnover in three tropical soils under pasture after deforestation. *Soil Sci. Soc. Am. J.* 58, 175-180.

Vrdoljak, G., and Sposito, G. 2002. Soil aggregate hierarchy in a Brazilian Oxisol. In *Developments in Soil Science*, vol. 28A, (ed. A. Violante *et al.*) pp. 197-217, Elsevier Science, Amsterdam.

Wada, K. 1995. Role of aluminium and iron in the accumulation of organic matter in soils with variable charge. In *Environmental Impact of Soil Component Interactions, vol. I.*,(ed. P. M. Huang *et al.*) pp. 47-58, CRC Lewis, Boca Raton, Florida.

Weidler, P.G. and Stanjek, H. 1998. The effect of dry heating of synthetic 2-line and 6-line ferrihydrite: II. surface area, porosity and fractal dimension. *Clay Min.* 33, 277-284.

Wiseman, C. L. S. and Puttmann, W. 2004. Soil organic carbon and its sorptive preservation in central Germany, *Eur. J. Soil Sci.,* (DOI:10.1111/j.1351-0754.2004.00655.x., in press).

Young, R. W., Carder, K. L., Betzer, P. R., Costello, D. K., Duce, R. A., Ditullio, G. R., Tindale, N. W., Laws, E. A., Uematsu, M., Merrill, J. T., and Feely, R. A. 1991. Atmospheric iron inputs and primary productivity: phytoplankton responses in the North Pacific. *Global Biogeochem. Cycles,* 5, 119-34.

Zimmerman, A. R., Goyne, K. W., Chorover, J., Komarneni, S., and Brantley, S. L. 2004. Mineral mesopore effects on nitrogenous organic matter adsorption. *Org. Geochem.* 35, 355-375

BIOGRAPHY OF THE AUTHOR

Rota Wagai was born in Tokyo, Japan on January 10, 1973. He was raised in Shirahama, Chiba and then in Bunkyo-ku, Tokyo. He graduated from Bunkyo Daini Junior High School in 1987 and from Sundai Kofu Highschool in 1990. He completed the general education requirement at Shizuoka University in 1992. During his years at Shizuoka Univeristy, he worked in the Forest Ecology Lab of Dr. Kakubari and inspired to study forest ecosystem science. He transfered to University of Wisconsin-Madison in 1993 and graduated from UW-Madison with a Bachelor of Science in Forest Ecology and Management with specialization in Soil Science in 1996. He received his Master of Science degree in Forest Science in September 1999 from Oregon State Univerisity. He enrolled in the Ecology and Environmental Science Ph.D. program in the Department of Plant, Soil, and Environmental Science Department at University of Maine immediately following completion of his Masters work. He moved to Darling Marine Center in 2000. Rota is a candidate for the Doctor of Philosophy degree in Ecology and Environemntal Sciences from The University of Maine in May, 2005.